Expanding the scope of H2O2-driven biocatalysis

Xu, X.

Important note
To cite this publication, please use the final published version (if applicable).
Please check the document version above.

Expanding the scope of H$_2$O$_2$-driven biocatalysis

Dissertation

for the purpose of obtaining the degree of doctor

at Delft University of Technology

by the authority of the Rector Magnificus, prof.dr.ir. T.H.J.J. van der Hagen

chair of the Board for Doctorates

to be defended publicly on

Wednesday 21 December 2022 at 10:00 o'clock

by

Xiaomin XU

Master of Engineering in Biotechnology Engineering, South China University of Technology, China

born in Hubei, China

Composition of the doctoral committee:

Rector Magnificus,	chairperson
Prof.dr. F. Hollmann	TU Delft, promotor
Dr. C.E. Paul	TU Delft, copromotor

Independent members:

Prof.dr.-ing. D. Holtmann	Technische Hochschule Mittelhessen, Germany
Prof.dr. I.W.C.E. Arends	Utrecht University, The Netherlands
Prof.dr. U. Hanefeld	TU Delft
Prof.dr. M. Alcalde Galeote	ICP-CSIC, Spain
Dr. S. Schmidt	University of Groningen, The Netherlands

Reserve member:

Prof.dr. E.A. Pidko	TU Delft

ISBN: 978-90-832797-7-0

Cover by: Xiaomin Xu

Copyright © 2022 by Xiaomin Xu

Printed by Proefschriftspecialist

An electronic version of the dissertation is available at TU Delft library

致家人

感谢你们无条件的支持与鼓励

Table of Contents

1

Summary

H_2O_2 is a relatively 'green' oxidant because its by-products are only H_2O. In recent years, an increasing number of enzymatic synthesis methods based on H_2O_2 have been established. H_2O_2-driven reactions are usually applied as an alternative to NAD(P)H-dependent reactions to avoid complicated cofactor regeneration systems.

The aim of this thesis was to develop H_2O_2-driven peroxizymes-catalysed reactions. Four approaches were studied: (1) UPO-ADHs combinations for the synthesis of enantiomerically pure (*R*)- and (*S*)-phenylethanol derivatives; (2) UPO-catalysed selective oxidation of silane to silanol; (3) VCPO-catalysed oxidative decarboxylation of glutamic acid to the corresponding nitrile at semi-preparative scale; (4) The investigation of the formate oxidase (*Ao*FOx)-driven H_2O_2 generation system.

In Chapter 3, UPO-catalysed hydroxylation of ethylbenzene could only produce (*R*)-phenylethanol exclusively. We therefore developed a bienzymatic reaction to produce not only (*R*)- but also (*S*)-phenylethanols with the combination of a peroxygenase and complementary alcohol dehydrogenases. The results obtained are promising (10 samples, >91% *ee*). Reaction conditions for this one-pot two-step system would require further study and optimisation.

In Chapter 4, a peroxygenase-catalysed hydroxylation of organosilanes is reported. *Aae*UPO enabled efficient conversion of a broad range of silane starting materials in attractive productivities (up to 300 mM h^{-1}) and catalyst usage (up to 84 s^{-1} and more than 120,000 catalytic turnovers). As this enzymatic Si-H oxyfunctionalisation route is a completely new application of UPOs, there are still some limitations that need further research and investigation.

In Chapter 5, the chemoenzymatic oxidative decarboxylation of glutamic acid to the corresponding nitrile using the vanadium chloroperoxidase (*Cl*VCPO) has been investigated. 1,630,000 turnovers and k_{cat} of 75 s^{-1} were achieved using 100 mM glutamate. The semi-preparative enzymatic oxidative decarboxylation of glutamate was also demonstrated. Product inhibition was identified as a major limitation.

In Chapter 6, the formic acid oxidase (*Ao*FOx) driven H_2O_2 generation system was used to drive the *Aae*UPO-catalysed hydroxylation of ethylbenzene derivatives. The investi-

gation of factors such as formate and enzyme spiking, pH, oxidase concentration, co-solvent, O_2 supply and production inhibition did not solve the premature ending of the reaction. In our opinion, the nature of the electronic donor for *Ao*FOx could be the breakthrough.

The results of this thesis contribute to the application of H_2O_2-driven peroxyzymes. The achievements and challenges noted in the thesis will promote the future implementation and popularisation of enzymatic oxyfunctionalisation reactions.

Samenvatting

H_2O_2 is een relatief "groene" oxidant omdat alleen de bijproducten H_2O gevormd worden. De laatste jaren zijn er een toenemend aantal enzymatische synthesemethoden op basis van H_2O_2 ontwikkeld. H_2O_2-gedreven reacties worden gewoonlijk toegepast als een alternatief voor NAD(P)H-afhankelijke reacties om ingewikkelde cofactor regeneratiesystemen te vermijden.

Het doel van dit proefschrift is om H_2O_2-gedreven peroxyzym gekatalyseerde reacties te ontwikkelen. Vier benaderingen werden bestudeerd: (1) UPO-ADHs combinaties voor de synthese van enantio-zuivere (*R*)- en (*S*)-fenylethanol derivaten; (2) UPO-gekatalyseerde selectieve oxidatie van silaan tot silanol; (3) Semi-preparatieve VCPO-gekatalyseerde oxidatieve decarboxylering van glutaminezuur tot zijn overeenkomstige nitril; (4) Onderzoek van het (*Ao*FOx)-gedreven H_2O_2-generatie systeem.

In hoofdstuk 3, werd met de UPO-gekatalyseerde hydroxylering van ethylbenzeen alleen (*R*)-fenylethanol geproduceerd. Dit was niet voldoende. Een nieuwe bi-enzymatische reactie werd ontwikkeld om tegelijkertijd (*R*)- en (*S*)-phenylethanolen te produceren met de combinatie van een peroxygenase en een alcohol dehydrogenase. De verkregen resultaten zijn veelbelovend (10 monsters, >91% *ee*), maar de reactiecondities voor de "één-pot twee-staps"-systeem vereisen een verdere studie en optimalisatie.

In hoofdstuk 4, wordt een peroxygenase-gekatalyseerde hydroxylering van organosilanen beschreven. Een efficiënte omzetting met *Aae*UPO is mogelijk met een breed scala aan silaan uitgangsmaterialen dat resulteert tot een aantrekkelijke productiviteit (tot 300 mM h^{-1}) en katalysatorgebruik (tot 84 s^{-1}) en een turnover van meer dan 120,000. Aangezien deze enzymatische Si-H-oxyfunctionaliseringsroute een volledig nieuwe toepassing van UPO's is, zijn er nog enkele beperkingen die verder onderzoek en bestudering behoeven.

In hoofdstuk 5, wordt de chemo-enzymatische oxidatieve decarboxylering van glutaminezuur naar zijn overeenkomstige nitril met behulp van vanadium chloroperoxidase (*Cn*VCPO) onderzocht. Een turnover van 1,630,000 en een k_{cat} van 75 s^{-1} werd bereikt met 100 mM glutamaat. Er werd aangetoond dat de semi-preparatieve enzymatische oxidatieve decarboxylering van glutamaat mogelijk is. Productremming werd geïdentificeerd als een belangrijke beperking.

In hoofdstuk 6, werd formaat oxidase (*Ao*FOx) aangedreven H_2O_2 generatie systeem gebruikt om de *Aae*UPO-gekatalyseerde hydroxylering van ethylbenzeenderivaten te stimuleren. Factoren zoals formaat, enzym spiking, pH, oxidase concentratie, co-solvent, en O_2-toevoer waren geen oplossing voor het voortijdig beëindigen van de reactie. Naar onze mening zou de aard van de elektronische donor voor *Ao*FOx een doorbraak kunnen betekenen.

De resultaten van dit proefschrift leveren een bijdrage voor de toepassing van H_2O_2-gedreven peroxyzym reacties. De resultaten en uitdagingen in dit proefschrift zullen de toepassing en popularisering van enzymatische oxyfunctionaliseringsreacties bevorderen.

2

Introduction

Biocatalysis is an attractive tool in chemical transformations because of its specific selectivity and mild reaction conditions.[1] The use of enzymes has spread to the production of food, pharmaceuticals, biodiesel, polymers and other commodities.[2]

Especially the oxyfunctionalisation of organic molecules remains a challenge in organic chemistry, as chemical catalysts commonly lack selectivity, resulting in a (more or less) intricate mixture of products. Oxidoreductase exhibit specific selectivity, giving them an unrivalled advantage in catalysing selective C-H bond oxyfunctionalisation.

2.1. Selective oxyfunctionalisation reactions catalysed by P450 monooxygenases and peroxygenases – a bright future for sustainable chemical synthesis.
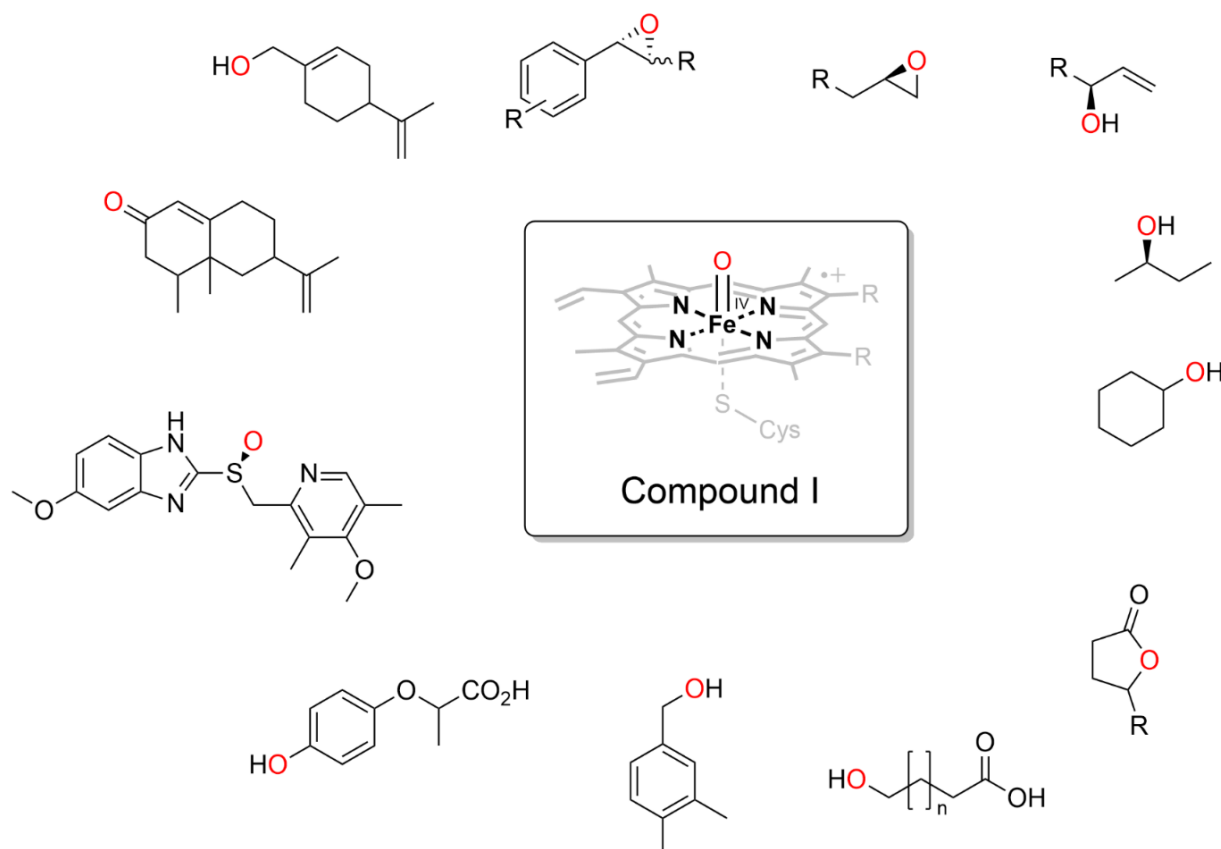

Figure 1. Compound I as an active catalyst within P450 monooxygenase and peroxygenase for selective oxygen functionalisation reactions.

Oxyfunctionalisations comprise chemical transformations inserting oxygen atoms into (non-activated) C-H-, C-C-, C=C-bonds or onto heteroatoms. The general inertness of these bonds requires potent oxygen-transfer reagents such as high-valent metal-oxo complexes or organic peroxides. These reagents, however, are challenged by low selectivity resulting in complex product mixtures and isolation of the desired product can be tedious and time- and resource-intensive. Interestingly, many of the aforementioned oxy-functionalising agents are 'biomimetic' i.e. they are inspired by natural catalysts such as iron- or flavin-dependent monooxygenases.[3,4] The fundamental difference between 'chemical' and enzymatic oxyfunctionalisation catalysts lies in the environment around the oxyfunctionalising catalyst. In case of chemical catalysts, this space is populated by simple ligands and solvent whereas enzymes provide a well-defined cavity (active site) that not only controls the orientation of the starting material towards the catalyst but also participates in the catalytic mechanism. Hence, it is not astonishing that monooxygenases usually excel over their 'chemical' counterparts in terms of catalytic performance and selectivity.

Cytochrome P450 monooxygenases have been at the centre of attention for decades[5] but are increasingly challenged by so-called unspecific peroxygenases (UPOs).[6,7] In this introduction we aim at providing a comparison between both enzyme classes with respect to their practical applicability based on recent scientific literature comparing their advantages and disadvantages.

Mechanistic similarities and differences between P450 MOs and UPOs

Both enzyme classes make use of Compound I (CpdI, Scheme 1C) as the active reagent to insert an oxygen atom into their substrates. However the mechanism, via which CpdI is formed, differs significantly between both enzyme classes. P450 monooxygenases utilise molecular oxygen as a source of oxygen atom and activate it reductively (Scheme 1A). The reducing equivalents required for this reduction are obtained from a nicotinamide cofactor (NAD(P)H) via more or less complex electron transport chains.[8,9] NAD(P)H itself is applied in catalytic amounts for economic reasons and regenerated *in situ* by the enzymatic oxidation of a stoichiometric co-substrate. Peroxygenases are much simpler as they

15

directly utilise reduced oxygen in the form of hydrogen peroxide or organic hydroperoxides (Scheme 1B).
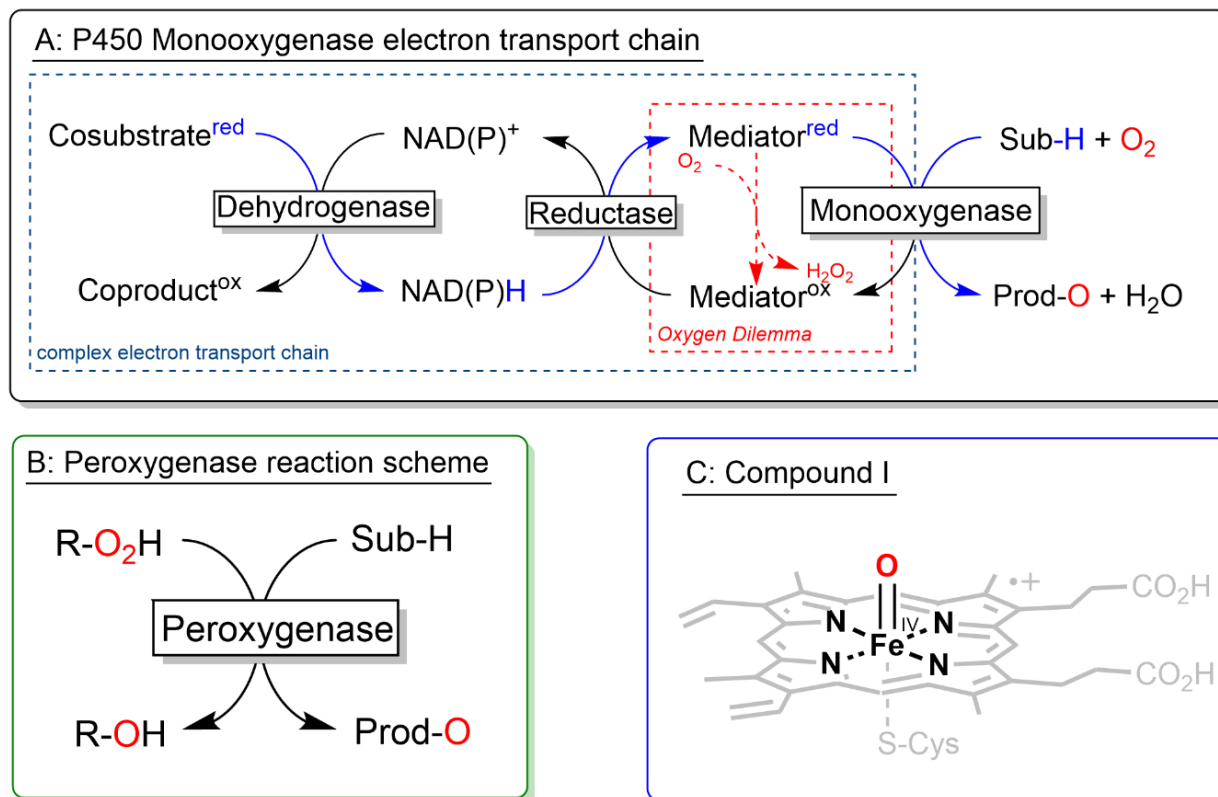
Scheme 1**.** Comparison of substrate oxidation via Compound I (C) formation in cytochrome P450 monooxygenases (A) and peroxygenases (B).

A comparison based on performance indicators

Evaluating the environmental impact of a given (catalytic) reaction is a complex task for which many factors have to be taken into account. Nevertheless, we believe that already some simple indicators such as catalyst turnover number (TN) and product concentration already give a reasonable indication of the economic and environmental attractiveness of a given catalytic reaction.

The importance of product concentration/yield is rather obvious: highly diluted reaction mixtures not only use the production infrastructure insufficiently but also result in high

amounts of solvent wastes and necessitate additional (time-, resource- and energy-intensive) downstream processing operations to obtain the product of interest (Figure 2A). Also, it should be taken into account that energy required for heating/cooling, mixing etc., is mostly spent on the solvent. Consequently, maximisation of the product concentration is mandatory from both an economic and environmental point-of-view. As shown in Figure 2C, the majority of recent P450- and peroxygenase-publications deal with highly diluted reaction mixtures with product concentrations below 10 mM corresponding to the solvent (i.e. aqueous buffer) representing more than 99% of the reaction mixture. However, while in the case of P450 monooxygenases, the highest product concentrations reported so far lie around 50-60 mM,[10,11] the situation is more promising in the case of peroxygenases with increasingly more examples of non-aqueous applications reported, culminating in 360 mM as the highest product concentration so far. A particularly attractive feature of peroxygenases is that they can be applied under non-aqueous reaction conditions, thereby circumventing the low solubility issue of many reagents of interest in aqueous media.[12–16] Nevertheless, in both cases significant improvements in final product titres are mandatory. Fortunately, the tools (such as multi-phase reactions and other non-conventional reaction media) principally exist[17,18] and are waiting to be implemented more in biocatalytic oxy-functionalisation chemistry.

High catalyst turnover numbers (i.e. number of catalytic cycles) are desirable from an economic point-of-view to minimise the cost contribution and environmental impact of the catalyst on the final product (Figure 2B). According to Woodley *et al.*[19] a minimal turnover number for an enzyme (produced on a large scale) of roughly 3,000, 20,000 and 1,000,000 can be estimated to achieve acceptable cost contributions for pharmaceuticals, fine chemicals and bulk chemicals, respectively (Figure 2B). Furthermore, it should be kept in mind that the catalyst preparation causes environmental impact by consuming resources and energy.[20,21] As shown in Figure 2D, the majority of both, P450 monooxygenase- and peroxygenase TNs fall more into the range of pharma- and fine-chemicals. Again, however, only with peroxygenases higher TNs approaching those required for the synthesis of bulk chemicals have been reported yet.
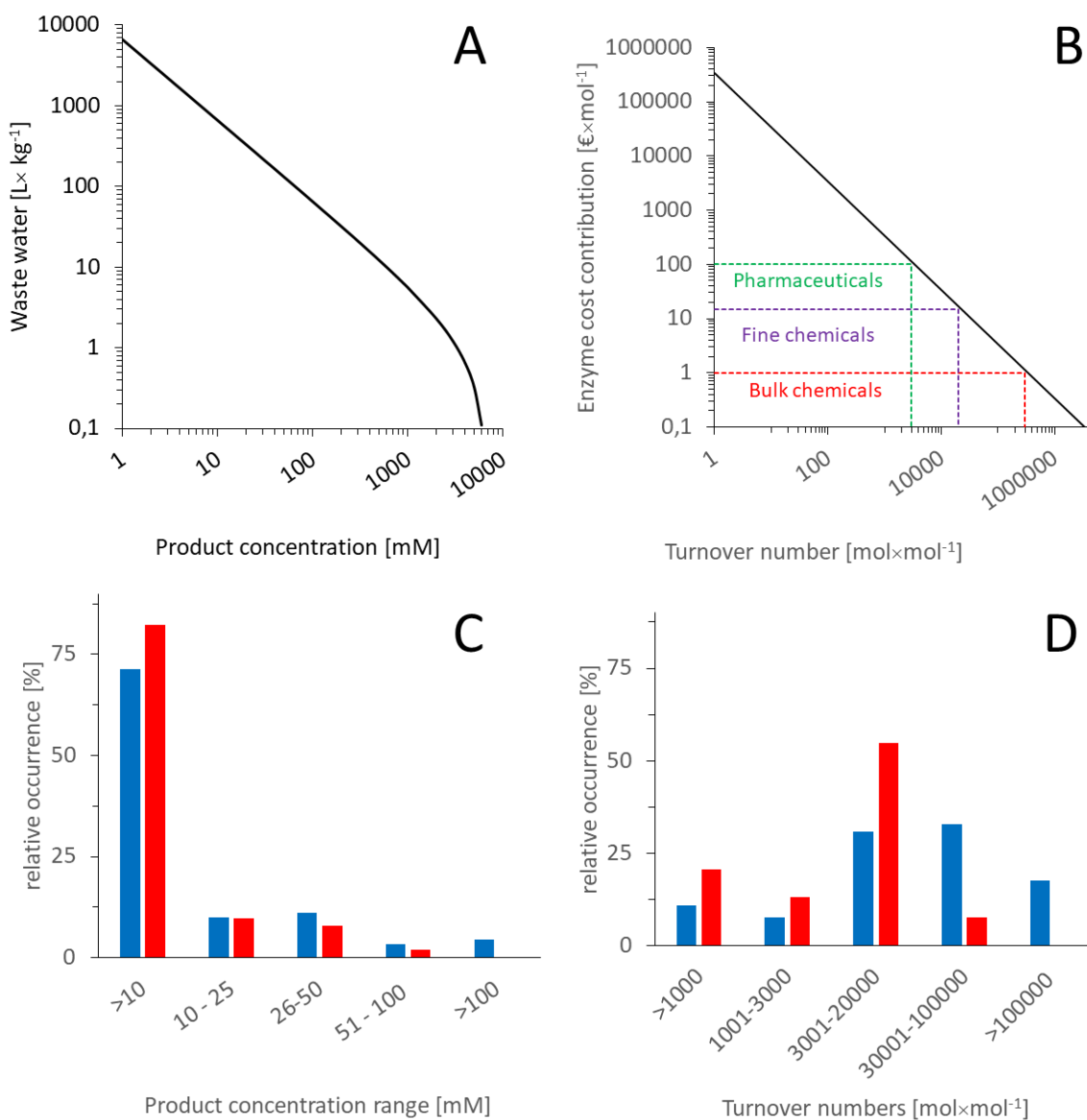
Figure 1. Performance indicators for biocatalytic oxyfunctionalisation reactions. A: Solvent (water) wastes generated with varying product concentrations; B: Influence of biocatalyst TN on its contribution to the final product (assumptions made: M_W(Enzyme) = 50 kDa, Enzyme price: 1000 € kg^{-1}, M_W(Product) = 150 g mol^{-1}); C and D: results of a literature analysis covering 91 peroxygenase reactions and 53 P450 monooxygenase reactions.

Substrate scope/engineering and recombinant expression

Today, a variety of different P450s and variants thereof are known and available for organic chemist.[22,23] Currently, online databases include more than 300,000 P450 se-

quences from all parts of the tree of life underlining the enormous diversity of P450 bio-catalysts.[24] Furthermore, enzyme engineering has proven an efficient tool to tailor P450 monooxygenases to the substrate scope-, selectivity- or stability needs of organic chemists.[22,25] Scheme 2 gives some examples of engineered P450 BM3 to selectively hydroxylate complex starting materials at user-defined positions, thereby overcoming its natural selectivity.[26]
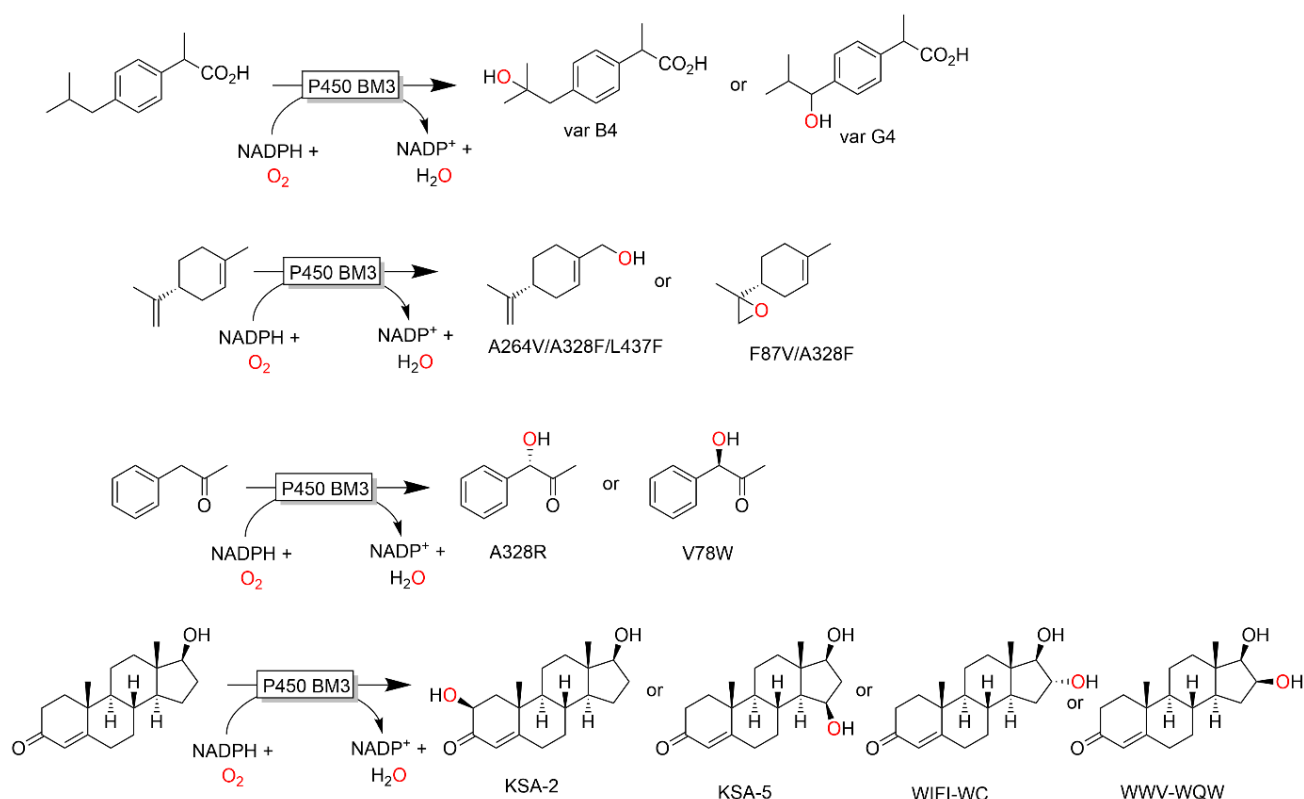
Scheme 2. Selected examples of tailored P450 (BM3) selectivity achieved via enzyme engineering.[26] hydroxylation of a) ibuprofen,[27] b) limonene,[28,29] c) phenylacetone,[30] d) testosterone.[31,32]

With peroxygenases we currently cannot access such a wealth of diversity. Though principally thousands of putative peroxygenase genes have been identified[33], only a handful of them have so far been functionally expressed and initially characterised.[6] Future characterisation studies will reveal whether peroxygenases are competitive in covering the broad substrate spectrum and diverse product selectivities of P450 enzymes.

Currently, the chemical space of selective oxyfunctionalisation accessible via P450 monooxygenases is enormous and approaches truly rational design. Compared to this, peroxygenase-catalysis still largely relies on wild-type enzymes, limiting their synthetic applicability.

Recombinant expression systems are crucial for both, cost-efficient production of biocatalysts and their engineering. Especially prokaryotic P450 monooxygenases can nowadays be expressed in simple bacterial expression systems such as *Escherichia coli*, putting the basis for mutant libraries and large-scale production.[5,34] Comparable, robust and simple expression systems for peroxygenases are still lacking today, which complicates the functional expression of larger libraries.[6,35,36] The enzyme titres achievable for both heme enzymes are in the range of 0.5-7.5 μmol L^{-1} (corresponding to approx. 25-375 mg L^{-1}),[35–37] which, compared to typical enzyme yield achievable with recombinant *E. coli* systems (often significantly above 5-10 g L^{-1}) leaves room for improvement. Nevertheless, *E. coli*-based expression systems appear more favourable for enzyme production than *Pichia* simply for the dramatically reduced fermentation times (2-3 days compared to ca. 2 weeks).

Cosubstrates/Coproducts

As redox reactions, oxyfunctionalisation reactions require stoichiometric cosubstrates. P450 monooxygenases require molecular oxygen and reducing equivalents for their catalytic mechanism whereas peroxygenases rely on hydrogen peroxide or organic hydroperoxides (Scheme 1). Envisioning larger scale applications of either enzyme class, the cosubstrate/coproduct selection has a significant impact on the economics and environmental footprint of the process.

In case of P450 monooxygenases, glucose is a popular sacrificial electron donor because the corresponding regeneration enzyme is very active, easy to express and recycles both NAD and NADP cofactors.[38] Issues related to this approach however are: low atom efficiency as only one out of the six available carbon atoms is actually oxidised, glucose being

edible and the high viscosity of aqueous solutions containing high concentrations of glucose. Therefore, the large-scale applicability of glucose dehydrogenase is questionable. A few other relevant cosubstrates are listed in Table 1. Overall, a broad range of practical *in situ* NAD(P)H regeneration systems are available today. They enable lab-scale applications of P450 monooxygenases and industrial applications for the synthesis of fine chemicals and active pharmaceutical intermediates but show little potential for larger scale implementation for cost and waste reasons.

To promote peroxygenase reactions, stoichiometric supply with H_2O_2 or organic hydroperoxides is needed. As H_2O_2 also inactivates the enzymes either controlled dosage or *in situ* generation of H_2O_2 via O_2 reduction is generally applied (Table 1).[39]

Table 1. Examples for P450 monooxygenase- and peroxygenase- *in situ* regeneration systems.

Coproduct[ox] ← / → NAD(P)H ⌒ / ⌐ Sub-H + O_2

Dehydrogenase   Monooxygenase

Cosubstrate[red] ⌐ / ⌐ NAD(P)+ ← / → Prod-O + H_2O

Cosubstrate / coproduct	Dehydrogenase	Waste [g mol^{-1}$_{NAD(P)H}$]	refs
Glucose / Gluconolactone	GDH[a]	176	40–43
Formic acid / CO_2	FDH[a]	44	44,45
Isopropanol / Acetone	ADH[a]	58	46
H_2 / H+	Hase[a]	-	47,48

Coproduct[ox] ← / → H_2O_2 ⌒ / ⌐ Sub-H

Catalyst   Peroxygenase

Cosubstrate[red] ⌐ / ⌐ O_2 H_2O → Prod-OH

Cosubstrate / coproduct	Catalyst / energy source	Waste [g mol^{-1}$_{H_2O_2}$]	ref
MeOH / CO_2	AlcOx, FDM, FDH, NAD, FMN / hν[a] FOx[a]	14.7	49,50
H_2O / O_2	TiO_2/ hν	32 (O_2)	51
	- / plasma		52
	- / ^{60}Co or ^{238}U		53
	Bi_2Te_3 / heat		54
	BiOCl / ultrasound		55
e$^-$ / 'none'	Cathode	'none'[b]	56–59
H_2 / H+	Hase[a]	-	60

[a] GDH: glucose dehydrogenase, FDH: formate dehydrogenase, ADH: alcohol dehydrogenase, Hase: hydrogenase, AlcOx: alcohol oxidase, FDM: formaldehyde dismutase, NAD: nicotinamide adenine dinucleotide; FMN: flavin mononucleotide; [b] depending on the CO_2 footprint of the electricity used.

As mentioned above, large-scale applications of monooxygenases or peroxygenases have to rely on readily available, easy to handle, cost-effective and low waste-generating energy sources to promote the biocatalytic oxyfunctionalisation reaction. Electrochemical regeneration using emission-free electrical power would represent an environmentally attractive solution to the 'regeneration issue'. First trials were reported in the late 1990s by Vilkner and coworkers.[61] Unfortunately, ever since then there has not been fundamental improvements in the productivity and robustness of direct or indirect electrochemical regeneration of P450 monooxygenases. Possibly the direct cathodic reduction of O_2 (another embodiment of the *Oxygen Dilemma*) poses too large technical hurdles to be solved at more than a proof-of-concept level. In contrast, this direct cathodic O_2 reduction to H_2O_2 offers, in case of peroxygenases, a promising approach for scalable and robust reaction schemes.[56,59]

Hydrogen represents another promising, waste-free cosubstrate. With the advent of O_2-tolerant hydrogenases[62] now also H_2-driven P450 monooxygenase[47,48] and peroxygenase-driven[60] oxyfunctionalisation reactions are coming into reach. This approach, however, is still in its infancy and necessitates further development to be able to judge its practicability.

Finally, water-derived reducing equivalents would be an elegant method to regenerate P450 monooxygenases and peroxygenases. The thermodynamic and kinetic inertness of water oxidation, however, necessitates external energy sources and catalysts. In case of monooxygenases, natural photosynthesis appears to be the most promising route *en route* to a water-driven oxyfunctionalisation chemistry.[63–66] The energy repertoire for *in situ* H_2O_2 generation from water and O_2 to drive peroxygenases is somewhat broader ranging from visible light[51,67,68] via γ-radiation (e.g. from nuclear waste),[53] cold plasma[52] to waste-heat.[54] Also wastes such as microplastics or lignin can serve as alternative electron donors.[69] Again, the early stage of development of the aforementioned approaches makes it difficult to predict if they are applicable on large-scale.

Conclusions and outlook

P450 monooxygenases and peroxygenases bear an enormous potential for selective chemical oxyfunctionalisation chemistry. Both enzyme classes exhibit specific advantages and disadvantages over the other.

Practical application of peroxygenases is much simpler than that of P450 monooxygenases as complex and vulnerable regeneration systems can be avoided simply by adding H_2O_2 (or organic hydroperoxides) or utilising one of the various *in situ* H_2O_2 generation systems. As a consequence, turnover numbers reachable with peroxygenase-catalysts appear to exceed those of P450 monooxygenases, which gives the first an advantage in terms of cost-contribution of the enzyme catalyst to the final product. Also the application of peroxygenases in non-aqueous reaction systems appears more straightforward (yet), which is important to reduce solvent wastes and increase the productivity of the reactions.

P450 monooxygenases, on the other hand, excel in terms of recombinant expression and ease of setting-up larger mutant libraries. As a consequence, many P450 monooxygenase mutants with tailored selectivity are available whereas this number is much smaller in case of peroxygenases. Overall, right now, it is not possible to define a 'clearly more promising' enzyme class.

UPO-catalyzed hydroxylation of ethylbenzene could only produce (*R*)-phenylethanol, this was not sufficient. This motivated us to find a way to produce (*R*) and (*S*)-phenylethanol at the same time. **Chapter 3** demonstrates the details.

The reactions that can be catalysed by UPO are mainly related to the oxidation of C-H bonds. Arnold *et al.* used P450 to catalyse the oxidation of Si-H motivated us to consider whether UPO could also be applied to the oxidation of Si-H bonds, as described in **Chapter 4.**

2.2 Vanadium-dependent haloperoxidases

Vanadium-dependent enzymes have a different active site structure as heme enzymes, which can protect them from the oxidative inactivation by H_2O_2.[70–75] Vanadium-dependent

haloperoxidases (VCPOs) are quite stable. It can maintain activity in organic solvents for several weeks.[71,72] Its thermal stability is very high, with VCPO from *Curvularia inaequalis* reaching a denaturation midpoint temperature of 90 °C. Moreover, their stability to H_2O_2 is also impressive, as they can withstand up to 0.5 M H_2O_2.[75]
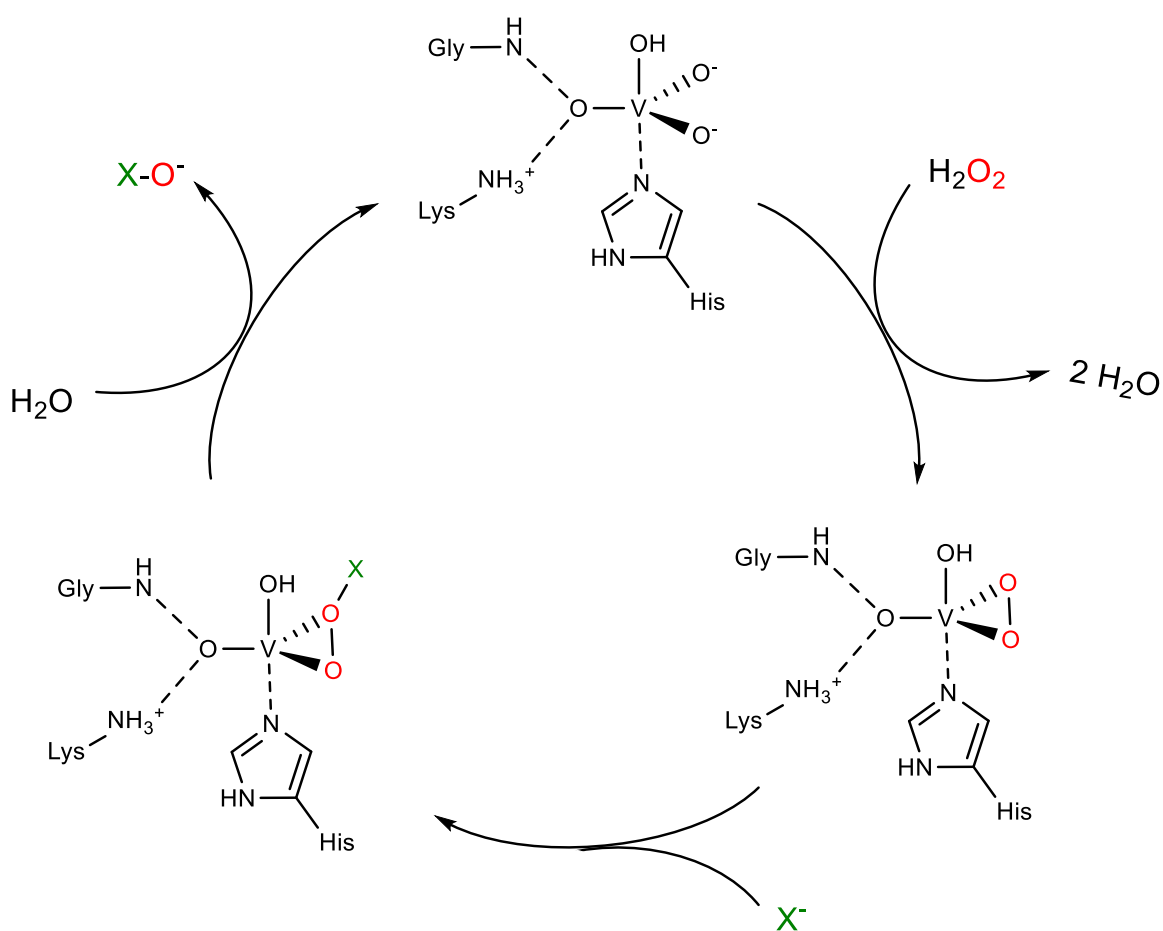

Figure 3. Simplified halide oxidation mechanisms of haloperoxidases.[76]

The catalytic mechanism of vanadate-dependent haloperoxidases (VCPO) is that the enzyme oxidises halogen ions (X^-) to their corresponding hypohalous acids in the presence of H_2O_2, after that hypohalites usually diffuse freely into the reaction system and react with the substrate, that means the subsequent halogenation reaction is not related to the enzyme (Figure 3). Therefore, the major shortcoming of using this enzyme for halogenation is lack of regio- or regio- or stereoselectivity.

$$H_2O_2 + X^- \longrightarrow \boxed{CiVCPO} \longrightarrow H_2O + OX^-$$

Halogenation of activated arenes

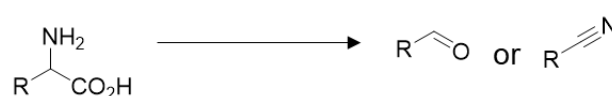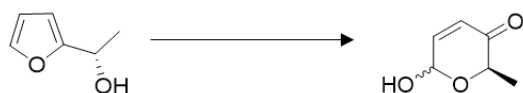Halocyclisation reactions

Halohydroxylation of alkenes

Oxidative decarboxylation

Achmatowicz reaction

Scheme 3. Selected reactions performed by CiVCPO.[76]

In recent years, a certain amount of reactions have been developed using CiVCPO.[72,77–80] However, research in this area is still in its early stages. The reported reactions are generally limited to a low substrate loading (≤5 mM). This was motivated us to develop a approach for higher substrate loading and scale-up preparation in **Chapter 5**.

2.3 Enzymatic driven H₂O₂ generation system.

Peroxygenases are effective biocatalysts towards the selective oxyfunctionalisation.[7,81] Its high catalytic activity and the ease-of-use are difficult to be replaced by chemical catalysts. However, in an excess of H_2O_2, peroxygenases will be inactivated.[82] The H_2O_2 system generate a catalytically effective amount of hydrogen peroxide, this mild H_2O_2 addition way can effectively reduce the inactivation of peroxygenase.[52,57] A wide range of H_2O_2 generation systems have been set up, including biocatalysis,[83,84] photochemistry,[68,85]

electrochemistry[54,86] and heterogeneous catalysis[87] methods. Of these, biocatalysis offers certain advantages with regard to environmental issues.

Table 2. Some enzymatic driven H_2O_2 generation system

H_2O_2 enzyme	Substrate	By-product	Peroxygenase, substrate	TTN	Ref
GDH	glucose	gluconolactone	*Cf*CPO, thianosole	TTN$_{CfCPO}$: 250000	[88]
*Pp*AOx	methanol	formaldehyde	*Aae*UPO, ethylbenzene	TTN$_{AaeUPO}$: 100000	[50]
SO	sulfite	sulfate	*Aae*UPO, ethylbenzene	TTN$_{SO}$: 77000 TTN$_{AaeUPO}$: 30800	[84]
*An*ChOx	choline chloride	betaine	*Aae*UPO, thianosole	TTN$_{AnChOx}$: 2100 TTN$_{AaeUPO}$: 150000	[89]

Some typical examples are shown in Table 2, these enzymes produce more or less by-products, which have a certain influence on the reaction system. Recently it has been reported that formic oxidase from *Aspergillus oryzae*, which could oxidise formate to CO_2 and H_2O_2, seems to be a very clean H_2O_2 generating system.[83] Our motivation was to study the system for further development, as shown in **Chapter 6.**

In this thesis, four systems related to *Aae*UPO, *Ci*VCPO and *Ao*FOx have been developed and studied. The goal was to provide more application possibilities for enzymatic selective oxyfunctionalisation.

Reference

1. T. K. Hyster, *Synlett* **2020**, *31*, 223.

2. R. De Regil, G. Sandoval, *Biomolecules* **2013**, *3*, 812.

3. L. M. Blank, B. E. Ebert, K. Buehler, B. Bühler, *Antioxid. Redox Signal.* **2010**, *13*, 349.

4. E. Roduner, W. Kaim, B. Sarkar, V. B. Urlacher, J. Pleiss, R. Gläser, W. D. Einicke, G. A. Sprenger, U. Beifuß, E. Klemm, C. Liebner, H. Hieronymus, S. F. Hsu, B. Plietker, S. Laschat, *ChemCatChem* **2013**, *5*, 82.

5. V. B. Urlacher, M. Girhard, *Trends Biotechnol.* **2012**, *30*, 26.

6. A. Beltrán-Nogal, I. Sánchez-Moreno, D. Méndez-Sánchez, P. Gómez de Santos, F. Hollmann, M. Alcalde, *Curr. Opin. Struct. Biol.* **2022**, *73*, 102342.

7. M. Hobisch, D. Holtmann, P. Gomez de Santos, M. Alcalde, F. Hollmann, S. Kara, *New Trends Ind. Biocatal.* **2021**, *51*, 107615.

8. F. Hannemann, A. Bichet, K. M. Ewen, R. Bernhardt, *Biochim. Biophys. Acta BBA - Gen. Subj.* **2007**, *1770*, 330.

9. D. Holtmann, F. Hollmann, *ChemBioChem* **2016**, *17*, 1391.

10. W. Lu, J. E. Ness, W. Xie, X. Zhang, J. Minshull, R. A. Gross, *J. Am. Chem. Soc.* **2010**, *132*, 15451.

11. I. Kaluzna, T. Schmitges, H. Straatman, D. van Tegelen, M. Müller, M. Schürmann, D. Mink, *Org. Process Res. Dev.* **2016**, *20*, 814.

12. F. E. H. Nintzel, Y. Wu, M. Planchestainer, M. Held, M. Alcalde, F. Hollmann, *Chem. Commun.* **2021**, *57*, 5766.

13. M. Hobisch, M. M. C. H. van Schie, J. Kim, K. Røjkjær Andersen, M. Alcalde, R. Kourist, C. B. Park, F. Hollmann, S. Kara, *ChemCatChem* **2020**, *12*, 4009.

14. M. C. R. Rauch, F. Tieves, C. E. Paul, I. W. C. E. Arends, M. Alcalde, F. Hollmann, *ChemCatChem* **2019**, *11*, 4519.

15. J. S. Dordick, M. A. Marletta, A. M. Klibanov, *Proc. Natl. Acad. Sci.* **1986**, *83*, 6255.

16. A. Zaks, A. M. Klibanov, *Science* **1984**, *224*, 1249.

17. M. M. C. H. van Schie, J. D. Spöring, M. Bocola, P. D. de María, D. Rother, *Green Chem.* **2021**, *23*, 3191.

18. B. O. Burek, A. W. H. Dawood, F. Hollmann, A. Liese, D. Holtmann, *Front. Catal.* **2022**, *2*.

19. P. Tufvesson, J. Lima-Ramos, M. Nordblad, J. M. Woodley, *Org. Process Res. Dev.* **2011**, *15*, 266.

20. F. Tieves, F. Tonin, E. Fernández-Fueyo, J. M. Robbins, B. Bommarius, A. S. Bommarius, M. Alcalde, F. Hollmann, *Tetrahedron* **2019**, *75*, 1311.

21. Y. Ni, D. Holtmann, F. Hollmann, *ChemCatChem* **2014**, *6*, 930.

22. G.-D. Roiban, M. T. Reetz, *Chem. Commun.* **2015**, *51*, 2208.

23. N. D. Fessner, *ChemCatChem* **2019**, *11*, 2226.

24. D. R. Nelson, *Biochim. Biophys. Acta BBA - Proteins Proteomics* **2018**, *1866*, 141.

25. S. N. Charlton, M. A. Hayes, *ChemMedChem* **2022**, *17*, e202200115.

26. H. Alwaseem, R. Fasan, in *Protein Engineering*, John Wiley & Sons, Ltd, **2021**, pp. 207–242.

27. A. Rentmeister, T. R. Brown, C. D. Snow, M. N. Carbone, F. H. Arnold, *ChemCatChem* **2011**, *3*, 1065.

28. A. Seifert, M. Antonovici, B. Hauer, J. Pleiss, *ChemBioChem* **2011**, *12*, 1346.

29. A. Seifert, S. Vomund, K. Grohmann, S. Kriening, V. B. Urlacher, S. Laschat, J. Pleiss, *ChemBioChem* **2009**, *10*, 853.

30. R. Agudo, G. D. Roiban, R. Lonsdale, A. Ilie, M. T. Reetz, *J. Org. Chem.* **2015**, *80*, 950.

31. C. G. Acevedo-Rocha, A. Li, L. D'Amore, S. Hoebenreich, J. Sanchis, P. Lubrano, M. P. Ferla, M. Garcia-Borràs, S. Osuna, M. T. Reetz, *Nat. Commun.* **2021**, *12*, 1621.

32. A. Li, C. G. Acevedo-Rocha, L. D'Amore, J. Chen, Y. Peng, M. Garcia-Borràs, C. Gao, J. Zhu, H. Rickerby, S. Osuna, J. Zhou, M. T. Reetz, *Angew. Chem.* **2020**, *132*, 12599.

33. M. Faiza, S. Huang, D. Lan, Y. Wang, *BMC Evol. Biol.* **2019**, *19*, 76.

34. S. Pflug, S. M. Richter, V. B. Urlacher, *J. Biotechnol.* **2007**, *129*, 481.

35. P. Gomez de Santos, M. D. Hoang, J. Kiebist, H. Kellner, R. Ullrich, K. Scheibner, M. Hofrichter, C. Liers, M. Alcalde, *Appl. Environ. Microbiol.* **2021**, *87*, e00878.

36. P. Molina-Espeja, S. Ma, D. M. Mate, R. Ludwig, M. Alcalde, *Enzyme Microb. Technol.* **2015**, *73–74*, 29.

37. J. Hausjell, H. Halbwirth, O. Spadiut, *Biosci. Rep.* **2018**, *38*, BSR20171290.

38. J. C. Moore, D. J. Pollard, B. Kosjek, P. N. Devine, *Acc. Chem. Res.* **2007**, *40*, 1412.

39. B. O. Burek, S. Bormann, F. Hollmann, J. Z. Bloh, D. Holtmann, *Green Chem.* **2019**, *21*, 3232.

40. S. Staudt, C. A. Müller, J. Marienhagen, C. Böing, S. Buchholz, U. Schwaneberg, H. Gröger, *Beilstein J. Org. Chem.* **2012**, *8*, 186.

41. T. Pongtharangkul, P. Chuekitkumchorn, N. Suwanampa, P. Payongsri, K. Honda, W. Panbangred, *AMB Express* **2015**, *5*, 68.

42. J. Brummund, M. Müller, T. Schmitges, I. Kaluzna, D. Mink, L. Hilterhaus, A. Liese, *J. Biotechnol.* **2016**, *233*, 143.

43. H. Wang, Y. Zheng, F. Chen, J. Xu, H. Yu, *ChemCatChem* **2020**, *12*, 2077.

44. H. Park, G. Park, W. Jeon, J.-O. Ahn, Y.-H. Yang, K.-Y. Choi, *Biotechnol. Adv.* **2020**, *40*, 107504.

45. M. L. Corrado, T. Knaus, F. G. Mutti, *ChemBioChem* **2018**, *19*, 679.

46. T. Hilberath, A. Raffaele, L. M. Windeln, V. B. Urlacher, *AMB Express* **2021**, *11*, 162.

47. T. H. Lonsdale, L. Lauterbach, S. H. Malca, B. M. Nestl, B. Hauer, O. Lenz, *Chem. Commun.* **2015**, *51*, 16173.

48. J. Preissler, H. A. Reeve, T. Zhu, J. Nicholson, K. Urata, L. Lauterbach, L. L. Wong, K. A. Vincent, O. Lenz, *ChemCatChem* **2020**, *12*, 4853.

49. S. J. P. Willot, M. D. Hoang, C. E. Paul, M. Alcalde, I. W. C. E. Arends, A. S. Bommarius, B. Bommarius, F. Hollmann, *ChemCatChem* **2020**, *12*, 2713.

50. Y. Ni, E. Fernández-Fueyo, A. G. Baraibar, R. Ullrich, M. Hofrichter, H. Yanase, M. Alcalde, W. J. H. van Berkel, F. Hollmann, *Angew. Chem. Int. Ed.* **2016**, *55*, 798.

51. W. Zhang, E. Fernández-Fueyo, Y. Ni, M. van Schie, J. Gacs, R. Renirie, R. Wever, F. G. Mutti, D. Rother, M. Alcalde, F. Hollmann, *Nat. Catal.* **2018**, *1*, 55.

52. A. Yayci, Á. G. Baraibar, M. Krewing, E. F. Fueyo, F. Hollmann, M. Alcalde, R. Kourist, J. E. Bandow, *ChemSusChem* **2020**, *13*, 2072.

53. W. Zhang, H. Liu, M. M. C. H. van Schie, P. L. Hagedoorn, M. Alcalde, A. G. Denkova, K. Djanashvili, F. Hollmann, *ACS Catal.* **2020**, *10*, 14195.

54. J. Yoon, H. Jang, M. W. Oh, T. Hilberath, F. Hollmann, Y. S. Jung, C. B. Park, *Nat. Commun.* **2022**, *13*, 3741.

55. J. Yoon, J. Kim, F. Tieves, W. Zhang, M. Alcalde, F. Hollmann, C. B. Park, *ACS Catal.* **2020**, *10*, 5236.

56. S. Bormann, D. Hertweck, S. Schneider, J. Z. Bloh, R. Ulber, A. C. Spiess, D. Holtmann, *Biotechnol. Bioeng.* **2021**, *118*, 7.

57. S. Bormann, M. M. C. H. van Schie, T. P. De Almeida, W. Zhang, M. Stöckl, R. Ulber, F. Hollmann, D. Holtmann, *ChemSusChem* **2019**, *12*, 4759.

58. L. Getrey, T. Krieg, F. Hollmann, J. Schrader, D. Holtmann, *Green Chem* **2014**, *16*, 1104.

59. C. Kohlmann, S. Lütz, *Eng. Life Sci.* **2006**, *6*, 170.

60. A. Al-Shameri, S. J. P. Willot, C. E. Paul, F. Hollmann, L. Lauterbach, *Chem. Commun.* **2020**, *56*, 9667.

61. V. Reipa, M. P. Mayhew, V. L. Vilker, *Proc. Natl. Acad. Sci.* **1997**, *94*, 13554.

62. L. Lauterbach, O. Lenz, *J. Am. Chem. Soc.* **2013**, *135*, 17897.

63. V. Jurkaš, F. Weissensteiner, P. De Santis, S. Vrabl, F. A. Sorgenfrei, S. Bierbaumer, S. Kara, R. Kourist, P. P. Wangikar, C. K. Winkler, W. Kroutil, *Angew. Chem. Int. Ed.* **2022**, *n/a*, e202207971.

64. A. Hoschek, B. Bühler, A. Schmid, *Angew. Chem.* **2017**, *129*, 15343.

65. E. Erdem, L. Malihan-Yap, L. Assil-Companioni, H. Grimm, G. D. Barone, C. Serveau-Avesque, A. Amouric, K. Duquesne, V. de Berardinis, Y. Allahverdiyeva, V. Alphand, R. Kourist, *ACS Catal.* **2022**, *12*, 66.

66. A. Tüllinghoff, M. B. Uhl, F. E. H. Nintzel, A. Schmid, B. Bühler, J. Toepel, *Front. Catal.* **2022**, *1*.

67. D. I. Perez, M. M. Grau, I. W. C. E. Arends, F. Hollmann, *Chem. Commun.* **2009**, 6848.

68. L. Schmermund, S. Reischauer, S. Bierbaumer, C. K. Winkler, A. Diaz-Rodriguez, L. J. Edwards, S. Kara, T. Mielke, J. Cartwright, G. Grogan, B. Pieber, W. Kroutil, *Angew. Chem. Int. Ed.* **2021**, *60*, 6965.

69. J. Kim, T. V. T. Nguyen, Y. H. Kim, F. Hollmann, C. B. Park, *Nat. Synth.* **2022**, *1*, 217.

70. R. Wever, R. Renirie, F. Hollmann, in *Vanadium Catalysis*, **2020**, pp. 548–563.

71. J. W. P. M. Van Schijndel, P. Barnett, J. Roelse, E. G. M. Vollenbroek, R. Wever, *Eur. J. Biochem.* **1994**, *225*, 151.

72. E. Fernández-Fueyo, M. van Wingerden, R. Renirie, R. Wever, Y. Ni, D. Holtmann, F. Hollmann, *ChemCatChem* **2015**, *7*, 4035.

73. R. Renirie, C. Pierlot, R. Wever, J. M. Aubry, *J. Mol. Catal. B Enzym.* **2009**, *56*, 259.

74. N. Tanaka, V. Dumay, Q. Liao, A. J. Lange, R. Wever, *Eur. J. Biochem.* **2002**, *269*, 2162.

75. R. Renirie, C. Pierlot, J. M. Aubry, A. F. Hartog, H. E. Schoemaker, P. L. Alsters, R. Wever, *Adv. Synth. Catal.* **2003**, *345*, 849.

76. G. T. Höfler, A. But, F. Hollmann, *Org. Biomol. Chem.* **2019**, *17*, 9267.

77. J. W. P. M. van Schijndel, E. G. M. Vollenbroek, R. Wever, *Biochim. Biophys. Acta BBA - Protein Struct. Mol. Enzymol.* **1993**, *1161*, 249.

78. J. J. Dong, E. Fernández-Fueyo, J. Li, Z. Guo, R. Renirie, R. Wever, F. Hollmann, *Chem. Commun.* **2017**, *53*, 6207.

79. G. T. Höfler, A. But, S. H. H. Younes, R. Wever, C. E. Paul, I. W. C. E. Arends, F. Hollmann, *ACS Sustain. Chem. Eng.* **2020**, *8*, 2602.

80. X. Xu, A. But, R. Wever, F. Hollmann, *ChemCatChem* **2020**, *12*, 2180.

81. Y. Wang, D. Lan, R. Durrani, F. Hollmann, *Curr. Opin. Chem. Biol.* **2017**, *37*, 1.

82. M. Ayala, C. V. Batista, R. Vazquez-Duhalt, *JBIC J. Biol. Inorg. Chem.* **2011**, *16*, 63.

83. F. Tieves, S. J. P. Willot, M. M. C. H. van Schie, M. C. R. Rauch, S. H. H. Younes, W. Zhang, J. Dong, P. Gomez de Santos, J. M. Robbins, B. Bommarius, M. Alcalde, A. S. Bommarius, F. Hollmann, *Angew. Chem. Int. Ed.* **2019**, *58*, 7873.

84. M. M. C. H. van Schie, A. T. Kaczmarek, F. Tieves, P. Gomez de Santos, C. E. Paul, I. W. C. E. Arends, M. Alcalde, G. Schwarz, F. Hollmann, *ChemCatChem* **2020**, *12*, 3186.

85. S. J. P. Willot, E. Fernández-Fueyo, F. Tieves, M. Pesic, M. Alcalde, I. W. C. E. Arends, C. B. Park, F. Hollmann, *ACS Catal.* **2019**, *9*, 890.

86. D. Holtmann, T. Krieg, L. Getrey, J. Schrader, *Catal. Commun.* **2014**, *51*, 82.

87. S. J. Freakley, S. Kochius, J. van Marwijk, C. Fenner, R. J. Lewis, K. Baldenius, S. S. Marais, D. J. Opperman, S. T. L. Harrison, M. Alcalde, M. S. Smit, G. J. Hutchings, *Nat. Commun.* **2019**, *10*, 4178.

88. P. C. Pereira, I. W. C. E. Arends, R. A. Sheldon, *Process Biochem.* **2015**, *50*, 746.

89. Y. Li, Y. Ma, P. Li, X. Zhang, D. Ribitsch, M. Alcalde, F. Hollmann, Y. Wang, *ChemPlusChem* **2020**, *85*, 254.

3

A Peroxygenase–Alcohol dehydrogenase cascade reaction to transform ethylbenzene derivatives into enantioenriched phenylethanols

In this study, we developed a new bienzymatic reaction to produce enantioenriched phenylethanols. In a first step, the recombinant, unspecific peroxygenase from *Agrocybe aegerita* (r*Aae*UPO) was used to oxidise ethylbenzene and its derivatives to the corresponding ketones (prochiral intermediates) followed by enantioselective reduction into the desired (*R*)- or (*S*)- phenylethanols using the (*R*)-selective alcohol dehydrogenase (ADH) from *Lactobacillus kefir* (*Lk*ADH) or the (*S*)-selective ADH from *Rhodococcus ruber* (ADH-A). In a one-pot two-step cascade, 11 ethylbenzene derivatives were converted into the corresponding chiral alcohols at acceptable yields and often excellent enantioselectivity.

This chapter is based on

Xiaomin Xu, Hugo Brasselet, Ewald Jongkind, Miguel Alcalde, Caroline E. Paul and Frank Hollmann

3.1 Introduction

Oxyfunctionalisation reactions (i.e. the insertion of O-atoms into C-H-, C=C-bonds) represent a central theme in organic synthesis and particularly in the manufacture of pharmaceutically active ingredients[1] and the quest for efficient (economically viable and environmentally acceptable) syntheses continues. The synthesis of chiral 1-phenylethanol derivatives for example has been the focus of various research groups. Chiral, α-functionalised benzene derivatives are found in approximately 15% of the 2020 top selling small molecule drugs[2] and various synthetic routes such as the enantioselective reduction of prochiral acetophenone derivatives[3,4] or the (dynamic) kinetic resolution of racemic 1-phenylethanols[5–8] have been established. Envisioning ethylbenzene derivatives as starting materials (i.e. obtaining chiral 1-phenylethanols through selective benzylic hydroxylation), heme-dependent enzymes appear to be the catalysts of choice.[9,10] One shortcoming of current enzymatic enantioselective hydroxylation, however, is a lack of enantiocomplementary oxygenases, often limiting access to only one enantiomer. Inspired by recent contributions from the groups of Flitsch[11] and Kroutil[12] we envisioned a bienzymatic cascade to give access to both enantiomers of 1-phenylethanol and its derivatives. Particularly, we propose to combine peroxygenase-catalysed oxyfunctionalisation yielding prochiral ketones followed by enantioselective alcohol dehydrogenase-catalysed reduction to the corresponding alcohols. In particular, we used the recombinant, evolved peroxygenase from *Agrocybe aegerita* (r*Aae*UPO)[13–16] for the benzylic oxidation via (*R*)-1-phenylethanol (derivatives) to the acetophenones of interest. To catalyse the stereoselective ketoreduction reaction we used either the (*R*)-selective alcohol dehydrogenase from *Lactobacillus kefir* (*Lk*ADH)[17] or the (*S*)-selective alcohol dehydrogenase from *Rhodococcus ruber* (ADH-A) (Scheme 1).[18,19]
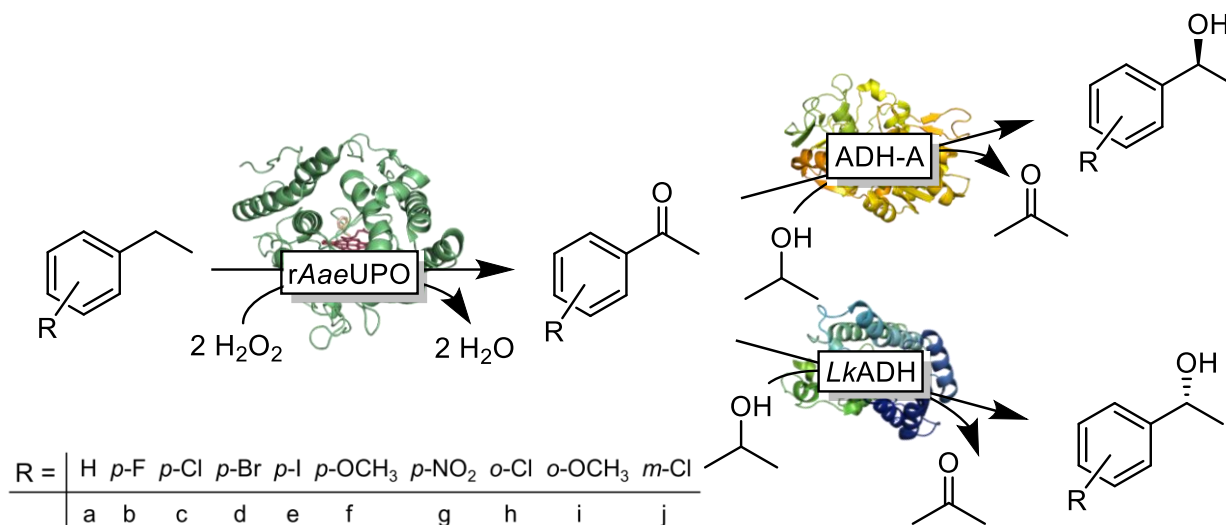
Scheme 1. Envisioned bienzymatic cascade to access both enantiomers of phenylethanols from non-functionalised ethylbenzenes. The first step comprises a peroxygenase from *Agrocybe aegerita*, r*Aae*UPO-catalysed double hydroxylation to the prochiral acetophenones followed by stereoselective reduction to (*R*)-phenylethanol (catalysed by the alcohol dehydrogenase from *Lactobacillus kefir*, *Lk*ADH) or to the (*S*)-alcohol (catalysed by the alcohol dehydrogenase from *Rhodococcus ruber*, ADH-A).
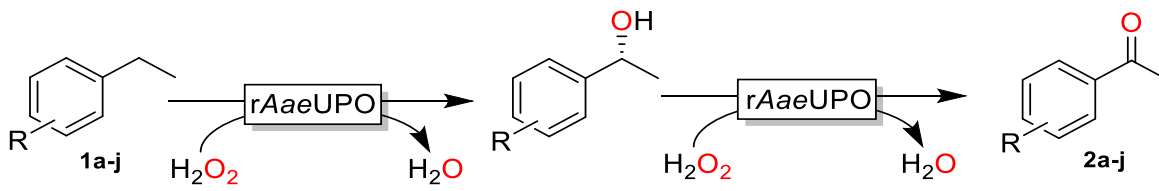
3.2 Results and Discussion

3.2.1 Selection of ethylbenzene derivatives converted by r*Aae*UPO.

In a first set of experiments we established the 'thorough oxidation' of various ethylbenzene derivatives to the corresponding acetophenone derivatives (Table 1). Expectedly, the first oxidation step proceeded highly enantioselectively yielding the (*R*)-phenylethanol derivative. Generally, the starting materials tested were smoothly converted into the corresponding ketone products with the exception of *p*-iodo- **1e** and *p*-methoxyethylbenzene **1f** (Table 1). In case of sluggish oxidation rates, increasing the r*Aae*UPO-concentration resulted in complete oxidation e.g. of *p*-iodoethylbenzene **1e** to the corresponding ketone product. Unfortunately, the mass balance was generally not closed, which can be attributed to either the experimental setup allowing for evaporation of the volatile reagents or the poor solubility of several reagents that led to quantification issue (see Supporting Information).

It should be mentioned that the reaction conditions chosen in these experiments, particularly the enzyme concentration and H_2O_2 feeding strategy have not been optimised neither

for space-time-yields nor for enzyme utilisation. However, already under these non-optimised conditions turnover numbers for the peroxygenase up to 42,300 (corresponding to approx.100 $g_{prod}×g_{rAaeUPO}^{-1}$) have been achieved.

Table 1. Selection of ethylbenzene derivatives converted by rAaeUPO.

Starting material	Starting material 1 [mM]	Alcohol [mM]	Ketone 2 [mM]
1a	0	0	35.8 ± 1.5
1b	0	0	41 ± 4.2
1c	0	0	46.4 ± 2.6
1d	0.4 ± 0.2	0.4 ± 0.4	42.3 ± 32.7
1e	20.3 ± 17.5	0.7 ± 0.1	18.5 ± 10.7
1e[a]	0	0	46.6 ± 4.5
1f	0	30.7 ± 4.0	11.5 ± 1.5
1g	0.5 ± 0.5	0	21.8 ± 1.9
1h	0.7 ± 0.7	2.2 ± 1.3	34.9 ± 3.1
1i	7.6 ± 3.8	7 ± 0.3	29.8 ± 0.9
1j	1.1 ± 0.2	2.1 ± 0.5	33.6 ± 1.1

Reaction conditions: [substrate **1**] = 50 mM, [rAaeUPO] = 2 µM, buffer: 50 mM KPi pH 7 containing 10% v/v acetonitrile, 25 °C, H_2O_2 dosing rate: 20 mM h^{-1}, reaction time: 6 h. Experiments were performed as duplicates. [a] [rAaeUPO] = 6 µM.

3.2.2 Enantioselective reduction of acetophenone

Next, we validated the possibility of enantioselective reduction of acetophenone with *Lk*ADH and ADH-A (Figure 1). For reasons of simplicity, we chose for a substrate-coupled NAD(P)H regeneration approach using isopropanol as sacrificial reductant.
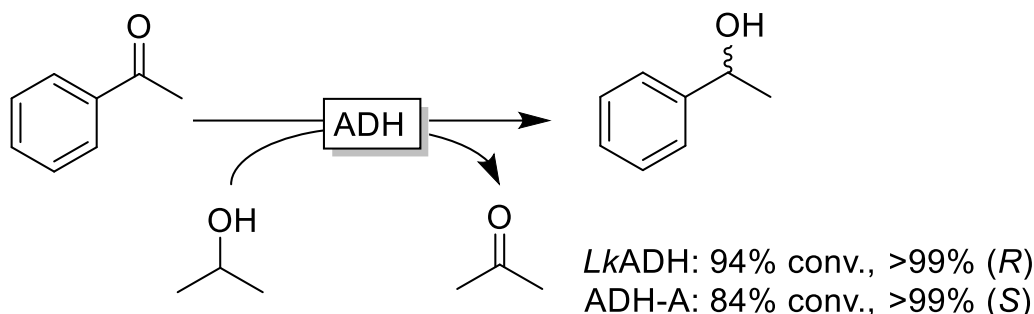

*Lk*ADH: 94% conv., >99% (*R*)
ADH-A: 84% conv., >99% (*S*)

Figure 1. Stereoselective reduction of acetophenone using two enantiocomplementary ADHs. Conditions: [acetophenone] = 15 mM, [NAD(P)H] = 0.1 mM, 10% v/v 2-propanol, [MgCl$_2$] = 2 mM, *Lk*ADH/ADH-A: 50 µL cell free extract or 20 mg lyophilised cells, 50 mM KPi buffer pH 7, 30 °C, 600 rpm, 24 h.

Having established the individual components of the envisioned cascade, we further combined both enzymatic steps in one pot. In a first try, we tested both enzymatic steps concurrently (one-pot one-step) using ethyl benzene as starting material. At first sight, the cascade was successful producing significant amounts of the desired phenylethanol (Table 2). However, a closer inspection of the optical purity of the alcohol products revealed a poor *ee* value of the (ADH-A-derived) (*S*)-phenylethanol **3a** of 19% *ee*. We observed a significant amount of r*Aae*UPO-derived (*R*)-phenylethanol had not been thoroughly oxidised to the ketone, thereby contaminating the ADH-A-derived (*S*)-enantiomer product. A plausible explanation for the decreased r*Aae*UPO-activity is the presence of isopropanol in the reaction, which competes with phenylethanol for r*Aae*UPO-catalysed oxidation thereby slowing down the oxidation steps of the cascade. Furthermore, the accumulating acetone decreases the thermodynamic driving force for the ADH-catalysed reduction step. Apparently, the oxidative and reductive partial steps are not compatible for a one-pot one-step procedure.

Table 2. Results from the one-pot one-step system.[a]

ADHs	Phenylethanol **3a** [mM]	*ee* [%]
*Lk*ADH	11.3 ± 0.1	98 (*R*)
ADH-A	15.1 ± 1.2	19 (*S*)

[a] Reaction conditions: [ethylbenzene **1a**] = 50 mM, [NAD(P)H] = 0.1 mM, 10% v/v 2-proponol, [MgCl$_2$] = 2 mM, [r*Aae*UPO] = 2 µM, *Lk*ADH or ADH-A = 50 µL cell-free extract, H$_2$O$_2$ dosing rate: 10 mM h^{-1} (10 h), 50 mM KPi buffer pH 7, 30 °C, 600 rpm. Data presented are averages of triplicate experiments.

3.2.3 One-pot two-step procedure

We therefore directed our attention to a one-pot two-step procedure, in which first the r*Aae*UPO-catalysed conversion of ethylbenzenes to the corresponding acetophenone derivatives occurs, followed by the ADH-catalysed reduction to the chiral alcohols. Concretely, in a first phase the r*Aae*UPO-catalysed ethylbenzene (50 mM) oxyfunctionalisation was conducted for 6 h with a H$_2$O$_2$-addition rate of 20 mMh^{-1}. This was followed by the addition of the ADH catalysts together with isopropanol (as sacrificial reductant) and incubation overnight. A first experiment combining r*Aae*UPO with ADH-A (Figure 2) gave promising results converting initial 55 mM of ethylbenzene into 1-phenylethanol (35.8 mM final concentration).
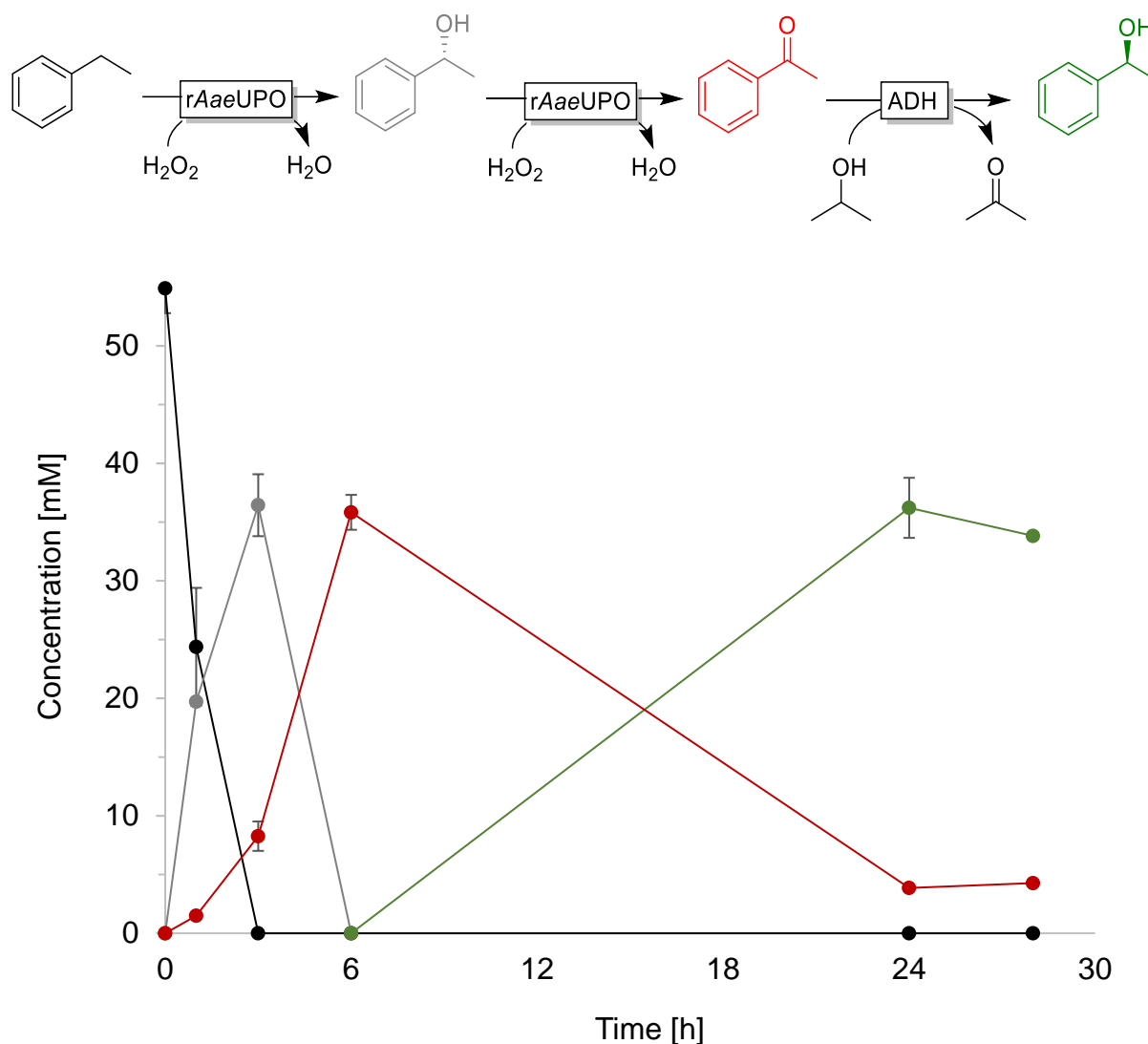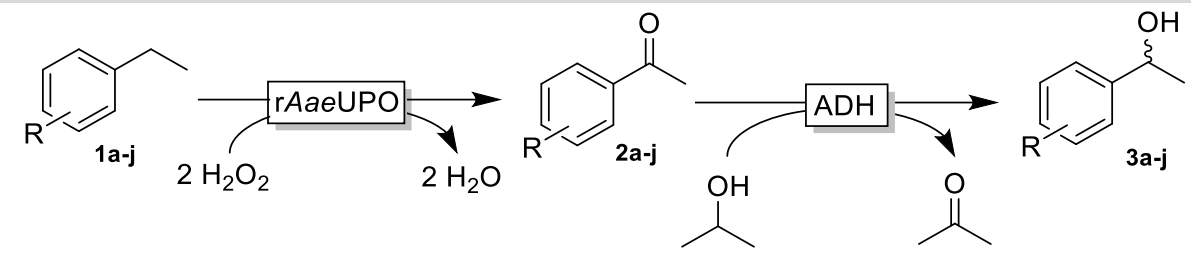
Figure 2. Representative time course of the bienzymatic one-pot two-step cascade converting ethylbenzene **1a** to (S)-phenylethanol **3a**. Reaction conditions: [ethylbenzene **1a**] = 50 mM, [rAaeUPO] = 2 μM, buffer: 50 mM KPi pH 7 containing 10% (v/v) of acetonitrile, 25 °C. The reaction was initiated by addition of H_2O_2 (20 mM h^{-1}), after 6 h H_2O_2 addition was stopped and the reaction mixture was supplemented with [NAD(P)H] = 0.1 mM, [MgCl$_2$] = 2 mM, 10% v/v 2-proponol, ADH-A (100 μL cell free extract) and incubated overnight. Experiments were performed as triplicates.

As this strategy proved to be successful, we further applied it for the conversion of the starting materials evaluated previous (*vide supra*). As shown in Table 3, the majority of ethylbenzene starting materials **1** was successfully converted into the corresponding (R)- or (S)-phenylethanols **3** at reasonable yields and generally good optical purities (Table 3). One notable exception was the o-methoxy derivate **1i** where in both cases low alcohol

Table 3. Results from the one-pot two-step conversion of ethylbenzene derivatives **1a–j** to the corre-
sponding phenylethanols **3a–j**.

Starting material	ADH-A		LkADH	
	Alcohol **3** [mM]	ee [%]	Alcohol **3** [mM]	ee [%]
1a	36.2 ± 2.6	>99 (S)	40.1 ± 1.0	>99 (R)
1b	38.6 ± 3.2	>99 (S)	36.7 ± 3.3	>99 (R)
1c	23.9 ± 11.5	98 (S)	34.0 ± 8.5	>99 (R)
1d	36.7 ± 0.6	>99 (S)	38.2 ± 0.8	>99 (R)
1e [a]	33.5 ± 6.7	>99 (S)	30.9 ± 1.2	>99 (R)
1f	37.9 ± 0.8	>99 (R)	37.6 ± 1.17	>99 (R)
1g	24.6 ± 4.8	>99 (S)	13.1 ± 1.9	>99 (R)
1h	27 ± 1.3	>99 (S)	35.8 ± 5.4	91(R)
1i	5.2 ± 0.1	>99 (R)	5.4 ± 0.3	>99 (R)
1j	47.7 ± 4.9	92 (S)	51.7 ± 0.9	>99 (R)

Reaction conditions: [substrate **1**] = 50 mM, [rAaeUPO] = 2 µM, buffer: 50 mM KPi pH 7 containing
10% v/v of acetonitrile, 25 °C, H_2O_2 dosing rate: 20 mM h^{-1}, reaction time: 6 h. For the second step the
reaction mixture was complemented with [NAD(P)H] = 0.1 mM, [MgCl₂] = 2 mM, 10% v/v 2-propanol,
LkADH or ADH-A (100 µL cell-free extract), and incubated overnight. Experiments were performed as
triplicates. [a] [rAaeUPO] = 6 µM.

concentrations of the (R)-alcohol were observed. Although a better understanding of the
issue with this substrate necessitates further experiments, it may be assumed that the
LkADH and ADH-A exhibited low to no activity towards the ketone intermediate **2i**.[20] We
currently cannot explain the (R) enantiomeric reduction product for the p-methoxy deriva-
tive **3f** with ADH-A.

3.2.4 E-factor analysis

Overall, we have established a bienzymatic cascade reaction to obtain both enantiomers of a range of phenylethanol derivatives. To assess the environmental impact of the reaction and to identify the bottlenecks of the current reaction system we performed an E-factor analysis[21] of the reaction (at the example of *p*-chloroethylbenzene **1c**, Figure 3).

The wastes generated in the current setup correspond to approx. 262 $kg_{waste} \times kg^{-1}_{product}$, of which 99% are caused by the (co-)solvents. Non reacted starting material and ketone intermediate contribute to less than 0.5% (E-factor contribution of 0.37 $kg \times kg^{-1}$), and the contribution of the catalysts (r*Aae*UPO, ADH-A, NAD: approx. 0.02 $kg \times kg^{-1}$) or of the buffer salts are negligible. Evidently a simple E-factor analysis does not give a complete picture as it neglects the pre-history of the reagents and catalysts used as well as energy requirements[22] and therefore can only give a first indication about the real environmental impact. Nevertheless, the dominance of (co-)solvents points out in which direction further improvements are necessary. First, the product concentration needs to be increased dramatically.[23] Fed-batch strategies adding the reagents over time appear particularly suitable to obtain high concentrations. Possibly, this will require higher concentrations of the cosolvent (acetonitrile or environmentally more acceptable alternatives)[24] to reduce the water consumption. In this way, the reaction system will also meet the requirements formulated by Huisman and co-workers for the biocatalytic synthesis of APIs.[25] Isopropanol also contributed significantly to the E-factor (21 $kg \times kg^{-1}$ corresponding to 8% of the overall E-factor). Considering that the isopropanol's main function was to shift the equilibrium of the ADH-catalysed reduction reaction, smarter, irreversible regeneration systems for the reduced nicotinamide cofactor[26] or switching to enzyme-coupled regeneration approaches[27] appear attractive to reduce this contribution.
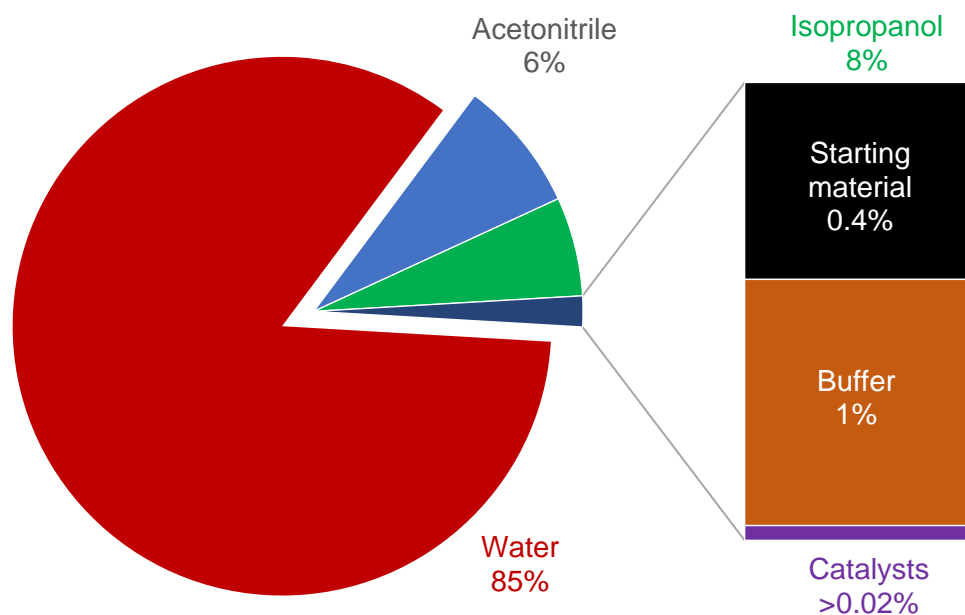
Figure 3. E-Factor analysis of the bienzymatic conversion of *p*-chloroethylbenzene **1c** to (*S*)-*p*-chlorophenylethanol **3c**.

3.3 Conclusions

Overall, we have established a biocatalytic access to complementary chiral phenylethanols from simple ethylbenzene derivatives by combining the peroxygenase-catalysed thorough oxidation of alkyl benzenes to the corresponding ketones, followed by stereoselective alcohol dehydrogenase-catalysed synthesis of enantiomerically enriched alcohols. Further steps will comprise broadening the substrate scope (e. g. to heteroaromatic starting materials) and increasing the substrate loading in order to turn this approach into an economically and ecologically interesting methodology for the synthesis of fine chemicals and APIs.

3.4 Experimental section

3.4.1 General information

Unless otherwise mentioned, all chemicals were purchased from Sigma-Aldrich, TCI-Europe or abcr GmbH, and used without further purification. Columns and column material for enzyme purification were purchased from GE Healthcare.

3.4.2 Enzyme preparation

The recombinant PaDaI variant of the evolved unspecific peroxygenase mutant from *A. aegerita* was expressed in *P. pastoris* and purified by using following procedures, which was described in the previous report.[15,16,20]

The alcohol dehydrogenases ADH-A from *Rhodococcus ruber* and *Lk*ADH from *Lactobacillus brevis*, were recombinantly produced in *E. coli* (see supplementary information) by using following procedures, which was described in the previous report.[28,29]

3.4.3 Synthesis of acetophenone derivatives

In a 20 mL glass vial the reaction mixture (6.5 mL total volume) contained 2 µM r*Aae*UPO, 50 mM substrate, and 10% v/v CH_3CN in 50 mM KPi buffer pH 7.0. The reaction started by addition of H_2O_2, which was supplied with a continuous flow rate of 20 mM/h and run at room temperature (about 20 °C), 600 rpm, 6 h. A ThermoMixer C from Eppendorf was used for the reactions at a speed of 600 rpm.

3.4.4 Acetophenone reduction by ADHs

In a 1.5 mL GC glass vial the reaction mixture (700 µL total volume) contained 2 mM $MgCl_2$, 0.1 mM NAD(P)H, 50 µL cell-free extract or 20 mg lyophilised cells of *Lk*ADH or ADH-A, 10% v/v 2-propanol and 15 mM acetophenone in 50 mM KPi buffer pH 7.0. The reaction was run at 30 °C, 600 rpm, overnight. A ThermoMixer C from Eppendorf was used to control the temperature at 30 °C and speed at 600 rpm.

3.4.5 One-pot one-step system

In a 1.5 mL GC glass vial the reaction mixture (700 µL total volume) contained 2 µM r*Aae*UPO, 50 mM ethylbenzene, 2 mM MgCl$_2$, 0.1 mM NAD(P)H, 10% v/v 2-propanol, 50 µL of ADH-A or *Lk*ADH cell-free extract in 50 mM KPi buffer pH 7.0. The reaction was started by addition of H$_2$O$_2$, which was supplied with a continuous flow rate 10 mM/h with 10 h, and run at 30 °C, 600 rpm, 24 h. A ThermoMixer C from Eppendorf was used to control the temperature at 30 °C and speed at 600 rpm.

3.4.6 One-pot two-step system

In a 20 mL glass vial the reaction mixture (6.5 mL total volume) contained 2 µM r*Aae*UPO, 50 mM substrates, 10% v/v CH$_3$CN in 50 mM KPi buffer pH 7.0. The reaction was started by addition of H$_2$O$_2$, which was supplied with a continuous flow rate of 20 mM/h and run at room temperature (about 20 °C), 600 rpm. After 6 h, 365 µL of the reaction mixture was taken into a 1.5 mL glass vial, then 2 mM MgCl$_2$, 0.1 mM NAD(P)H, 10% v/v 2-propanol, 100 µL of ADH-A or *Lk*ADH cell-free extract was added and run at 30 °C, 600 rpm, overnight.

Thermomixers were used for controlling temperature and shaking. For each sampling over time, 100 µL of reaction mixture was extracted with 500 µL ethyl acetate containing 5 mM *n*-octanol as internal standard. The extraction was then dried by MgSO$_4$ and analysed by achiral and chiral gas chromatography. Details of gas chromatography and temperature profiles are shown in the Supporting Information.

3.4.7 Analysis procedures

3.4.7.1 Determination of r*Aae*UPO activity

The volumetric activity was determined via the ABTS-assay at 25 °C. The ABTS-assay was performed in sodium citrate buffer (50 mM, pH 4.4) containing H$_2$O$_2$ (2.0 mM), ABTS

(0.5 mM) and a diluted enzyme solution. The oxidation of ABTS was monitored by absorption change at 420 nm (ε_{420} = 36.0 mM^{-1} cm^{-1}). Reactions were performed in triplicates.

3.4.7.2 SDS-PAGE

10 µL Protein samples were diluted with distilled water and mixed with 9.5 µL staining agent (Laemmli Sample buffer 4x) and 0.5 µL reducing agent (DDT 20x) to a final volume of 20 µL. After heat incubation the samples, 10 µL samples were loaded onto the gel. A precast gel was used (Criterion^{TM} TGX Stain-Free) with 1x TGS running buffer. 10 µL of marker solution (Precision Plus Protein^{TM} Unstained Standard) was applied for every run. As running conditions, a constant voltage of 200 V and a starting current of 165 mA per gel with a running time of 45 min were applied.

3.4.7.3 GC measurements

GC measurements were performed on a Shimadzu GC-14A/FID or Shimadzu GC-2010 plus/FID equipped with different columns (see supplementary information). The reactions were stopped at different time points by addition of ethyl acetate containing *n*-octanol (5 mM) as internal standard. After extraction and centrifugation, the organic phase was dried with magnesium sulfate and analysed via gas chromatography. All concentrations reported, are based on calibration curves obtained from authentic and synthesised standards.

References

1. D. J. C. Constable, P. J. Dunn, J. D. Hayler, G. R. Humphrey, J. Johnnie L. Leazer, R. J. Linderman, K. Lorenz, J. Manley, B. A. Pearlman, A. Wells, A. Zaks, T. Y. Zhang, *Green Chem.* **2007**, *9*, 411.

2. N. A. McGrath, M. Brichacek, J. T. Njardarson, *J. Chem. Educ.* **2010**, *87*, 1348.

3. Y. Zheng, H. Yin, D. Yu, X. Chen, X. Tang, X. Zhang, Y. Xue, Y. Wang, Z. Liu, *Appl. Microbiol. Biotechnol.* **2017**, *101*, 987.

4. F. Hollmann, D. J. Opperman, C. E. Paul, *Angew. Chem. Int. Ed.* **2021**, *60*, 5644.

5. H. Cao, X. Zhu, D. Wang, Z. Sun, Y. Deng, X. Hou, D. Zhao, *ACS Catal.* **2015**, *5*, 27.

6. O. Pàmies, J. E. Bäckvall, *Chem. Rev.* **2003**, *103*, 3247.

7. B. A. Persson, A. L. E. Larsson, M. Le Ray, J. E. Bäckvall, *J. Am. Chem. Soc.* **1999**, *121*, 1645.

8. R. M. Haak, F. Berthiol, T. Jerphagnon, A. J. A. Gayet, C. Tarabiono, C. P. Postema, V. Ritleng, M. Pfeffer, D. B. Janssen, A. J. Minnaard, B. L. Feringa, J. G. de Vries, *J. Am. Chem. Soc.* **2008**, *130*, 13508.

9. V. B. Urlacher, M. Girhard, *Trends Biotechnol.* **2019**, *37*, 882.

10. M. Hobisch, D. Holtmann, P. Gomez de Santos, M. Alcalde, F. Hollmann, S. Kara, *New Trends Ind. Biocatal.* **2021**, *51*, 107615.

11. P. Both, H. Busch, P. P. Kelly, F. G. Mutti, N. J. Turner, S. L. Flitsch, *Angew. Chem. Int. Ed.* **2016**, *55*, 1511.

12. L. Schmermund, S. Reischauer, S. Bierbaumer, C. K. Winkler, A. Diaz-Rodriguez, L. J. Edwards, S. Kara, T. Mielke, J. Cartwright, G. Grogan, B. Pieber, W. Kroutil, *Angew. Chem. Int. Ed.* **2021**, *60*, 6965.

13. R. Ullrich, J. Nüske, K. Scheibner, J. Spantzel, M. Hofrichter, *Appl. Environ. Microbiol.* **2004**, *70*, 4575.

14. F. Tonin, F. Tieves, S. Willot, A. van Troost, R. van Oosten, S. Breestraat, S. van Pelt, M. Alcalde, F. Hollmann, *Org. Process Res. Dev.* **2021**, *25*, 1414.

15. P. Molina-Espeja, S. Ma, D. M. Mate, R. Ludwig, M. Alcalde, *Enzyme Microb. Technol.* **2015**, *73–74*, 29.

16. P. Molina-Espeja, E. Garcia-Ruiz, D. Gonzalez-Perez, R. Ullrich, M. Hofrichter, M. Alcalde, *Appl. Environ. Microbiol.* **2014**, *80*, 3496.

17. C. W. Bradshaw, W. Hummel, C. H. Wong, *J. Org. Chem.* **1992**, *57*, 1532.

18. C. E. Paul, I. Lavandera, V. Gotor-Fernández, W. Kroutil, V. Gotor, *ChemCatChem* **2013**, *5*, 3875.

19. I. Lavandera, A. Kern, V. Resch, B. Ferreira-Silva, A. Glieder, W. M. F. Fabian, S. de Wildeman, W. Kroutil, *Org. Lett.* **2008**, *10*, 2155.

20. W. Stampfer, B. Kosjek, K. Faber, W. Kroutil, *J. Org. Chem.* **2003**, *68*, 402.

21. R. A. Sheldon, *Green Chem.* **2017**, *19*, 18.

22. F. Tieves, F. Tonin, E. Fernández-Fueyo, J. M. Robbins, B. Bommarius, A. S. Bommarius, M. Alcalde, F. Hollmann, *Tetrahedron* **2019**, *75*, 1311.

23. D. Holtmann, F. Hollmann, *Mol. Catal.* **2022**, *517*, 112035.

24. R. K. Henderson, C. Jiménez-González, D. J. C. Constable, S. R. Alston, G. G. A. Inglis, G. Fisher, J. Sherwood, S. P. Binks, A. D. Curzons, *Green Chem.* **2011**, *13*, 854.

25. G. W. Huisman, J. Liang, A. Krebber, *Curr. Opin. Chem. Biol.* **2010**, *14*, 122.

26. S. Kara, D. Spickermann, J. H. Schrittwieser, C. Leggewie, W. J. H. van Berkel, I. W. C. E. Arends, F. Hollmann, *Green Chem.* **2013**, *15*, 330.

27. R. Wichmann, D. Vasic-Racki, in *Technology Transfer in Biotechnology: From lab to Industry to Production*, ed. by Udo Kragl, Springer Berlin Heidelberg, Berlin, Heidelberg, **2005**, pp. 225–260.

28. K. Edegger, C. C. Gruber, T. M. Poessl, S. R. Wallner, I. Lavandera, K. Faber, F. Niehaus, J. Eck, R. Oehrlein, A. Hafner, W. Kroutil, *Chem. Commun.* **2006**, 2402.

29. A. Weckbecker, W. Hummel, *Biocatal. Biotransformation* **2006**, *24*, 380.
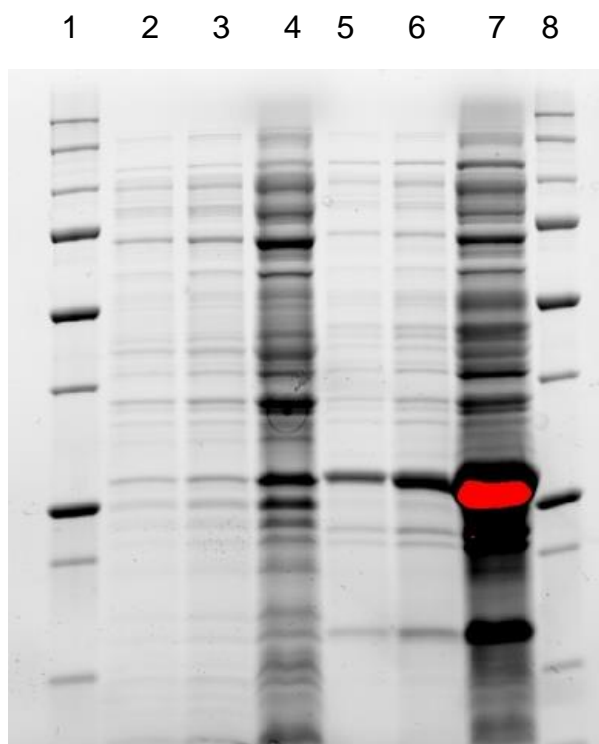
Supplementary information

Figure S1. SDS-PAGE of ADH-A and *Lk*ADH cell free extracts used. Line 1 and 8: Marker; lines 2-4: ADH-A at 3 dilutions; lines 5-7: *Lk*ADH at three dilutions.

Table S1. GC analytical data with achiral columns

Compound	GC column	Oven temperature program	Retention time
Ethylbenzene 1-Phenylethanol Acetophenone	CP-Wax 52 CB (Agilent) (25 m×0.25 mm×1.2 µm); carrier gas: N$_2$ Split 150	135°C hold 4 min 20°C/min to 200°C hold 6.0 min 25°C/min to 250°C hold 1.0 min	3.56 min ethylbenzene 7.73 min n-octanol (IS) 9.72 min acetophenone 11.76 min 1-Phenylethanol
1-Chloro-4-ethylbenzene 1-(4-Chlorophenyl)ethanol 4'-Chloroacetophenone	CP-Sil 5 CB (Agilent) (25 m×0.25 mm×1.2 µm); carrier gas: N$_2$ Split 150	165°C hold 9 min 25°C/min to 345°C hold 1.0 min	3.74 min n-octanol (IS) 3.98 min 1-Chloro-4-ethylbenzene 7.02 min 4'-Chloroacetophenone

			7.49 min 1-(4-Chlorophenyl)ethanol
1-Chloro-2-ethylbenzene 1-(2-Chlorophenyl)ethanol 2'-Chloroacetophenone	CP-Sil 5 CB (Agilent) (25 m×0.25 mm×1.2 µm); carrier gas: N$_2$ Split 150	110°C hold 3 min 20°C/min to 145°C hold 5.0 min 20°C/min to 170°C hold 3.0 min 25°C/min to 345°C hold 1.0 min	7.72 min 1-Chloro-2-ethylbenzene 7.90 min n-octanol (IS) 11.86 min 2'-Chloroacetophenone 12.67 min 1-(2-Chlorophenyl)ethanol
1-Chloro-3-ethylbenzene 1-(3-Chlorophenyl)ethanol 3'-Chloroacetophenone	CP-Wax 52 CB (Agilent) (50 m×0.53 mm×2.0 µm); carrier gas: N$_2$ Split 150	180°C hold 12 min 25°C/min to 250°C hold 1.0 min	1.58 min 1-Chloro-3-ethylbenzene 1.87 min n-octanol (IS) 4.97 min 3'-Chloroacetophenone 10.27 min 1-(3-Chlorophenyl)ethanol
1-Bromo-4-ethylbenzene 1-(4-Bromophenyl)ethanol 4'-Bromoacetophenone	CP-Sil 5 CB (Agilent) (25 m×0.25 mm×1.2 µm); carrier gas: N$_2$ Split 150	170°C hold 10 min 25°C/min to 345°C hold 1.0 min	2.93 min 1-Bromo-4-ethylbenzene 6.49 min n-octanol (IS) 9.90 min 4'-Bromoacetophenone 14.37 min 1-(4-Bromophenyl)ethanol
1-Ethyl-4-fluorobenzene 1-(4-Fluorophenyl)ethanol 4-Fluoroacetophenone	CP-Wax 52 CB (Agilent) (25 m×0.25 mm×1.2 µm); carrier gas: N$_2$ Split 150	160°C hold 11 min 20°C/min to 220°C hold 2.0 min 25°C/min to 250°C hold 1.0 min	3.36 min n-octanol (IS) 4.68 min 1-Ethyl-4-fluorobenzene 8.49 min 4-Fluoroacetophenone 9.06 min 1-(4-Fluorophenyl)ethanol
1-Ethyl-4-iodobenzene 1-(4-Iodophenyl)ethanol 4-Iodoacetophenone	CP-Sil 5 CB (Agilent) (25 m×0.25 mm×1.2 µm); carrier gas: N$_2$ Split 150	190°C hold 15 min 25°C/min to 345°C hold 1.0 min	2.75 min n-octanol (IS) 4.82 min 1-Ethyl-4-iodobenzene 8.41 min 4-Iodoacetophenone 8.75 min 1-(4-Iodophenyl)ethanol
4-Ethylnitrobenzene 1-(4-Nitrophenyl)ethanol 4-Nitroacetophenone	CP-Sil 5 CB (Agilent) (25 m×0.25 mm×1.2 µm); carrier gas: N$_2$ Split 150	170°C hold 22 min 25°C/min to 345°C hold 1.0 min	3.48 min n-octanol (IS) 8.50 min 4-Ethylnitrobenzene

			13.32 min 4-Nitroaceto-phenone
			18.14 min 1-(4-Nitro-phenyl)ethanol
4-Ethylanisole 1-(4-Methoxyphenyl)etha-nol 4'-Methoxyacetophenone	CP-Sil 5 CB (Agilent) (25 m×0.25 mm×1.2 µm); carrier gas: N$_2$ Split 150	160°C hold 6 min 20°C/min to 205°C hold 1.5 min 25°C/min to 345°C hold 1.0 min	4.05 min n-octanol (IS) 4.99 min 4-Ethylanisole 8.35 min 1-(4-Methoxy-phenyl)ethanol 9.12 min 4'-Methoxyace-tophenone
2-Ethylanisole 1-(4-Methoxyphenyl)etha-nol 2-Methoxyacetophenone	CP-Sil 5 CB (Agilent) (25 m×0.25 mm×1.2 µm); carrier gas: N$_2$; Split 150	180°C hold 10 min 25°C/min to 345°C hold 1.0 min	3.06 min n-octanol (IS) 3.36 min 2-Ethylanisole 5.74 min 1-(2-Methoxy-phenyl)ethanol 5.99 min 2-Methoxyace-tophenone
Isobutylbenzene 2-Methyl-1-phenyl-1-pro-panol Isobutyrophenone	CP-Sil 5 CB (Agilent) (25 m×0.25 mm×1.2 µm); carrier gas: N$_2$; Split 150	100°C hold 3 min 25°C/min to 345°C hold 1.0 min	9.38 min n-octanol (IS) 9.68 min Isobutylben-zene

Table S2. GC analytical data with chiral columns

Compound	GC column	Oven temperature program	Retention time
Ethylbenzene 1-Phenylethanol Acetophenone	CP-Chirasil-Dex-CB (Agilent) (25 m×0.32 mm×0.25 µm); carrier gas: He Split 150	100°C hold 16 min 20°C/min to 140°C hold 3.0 min 25°C/min to 225°C hold 1.0 min	3.49 min Ethylbenzene 10.07 min Acetophenone 14.16 min n-octanol (IS) 18.65 min (*R*)-1-Phe-nylethanol 19.10 min (*S*)-1-Phe-nylethanol
1-Chloro-4-ethylbenzene 1-(4-Chlorophenyl)ethanol 4'-Chloroacetophenone	CP-Chirasil-Dex-CB (Agilent) (25 m×0.32 mm×0.25 µm); carrier gas: He Split 150	150°C hold 10 min 25°C/min to 225°C hold 1.0 min	2.70 min 1-Chloro-4-ethylbenzene 2.95 min n-octanol (IS) 4.52 min 4'-Chloroaceto-phenone 7.54 min (*R*)-1-(4-Chloro-phenyl)ethanol

			8.08 min (*S*)-1-(4-Chloro-phenyl)ethanol
1-Chloro-2-ethylbenzene 1-(2-Chlorophenyl)ethanol 2'-Chloroacetophenone	CP-Chirasil-Dex-CB (Agilent) (25 m✕0.32 mm✕0.25 µm); carrier gas: He Split 150	150°C hold 10 min 25°C/min to 225°C hold 1.0 min	2,73 min 1-Chloro-2-ethylbenzene 2.96 min n-octanol (IS) 3.76 min 2'-Chloroaceto-phenone 6.89 min (*R*)-1-(2-Chloro-phenyl)ethanol 7.73 min (*S*)-1-(2-Chloro-phenyl)ethanol
1-Chloro-3-ethylbenzene 1-(3-Chlorophenyl)ethanol 3'-Chloroacetophenone	CP-Chirasil-Dex-CB (Agilent) (25 m✕0.32 mm✕0.25 µm); carrier gas: He Split 150	150°C hold 10 min 25°C/min to 225°C hold 1.0 min	2.77 min 1-Chloro-3-ethylbenzene 2.96 min n-octanol (IS) 4.12 min 3'-Chloroaceto-phenone 7.31 min (*R*)-1-(3-Chloro-phenyl)ethanol 7.68 min (*S*)-1-(3-Chloro-phenyl)ethanol
1-Bromo-4-ethylbenzene 1-(4-Bromophenyl)ethanol 4'-Bromoacetophenone	CP-Chirasil-Dex-CB (Agilent) (25 m✕0.32 mm✕0.25 µm); carrier gas: He Split 150	135°C hold 8 min 25°C/min to 225°C hold 1.0 min	2.37 min 1-Bromo-4-ethylbenzene 3.66 min 4'-Bromoaceto-phenone 3.92 min n-octanol (IS) 5.99 min (*R*)-1-(4-Bromo-phenyl)ethanol 6.41 min (*S*)-1-(4-Bromo-phenyl)ethanol
1-Ethyl-4-fluorobenzene 1-(4-Fluorophenyl)ethanol 4-Fluoroacetophenone	CP-Chirasil-Dex-CB (Agilent) (25 m✕0.32 mm✕0.25 µm); carrier gas: He Split 150	160°C hold 10 min 25°C/min to 225°C hold 1.0 min	2.72 min n-octanol (IS) 2.97 min 1-Ethyl-4-fluoro-benzene 5.02 min 4-Fluoroaceto-phenone 8.03 min (*R*)-1-(4-Fluoro-phenyl)ethanol 8.48 min (*S*)-1-(4-Fluoro-phenyl)ethanol
1-Ethyl-4-iodobenzene 1-(4-Iodophenyl)ethanol 4-Iodoacetophenone	CP-Chirasil-Dex-CB (Agilent) (25 m✕0.32 mm✕0.25 µm); carrier gas: He Split 150	175°C hold 8 min 25°C/min to 225°C hold 1.0 min	2.31 min n-octanol (IS) 2.89 min 1-Ethyl-4-iodo-benzene

			5.00 min 4-Iodoacetophe-none
			6.848 min (*R*)-1-(4-Iodo-phenyl)ethanol
			7.08 min (*S*)-1-(4-Iodo-phenyl)ethanol
4-Ethylnitrobenzene 1-(4-Nitrophenyl)ethanol 4-Nitroacetophenone	CP-Chirasil-Dex-CB (Agilent) (25 m✕0.32 mm✕0.25 μm); carrier gas: He Split 150	180°C hold 13 min 25°C/min to 225°C hold 1.0 min	2.31 min n-octanol (IS) 3.31 min 4-Ethylnitroben-zene 4.97 min 4-Nitroaceto-phenone 9.88 min (*R*)-1-(4-nitro-phenyl)ethanol 10.54 min (*S*)-1-(4-nitro-phenyl)ethanol
4-Ethylanisole 1-(4-Methoxyphenyl)etha-nol 4'-Methoxyacetophenone	CP-Chirasil-Dex-CB (Agilent) (25 m✕0.32 mm✕0.25 μm); carrier gas: He Split 150	110°C hold 3 min 20°C/min to 130°C hold 3.0 min 20°C/min to 170°C hold 3.0 min 25°C/min to 225°C hold 1.0 min	5.48 min 4-Ethylanisole 6.25 min n-octanol (IS) 10.39 min 4'-Methoxy-acetophenone 11.23 min (*R*)-1-(4-Meth-oxyphenyl)ethanol 11.38 min (*S*)-1-(4-Meth-oxyphenyl)ethanol
2-Ethylanisole 1-(2-Methoxyphenyl)etha-nol 2-Methoxyacetophenone	CP-Chirasil-Dex-CB (Agilent) (25 m✕0.32 mm✕0.25 μm); carrier gas: He; Split 150	110°C hold 3 min 20°C/min to 130°C hold 3.0 min 20°C/min to 180°C hold 5.0 min 25°C/min to 225°C hold 1.0 min	5.22 min 2-Ethylanisole 6.57 min n-octanol (IS) 10.83 min 2-Methoxyace-tophenone 12.95 min (*R*)-1-(2-Meth-oxyphenyl)ethanol

GC-MS chromatograms
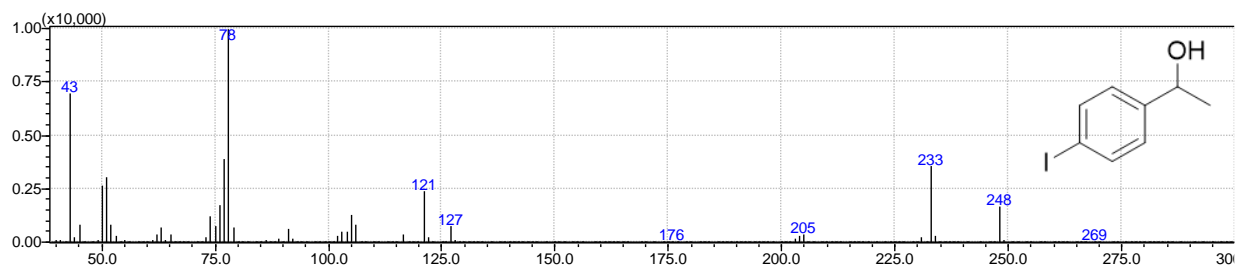
Figure S2. GC-MS mass spectrum 1-(4-iodophenyl)ethanol.
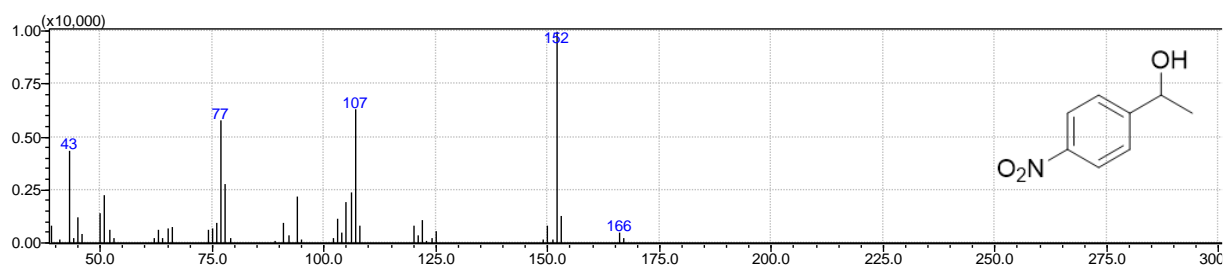
Figure S3. GC-MS mass spectrum 1-(4-nitrophenyl)ethanol.
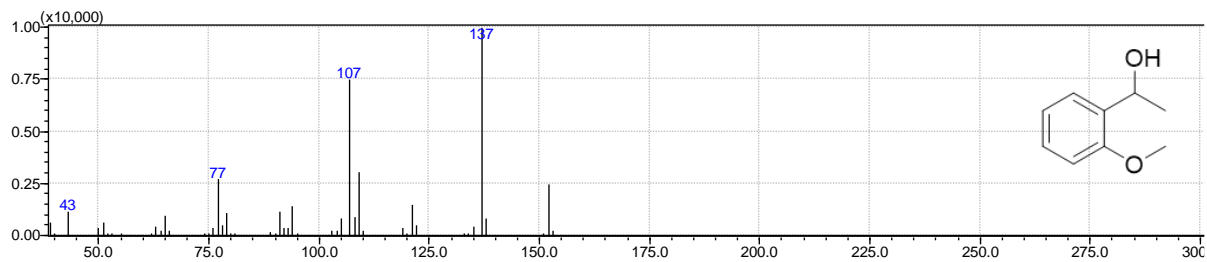
Figure S4. GC-MS mass spectrum 1-(2-methoxyphenyl)ethanol.

4

Peroxygenase–catalysed selective oxidation of silanes to silanols

A peroxygenase-catalysed hydroxylation of organosilanes is reported. The recombinant peroxygenase from *Agrocybe aegerita* (*Aae*UPO) enabled efficient conversion of a broad range of silane starting materials in attractive productivities (up to 300 mM h^{-1}) and catalyst usage (up to 84 s^{-1} and more than 120,000 catalytic turnovers). Molecular modelling of the enzyme-substrate interaction puts a basis for the mechanistic understanding of *Aae*-UPO selectivity.

Xiaomin Xu, Yejia Mao, Mireia Martinez, Sergi Roda, Martin Floor, Victor Guallar, Caroline E. Paul, Miguel Alcalde and Frank Hollmann

4.1 Introduction

Silanols represent an important product class in organic chemistry as precursors for sili-cones, as catalyst components or in medicinal chemistry.[1,2] Syntheses of the state-of-the-art typically start from already functionalised silanes such as chloro- or alkoxysilanes via hydrolysis and producing significant amounts of salt waste-products (Scheme 1a).[2,3] Less waste-intensive methods involving dehydrogenative,[4-12] O_2[13-15] or H_2O_2[16-19]-dependent oxidation of non-functionalised silanols are rare (Scheme 1b,c). Even less common are biocatalytic methods for the conversion of silanes.[20-22] Recently, Arnold and coworkers succeeded in evolving a cytochrome P450-BM3 variant which dramatically increased cat-alytic activity towards a range of organosilanes (Scheme 1d).[20]

a) hydrolysis of chlorosilanes

$$R_3Si\text{-}Cl + H_2O \longrightarrow R_3Si\text{-}OH + HCl$$

b) dehydrogenative oxidation of silanes

$$R_3Si\text{-}H + H_2O \xrightarrow{\boxed{Cat}} R_3Si\text{-}OH + H_2 + SiR_3\text{-}O\text{-}SiR_3$$

c) oxygen-driven oxidations

$$R_3Si\text{-}H + (H_2)O_2 \xrightarrow{\boxed{Cat}} R_3Si\text{-}OH + SiR_3\text{-}O\text{-}SiR_3 + H_2O$$

d) P450 monooxygenase-catalysed oxidation of silanes

$$R_3Si\text{-}H + NADPH + O_2 \xrightarrow{\boxed{P450}} R_3Si\text{-}OH + H_2O$$
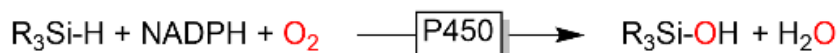
Scheme 1. Synthetic routes to silanols.

Inspired by these pioneering works, we asked ourselves whether so-called unspecific per-oxygenases (UPOs) may also be suitable catalysts for this type of transformation. Partic-ularly, we investigated the UPO from *Agrocybe aegerita* (*Aae*UPO)[23-26] as silane oxyfunc-

tionalisation catalyst. UPOs are attractive alternatives to established P450 monooxygenases as they enable drastically simplified, NAD(P)H-independent reaction schemes using simple H_2O_2 as stoichiometric oxidant (Scheme 2).[27]

a) P450-monooxygenase-catalysed hydroxylation
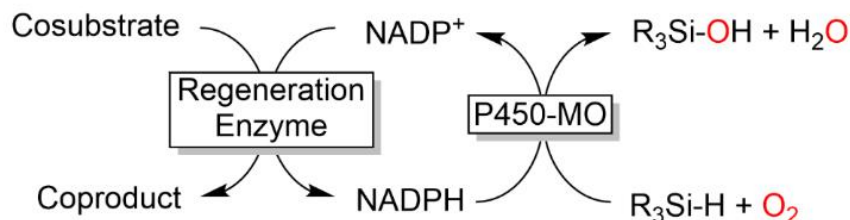
b) UPO-catalysed hydroxylation
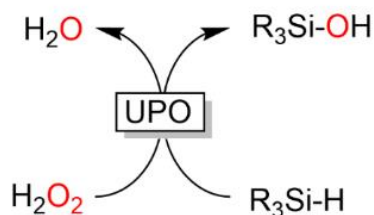
Scheme 2. Comparison of P450-monooxygenase-(a) and peroxygenase-(b) catalysed hydroxylation of silanes to silanols.

4.2 Results and Discussion

4.2.1 Time course

In a first experiment, we performed the H_2O_2-dependent hydroxylation of dimethylphenylsilane (**1a**) to the corresponding dimethylphenylsilanol (**1b**) catalysed by *Aae*UPO (Figure 1). Because of the poor water solubility of **1a,** 30% (v/v) of acetonitrile was added, which was feasible due to the extraordinary solvent tolerance of *Aae*UPO.[28] Using 1 µM of *Aae*UPO and a H_2O_2 feeding rate of 10 mM×h^{-1}, full conversion of the starting material was achieved within 5 h of reaction time, corresponding to an excellent total turnover number and turnover frequency for *Aae*UPO of 40,000 and 2.2 s^{-1}, respectively. No by-product formation was observed. Control reactions in the absence of *Aae*UPO or using thermally inactivated *Aae*UPO did not yield detectable conversion of **1a**.
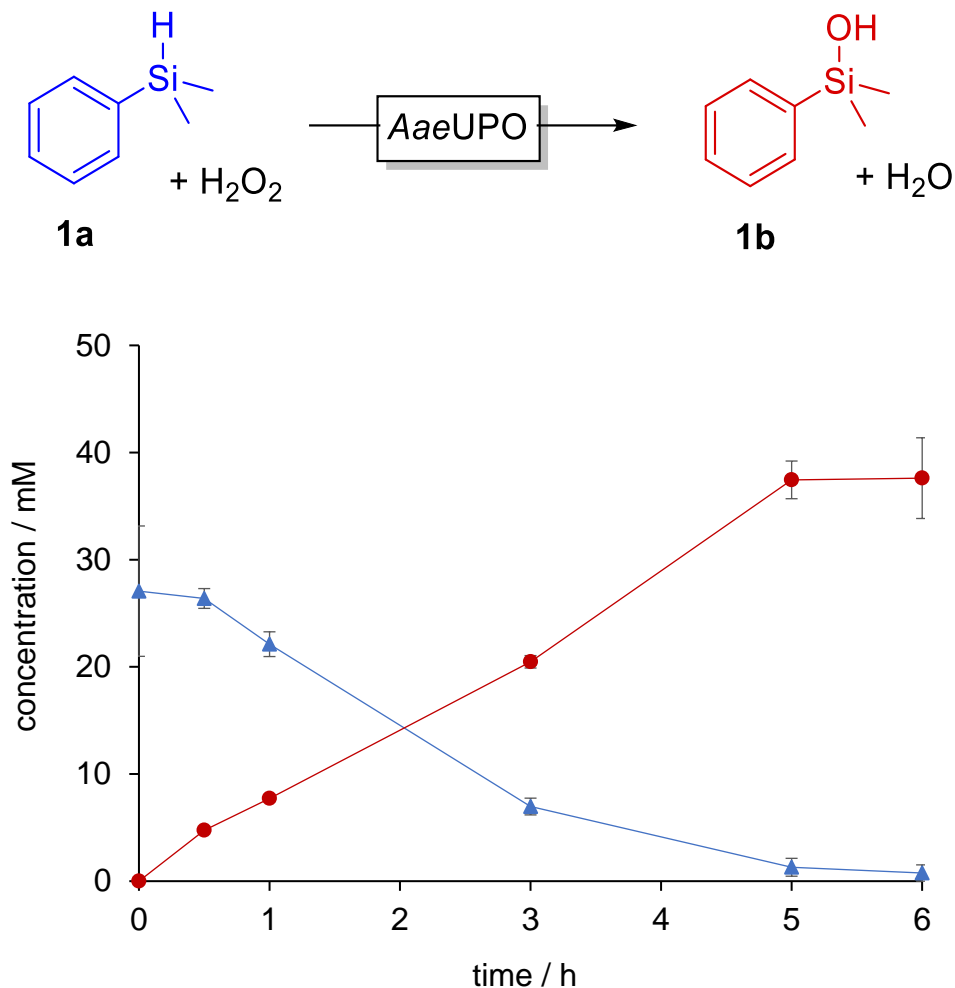
Figure 1. *Aae*UPO-catalysed hydroxylation of dimethylphenylsilane (**1a**) to dimethylphenylsilanol (**1b**). Conditions: [**1a**] = 50 mM, [*Aae*UPO] = 1 µM, buffer: 50 mM KPi pH 7.0 containing 30% (v/v) of acetonitrile, 25 °C, 600 rpm, H_2O_2 feeding-rate: 10 mM×h^{-1} (from a 1 M stock).
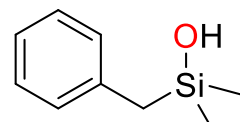
4.2.2 Substrate scope

Encouraged by the promising results obtained with dimethylphenylsilane (**1a**), we further explored the scope of the *Aae*UPO-catalysed hydroxylation of organosilanes to several commercially available starting materials (Figure 2). Overall, a broad range of organosilanes was converted by *Aae*UPO. Sterically demanding organosilanes such as **4a** and **5a** turned out to be relatively poor substrates which is in line with the active site architecture of *Aae*UPO.
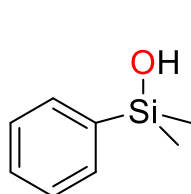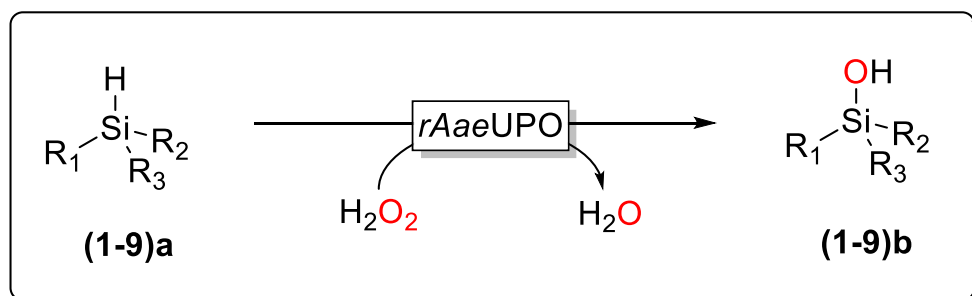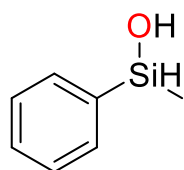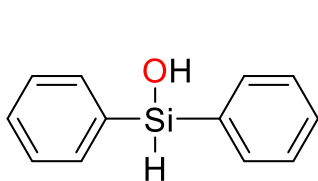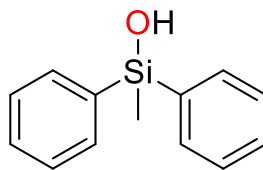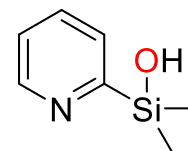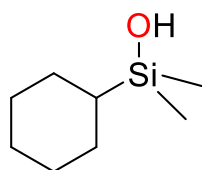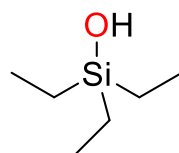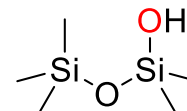
Figure 2. Substrate scope of *Aae*UPO-catalysed hydroxylation of organosilanes. Yields are given as averages of duplicate runs (see the Supporting Information for further details). General conditions: [organosilane] = 50 mM, [*Aae*UPO] = 1 µM, buffer: 50 mM KPi pH 7.0 containing 30% (v/v) of acetonitrile, 25 °C, 600 rpm. The reaction was initiated by adding H_2O_2 (10 mM×h^{-1} from a 1 M stock), 5 h. [a] negative controls gave similar results to the enzymatic reactions; [b] GC-results; [c] *in situ* NMR-results; [d] including the (spontaneous dimerisation product; [e] C-H hydroxylation product detected; n.c.: no conversion detected.

It should be noted that in case of **2a** and **4a**, the result of the enzymatic conversion was almost identical to the result of the negative control (in the absence of enzyme under otherwise identical conditions). Hence, for these two substrates no significant contribution of *Aae*UPO to the conversion can be assumed. Also, **5a** turned out to be a poor substrate, in line with the sterically rather constraint active site of *Aae*UPO.

It is interesting to note that the chemo/regioselectivity was not perfect with all substrates. With **2a**, approx. 50% of the product formed was identified as dimer, most probably stemming from a spontaneous monomer/dimer equilibrium. In case of **7a** and **8a**, considerable amounts of the α- or β-hydroxylation product (C-H-bond hydroxylation) was observed.

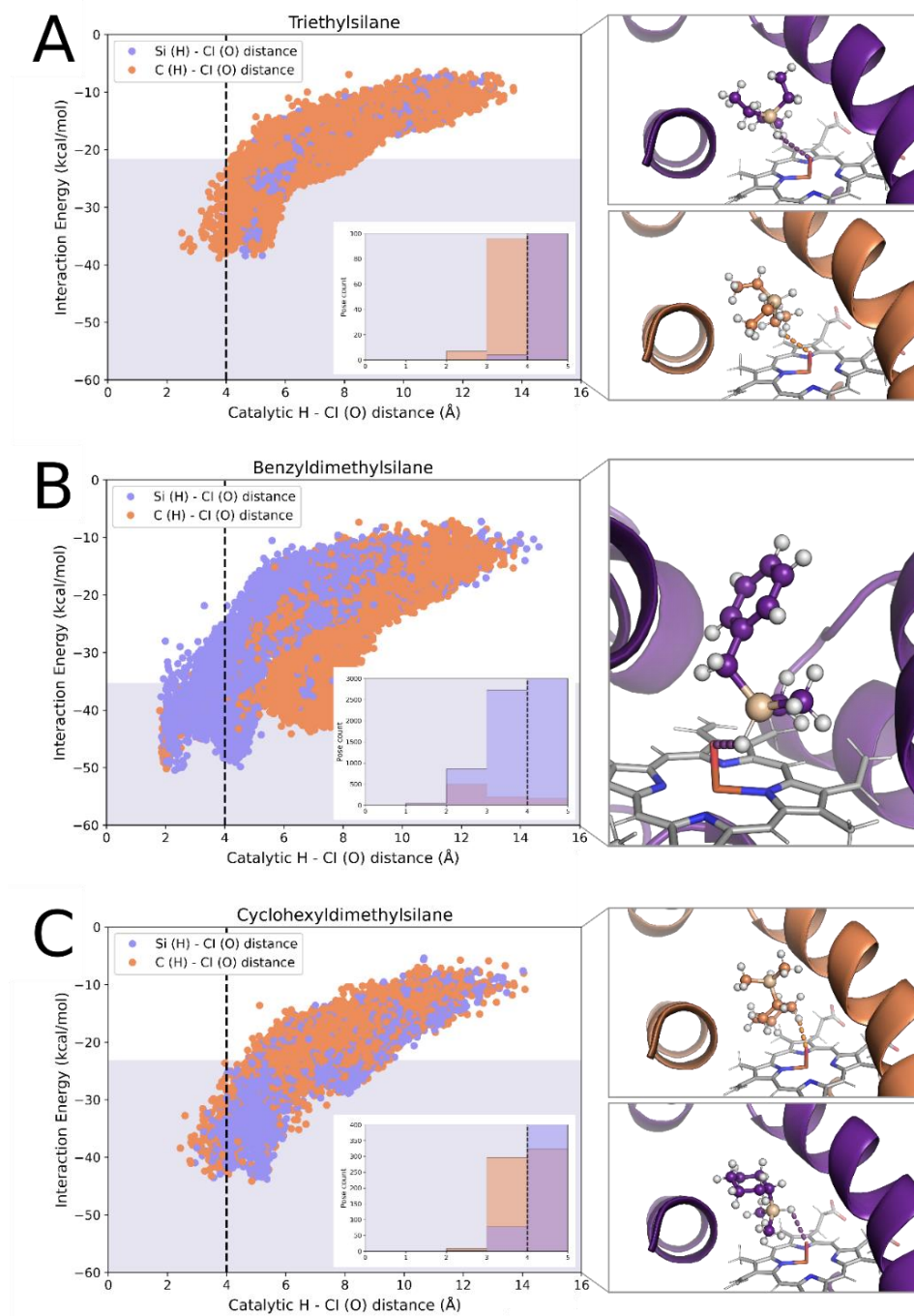## 4.2.3 Protein Energy Landscape Exploration (PELE) simulations

Figure 3. Selectivity results. Scatter plot of the substrate diffusion (left) and representative bound poses (right) for triethylsilane (A; **8a**), benzyldimethylsilane (B; **3a**); and cyclohexyldimethylsilane (C; **7a**) compounds on the *Aae*UPO's active site. Plots show the catalytic distance (in Å) between the reactive oxygen in CI and the silicon (purple) or carbon (orange) hydrogens, against the enzyme-substrate interaction energy; notice that only the shortest distance between these two atoms is shown for each PELE pose. The vertical dashed line marks a threshold for the catalytic distance. The grey area highlights the 20% lowest percentile regarding interaction energy. The inner histogram plot represents the number of accepted PELE poses of the mentioned grey area in different bindings of the catalytic distances.

To obtain further insights into the molecular basis for the selectivity of the *Aae*UPO-cata-lysed silane hydroxylation, Protein Energy Landscape Exploration (PELE) simulations[29] were performed. The distance between the heme compound I (CI) oxygen and silicon-bound hydrogens (Figure 3 and Figure S1) were chosen as reactive coordinates. Simulations indicate that steric effects in both the channel and active site explain most selectivities observed in the in enzymatic conversions. For instance, the only difference between **4a** and **5a** is a methyl group, an extra volume that hinders the access to the active site, as seen in PELE simulations where no poses below 4 Å were found for the bulkier substrate, in contrast to the smaller one (Figure S1). In addition, notice the correlation between the low yield percentage with the very few catalytic points observed for **4a** (in general large yields correspond to a significant number of catalytic poses, Figure S2). Concerning **6a**, while the energy profiles indicate a less pronounced funnel shape, when compared to **1a**, we still observed a significant number of catalytic poses. The lack of activity, however, can be explained if turning to electronic effects, rather than steric ones. The pyridine group pKa is sensitive to the particular environment; quantum mechanical calculations predict a pKa value of 6.15±0.493 in water ($\varepsilon \approx 80$) and 10.68±1.300 in DMSO ($\varepsilon \approx 48$). Besides the dielectric constant reduction in proteins ($\varepsilon \approx 3.24\pm0.04$),[30] *Aae*UPOs' active site presents a highly charged oxygen atom from CI, resulting in **6a** most likely being protonated. Hence, the H-atom abstraction will be highly hindered by the positive charge of the substrate, explaining why **1a** reacts while **6a** does not; a QM/MM H-atom abstraction scan shows a difference of ~5 kcal×mol^{-1} between them, and a ~7 kcal×mol^{-1} between the protonated and deprotonated species in **6a** (Figure S3).

Finally, at the modelling level, two reaction coordinates were defined for substrates showing additional reactivity towards carbon atoms, aiming to differentiate between carbon *vs.* silicon oxidative selectivity. As it can be seen, **3a** has more catalytic poses for the silicon-bound hydrogen compared to **8a** and **7a** (Figure 3). Hence, higher regioselectivity for the hydroxylation of the Si atom is expected in **3a**. In contrast, both **7a** and **8a** seem to prefer to bind the carbon-bound hydrogen catalytically.

4.2.4 Reaction conditions investigation

Next, we investigated the effect of H_2O_2 dosage on the rate and robustness of the *Aae*-UPO-catalysed hydroxylation of **1a** (Figure 4). With a dose rate of up to ca. 250 mM h^{-1} the initial product formation rate increased linearly with the increasing feed rate of H_2O_2. The slope in this linear region was around 0.78, indicating that approx. 22% of the H_2O_2 supplied was not used productively for product conversion. Most likely the known catalase activity of *Aae*UPO accounts for this observation.[31] The highest product formation rate observed in these experiments was 303 mM h^{-1} corresponding to a superb catalytic performance of *Aae*UPO of approx. 84 catalytic turnovers per second (ca. 109 U mg^{-1}). Quite expectedly, further increase of the H_2O_2 addition rate resulted in a decrease of the overall reaction rate, which most likely can be attributed to the irreversible, oxidative inactivation of the catalytic heme site of *Aae*UPO.
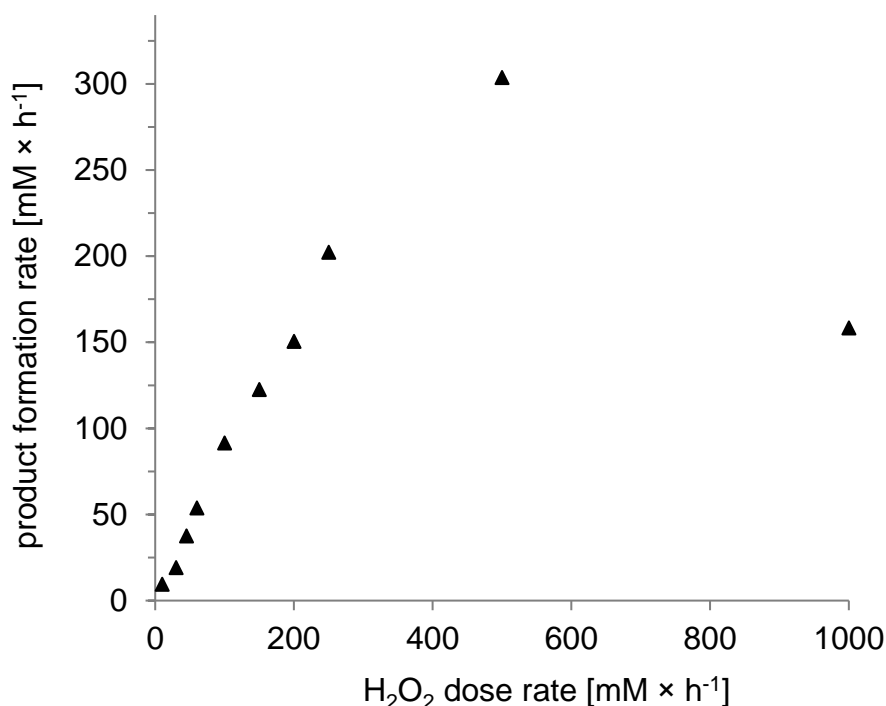

Figure 4. Influence of H_2O_2 addition rate on the rate of the conversion of **1a** to **1b**. Conditions: [dimethylphenylsilane, **1a**] = 50 mM, [*Aae*UPO] = 1 µM, buffer: 50 mM KPi pH 7 containing 30% (v/v) of acetonitrile, 25 °C, 600 rpm. The reaction was initiated by addition of H_2O_2 (0-1000 mM h^{-1} from a 1 M stock)

With future preparative-scale applications in mind we further investigated the influence of starting material- and product-concentration on the activity of the biocatalyst (Figures S8 & 9). While the activity of *Aae*UPO was hardly influenced by concentrations of **1a** up to 500 mM, there seemed to be a mild inhibitory effect of the silanol product **1b** with *Aae*UPO activity steadily decreasing in the presence of increasing concentrations of **1b**. Moreover, the volatility of the reagents, especially **1a**, represented a challenge to achieve a closed mass balance (Figure S4-6).

In future upscaling experiments, we will focus on the two liquid phase system approach wherein **1a** will be applied as second, water immiscible phase and serve as substrate reservoir and product sink. Already a preliminary experiment using this approach gave very promising results (Figure S7) and product concentrations (**1b**) of up to 121 mM, corresponding to more than 120,000 catalytic turnovers of *Aae*UPO.

4.3 Conclusions

Overall, in this study, we have demonstrated the potential of peroxygenases for the biocatalytic oxyfunctionalisation of organosilanes. Compared to recently reported P450 monooxygenase catalysts, *Aae*UPO excels not only in terms of simplicity of the reaction (simple H_2O_2 addition instead of *in situ* NADPH regeneration and O_2 addition) but also by its very high catalytic activity. Substrate induced fit binding simulations provide a good understanding of the selectivity/activity patterns, which will put the basis for tailored *Aae*-UPO variants and optimised reaction schemes will enable practical synthetic schemes.

4.4 Experimental section

4.4.1 Enzyme preparation

Recombinant expression and purification of the evolved unspecific peroxygenase mutant from *A. aegerita* in *P. pastoris* was performed following a previously described procedure.[24]

4.4.2 Silanol production

In a 20 mL glass vial the reaction mixture (4 mL total volume) contained 1 µM *Aae*UPO, 50 mM substrate, and 30% v/v CH_3CN in 50 mM KPi buffer pH 7.0. The reaction started with the addition of H_2O_2, which was supplied with a continuous flow rate of 10 mM/h and run at room temperature (about 20 °C), 600 rpm, 5 h. Thermomixer were used for controlling temperature and shaking. 100 µL of the reaction mixture was extracted with 500 µL ethyl acetate containing 5 mM n-octanol as internal standard for each sampling over time. The extraction was then dried by $MgSO_4$ and analysed by achiral gas chromatography. Details of gas chromatography and temperature profiles are shown in the supplementary information. The error bars represent the standard deviation of duplicate experiments.

4.4.3 Two liquid phase systems

In a 4 mL glass vial, 1 mL 50 mM KPi buffer pH 7.0 contained 1 µM of *Aae*UPO as the aqueous phase; In the meanwhile, 1 mL dimethylphenylsilane as the organic phase. H_2O_2 was added into the aqueous phase through a syringe pump with a 5 mM/h feeding rate (from a 1 M stock); the solution was mixed at 600 rpm with a magnetic stirrer. Samples were taken from the organic phase; 20 µL of the samples were diluted into 180 µL ethyl acetate containing 5 mM *n*-octanol as an internal standard. The extraction was then dried by $MgSO_4$ and analysed by achiral gas chromatography.

4.4.4 Enzyme activity assay

To evaluate the activity of *Aae*UPO, the standardised assay for the *Aae*UPO-ABTS assay was used. ABTS assay was performed in sodium citrate buffer (50 mM, pH 4.4) containing H_2O_2 (2.0 mM), ABTS (0.5 mM) and a diluted enzyme solution. The oxidation of ABTS was monitored by absorption change at 420 nm ($\varepsilon_{420} = 36.0$ mM^{-1} cm^{-1}). For inhibition of testing, the enzyme was incubated with different inhibitor concentrations before being tested. Reactions were performed in triplicates.

4.4.5 GC measurement

GC measurements were performed on a Shimadzu GC-14A/FID or Shimadzu GC-2010 plus/FID equipped with different columns. The reactions were stopped at different time points by adding ethyl acetate containing *n*-octanol (5 mM) as internal standard. After extraction and centrifugation, the organic phase was dried with magnesium sulfate and analysed via gas chromatography. All concentrations reported are based on calibration curves obtained from authentic and synthesised standards

4.4.6 NMR spectra

^{1}H NMR spectra were recorded on a Varian 400 (400 MHz) spectrometer in $CDCl_3$ or 10% D_2O. Chemical shifts (ppm), multiplicity (brs= broad singlet, s = singlet, d = doublet, t = triplet, q = quartet, m = multiplet), coupling constant (Hz), integration are given.

4.4.7 Protein preparation for in silico analysis.

The apo *Aae*UPO structure (PDB ID: 5OXU) was prepared and protonated at pH 7.0, the pH at which the experimental assays were performed, using the Protein Preparation Wizard.[32] In all cases, structural water molecules were included in the models. The heme group was modelled as the two-electron-oxidised compound C-I. A docking with Glide[33] was performed in order to place the ligands in the vicinity of the heme group for the PELE simulations. Substrates were built with the 2D Sketcher of the Schrödinger Suite and later on minimised.

4.4.8 Protein Energy Landscape Exploration (PELE) simulations

PELE was used to analyse the substrate specificity of *Aae*UPO. PELE is a Monte Carlo (MC)-based algorithm coupled with protein structure prediction methods.[34,35] The software begins with the heuristic sampling of the different microstates of the ligand (by applying small rotations and translations to it). The flexibility of the protein was also considered by

applying normal modes through the anisotropic network model (ANM) approach. After perturbing the whole system, side chains of the residues close to the ligand were sampled to avoid steric clashes. Finally, a truncated Newton minimisation with the OPLS2005 force field was performed[36] and the new microstate was accepted or rejected based on the Metropolis criterion. The Variable Dielectric Generalised Born Non-Polar (VDGBNP) implicit solvent model[37] was used to mimic the effect of water molecules around the protein.

4.4.9 QM and QM/MM calculations

All quantum mechanical calculations were performed using the Schrödinger Suite (Jaguar for QM and QSite for QM/MM).[37,38] In both cases, the calculations are at the DFT/B3LYP level of theory. The QM/MM scan calculation used the 6-31G** basis set, except for the Fe atom in the heme group where the LACVP* basis set was used. On the other hand, the pKa prediction used the 6-31G* basis set for the geometry optimisation of the protonated and deprotonated states and the cc-pVTZ(+) basis set for accurate single-point energies of the optimised geometries.

Reference

1. M. Jeon, J. Han, J. Park, *ACS Catal.* **2012**, *2*, 1539-1549.

2. V. Chandrasekhar, R. Boomishankar, S. Nagendran, *Chem. Rev.* **2004**, *104*, 5847-5910.

3. J. A. Cella, J. C. Carpenter, *J. Organomet. Chem.* **1994**, *480*, 23-26.

4. G. H. Barnes, N. E. Daughenbaugh, *J. Org. Chem.* **1966**, *31*, 885-887.

5. M. Lee, S. Ko, S. Chang, *J. Am. Chem. Soc.* **2000**, *122*, 12011-12012.

6. M. Shi, K. M. Nicholas, *J. Chem. Res.* **1997**, 400-401.

7. M. Yu, H. Jing, X. Liu, X. Fu, *Organometal.* **2015**, *34*, 5754-5758.

8. Y. Kikukawa, Y. Kuroda, K. Yamaguchi, N. Mizuno, *Angew. Chem. Int. Ed.* **2012**, *51*, 2434-2437.

9. E. A. Ison, R. A. Corbin, M. M. Abu-Omar, *J. Am. Chem. Soc.* **2005**, *127*, 11938-11939.

10. E. Matarasso-Tchiroukhine, *J. Chem. Soc., Chem. Commun.* **1990**, 681-682.

11. U. Schubert, C. Lorenz, *Inorg. Chem.* **1997**, *36*, 1258-1259.

12. A. K. Liang Teo, W. Y. Fan, *Chem. Comm.* **2014**, *50*, 7191-7194.

13. Y. Okada, M. Oba, A. Arai, K. Tanaka, K. Nishiyama, W. Ando, *Inorg. Chem.* **2010**, *49*, 383-385.

14. A. V. Arzumanyan, I. K. Goncharova, R. A. Novikov, S. A. Milenin, K. L. Boldyrev, P. N. Solyev, Y. V. Tkachev, A. D. Volodin, A. F. Smol'yakov, A. A. Korlyukov, A. M. Muzafarov, *Green Chem.* **2018**, *20*, 1467-1471.

15. H. Li, L. Chen, P. Duan, W. Zhang, *ACS Sus. Chem. Eng.* **2022**,*10*, 4642–4649.

16. W. Adam, C. M. Mitchell, C. R. Saha-Möller, O. Weichold, H. Garcia, *Chem. Commun.* **1998**, 2609-2610.

17. K. Wang, J. Zhou, Y. Jiang, M. Zhang, C. Wang, D. Xue, W. Tang, H. Sun, J. Xiao, C. Li, *Angew. Chem. Int. Ed.* **2019**, *58*, 6380-6384.

18. D. Limnios, C. G. Kokotos, *ACS Catalysis* **2013**, *3*, 2239-2243.

19. A. T. Kelly, A. K. Franz, *ACS Omega* **2019**, *4*, 6295-6300.

20. S. Bahr, S. Brinkmann-Chen, M. Garcia-Borras, J. M. Roberts, D. E. Katsoulis, K. N. Houk, F. H. Arnold, *Angew. Chem.Int. Ed.* **2020**, *59*, 15507-15511.

21. S. B. J. Kan, R. D. Lewis, K. Chen, F. H. Arnold, *Science* **2016**, *354*, 1048-1051.

22. R. J. Fessenden, R. A. Hartman, *J. Med. Chem.* **1970**, *13*, 52-54.

23. R. Ullrich, J. Nüske, K. Scheibner, J. Spantzel, M. Hofrichter, *Appl. Environ. Microbiol.* **2004**, *70*, 4575-4581.

24. F. Tonin, F. Tieves, S. Willot, A. van Troost, R. van Oosten, S. Breestraat, S. van Pelt, M. Alcalde, F. Hollmann, *Org. Proc. Res. Dev.* **2021**, *25*, 1414−1418.

25. P. Molina-Espeja, S. Ma, D. M. Mate, R. Ludwig, M. Alcalde, *Enz. Microb. Technol.* **2015**, *73–74*, 29-33.

26. P. Molina-Espeja, E. Garcia-Ruiz, D. Gonzalez-Perez, R. Ullrich, M. Hofrichter, M. Alcalde, *Appl. Environ. Microbiol.* **2014**, *80*, 3496-3507.

27. M. Hobisch, D. Holtmann, P. G. de Santos, M. Alcalde, F. Hollmann, S. Kara, *Biotechnol. Adv.* **2021**, *51*, 107615.

28. T. Hilberath, A. van Troost, M. Alcalde, F. Hollmann, *Front. Catal.* **2022**, 2*:882992*.

29. S. Acebes, E. Fernandez-Fueyo, E. Monza, M. F. Lucas, D. Almendral, F. J. Ruiz-Dueñas, H. Lund, A. T. Martinez, V. Guallar, *ACS Catal.* **2016**, *6*, 1624-1629.

30. M. Amin, J. Küpper, *ChemistryOpen* **2020**, *9*, 691-694.

31. M. Hofrichter, R. Ullrich, *Appl. Microbiol. Biotechnol.* **2006**, *71*, 276-288.

32. G. Madhavi Sastry, M. Adzhigirey, T. Day, R. Annabhimoju, W. Sherman, *J. Comput. Aided Mol. Des.* **2013**, *27*, 221-234.

33. R. A. Friesner, R. B. Murphy, M. P. Repasky, L. L. Frye, J. R. Greenwood, T. A. Halgren, P. C. Sanschagrin, D. T. Mainz, *J. Med. Chem.* **2006**, *49*, 6177-6196.

34. K. W. Borrelli, A. Vitalis, R. Alcantara, V. Guallar, *J. Chem. Theo. Compu.* **2005**, *1*, 1304-1311.

35. M. Municoy, S. Roda, D. Soler, A. Soutullo, V. Guallar, *J. Chem. Theo. Compu.* **2020**, *16*, 7655-7670.

36. J. L. Banks, H. S. Beard, Y. Cao, A. E. Cho, W. Damm, R. Farid, A. K. Felts, T. A. Halgren, D. T. Mainz, J. R. Maple, R. Murphy, D. M. Philipp, M. P. Repasky, L. Y. Zhang, B. J. Berne, R. A. Friesner, E. Gallicchio, R. M. Levy, *J. Comput. Chem.* **2005**, *26*, 1752-1780.

37. D. Bashford, D. A. Case, *Ann. Rev. Phys. Chem.* **2000**, *51*, 129-152.

38. A. D. Bochevarov, E. Harder, T. F. Hughes, J. R. Greenwood, D. A. Braden, D. M. Philipp, D. Rinaldo, M. D. Halls, J. Zhang, R. A. Friesner, *Int. J. Quantum Chem.* **2013**, *113*, 2110-2142.

39. R. B. Murphy, D. M. Philipp, R. A. Friesner, *J. Comput. Chem.* **2000**, *21*, 1442-1457.
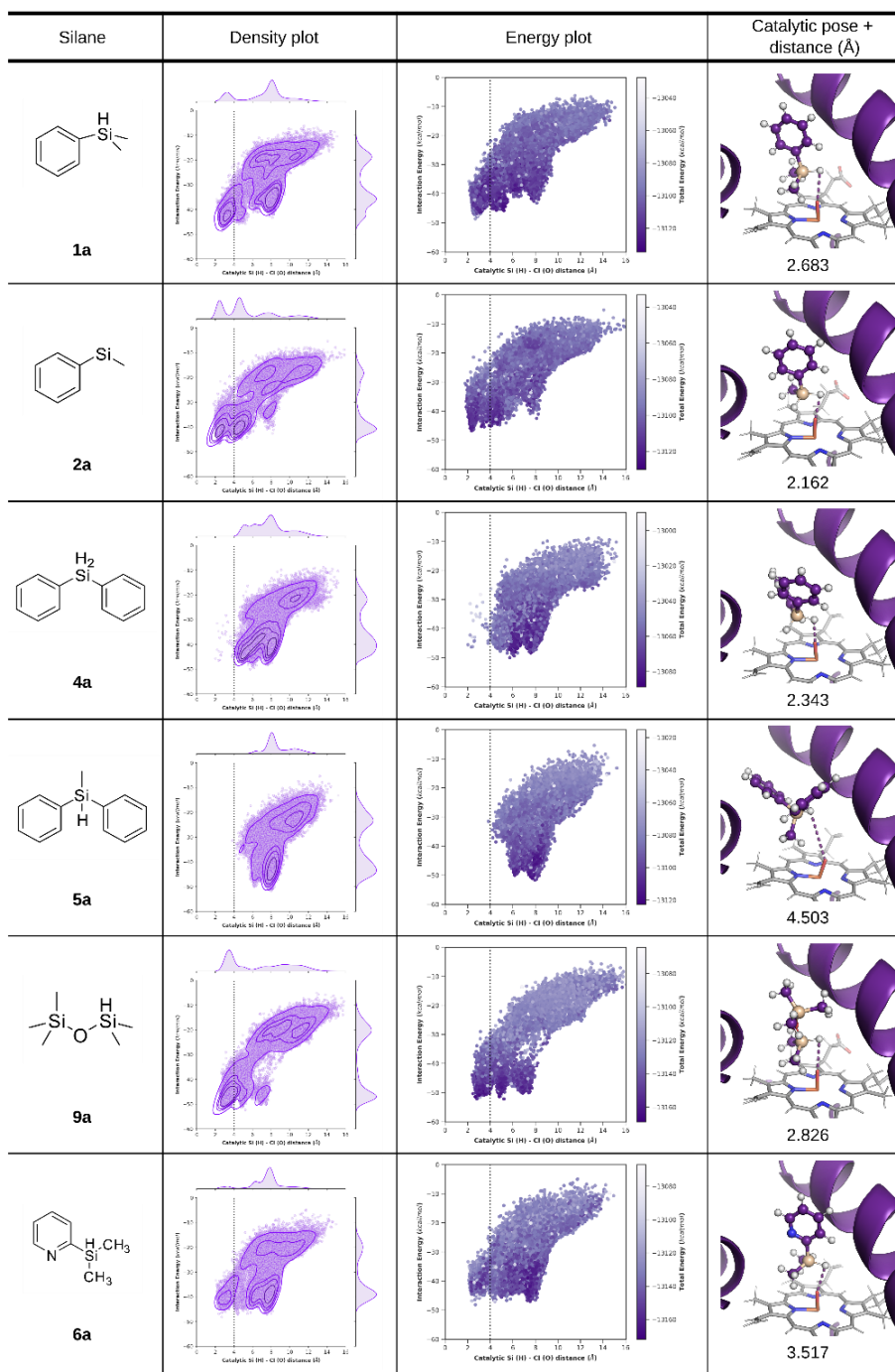
Supplementary information

Figure S1. Substrate diffusion and binding of the different silanes on r*Aae*UPO's active site. Plots of distances between the reactive oxygen in CI and the silicon hydrogen of the different substrates versus the corresponding interaction energies are shown (as density and energetic representations). Also, the poses of the substrates' lowest interaction energies (with the heme iron and oxo represented as sticks and the substrate as CPK filing) are shown on the right panels, together with the CI oxygen - silicon hydrogen distance (in Å).
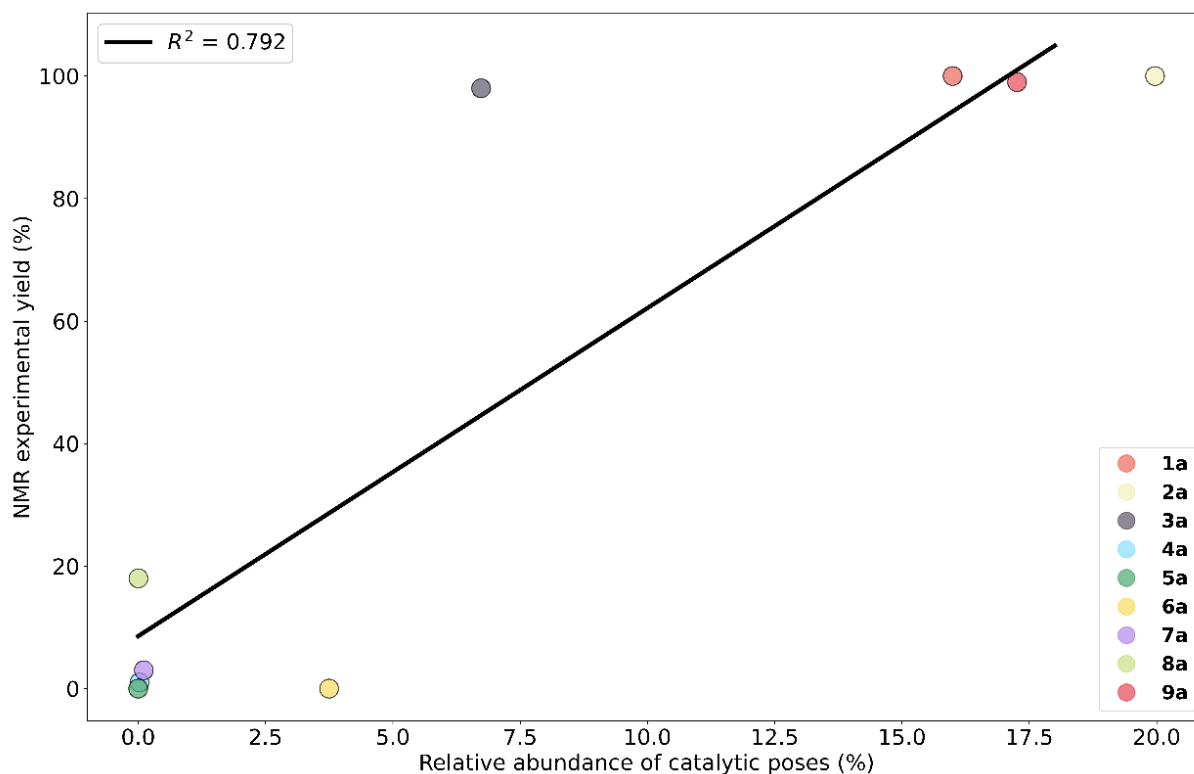
Figure S2. Linear regression plot between NMR's experimental yield and the relative abundance of catalytic poses (in the 20% lowest percentile regarding the interaction energy) of all the substrates (**1a** – **9a**). This relative abundance refers to the number of accepted PELE steps in a catalytic position (under 4Å and 20% best interaction energy) divided by the total number of accepted PELE steps. The coefficient of determination (R^2) is displayed in the graph.
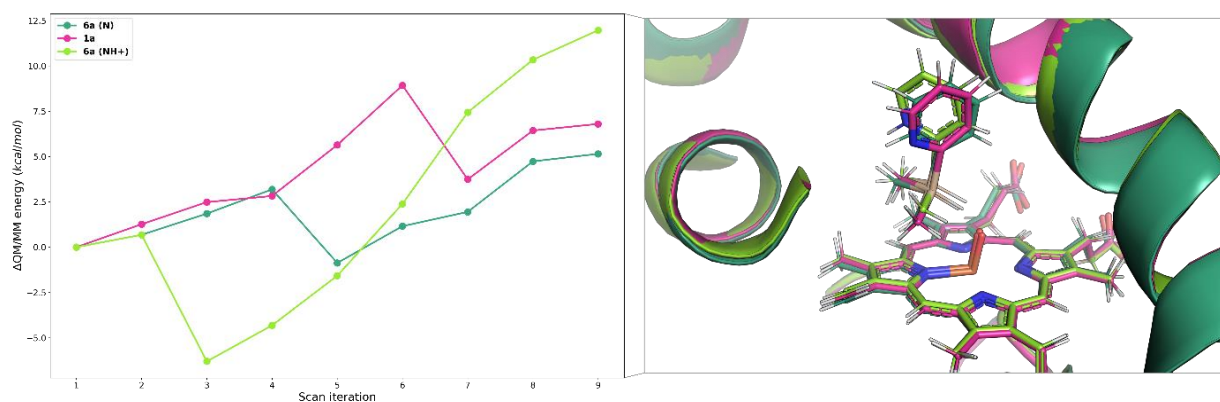

Figure S3. QM/MM H-atom abstraction scan results. Plot representing the scan iteration versus the ΔQM/MM energy (QM/MM energy$_{\text{iteration n}}$ - QM/MM energy$_{\text{iteration 0}}$) (left). Pose of the final step in the H-atom abstraction scan calculation in the tested substrates (right).
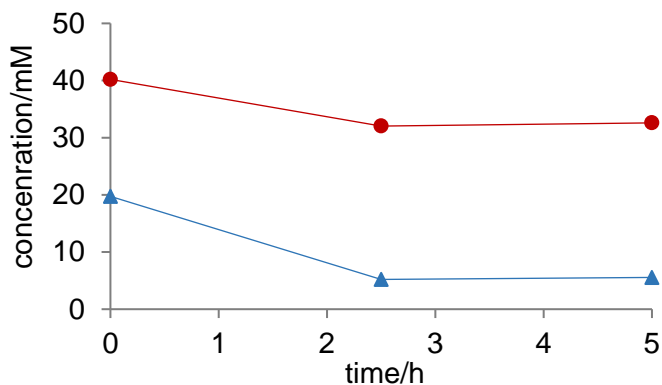
Figure S4. Volatility test of blue: dimethylphenylsilane (**1a**) and red: dimethylphenylsilanol (**1b**). Conditions: [**1a**] = 50 mM, [**1b**] = 50 mM, buffer: 50 mM KPi pH 7 containing **30% (v/v)** of acetonitrile, 25 °C, 600 rpm, H_2O_2 feeding-rate: 10 mM×h^{-1} (from a 1 M stock).

Figure S5. Volatility test of blue: dimethylphenylsilane (**1a**) and red: dimethylphenylsilanol (**1b**). Conditions: [**1a**] = 50 mM, [**1b**] = 50 mM, buffer: 50 mM KPi pH 7 containing **50% (v/v)** of acetonitrile, 25 °C, 600 rpm, H_2O_2 feeding-rate: 10 mM×h^{-1} (from a 1 M stock).
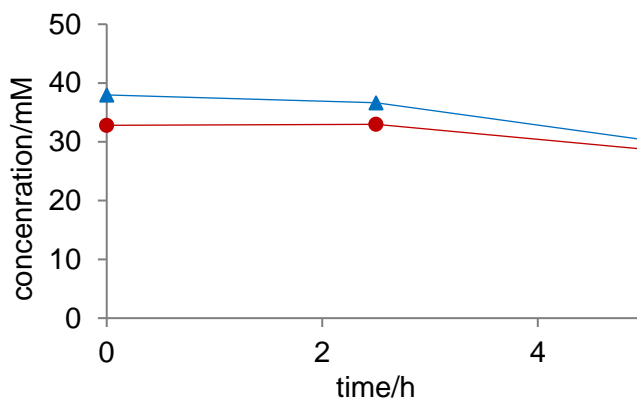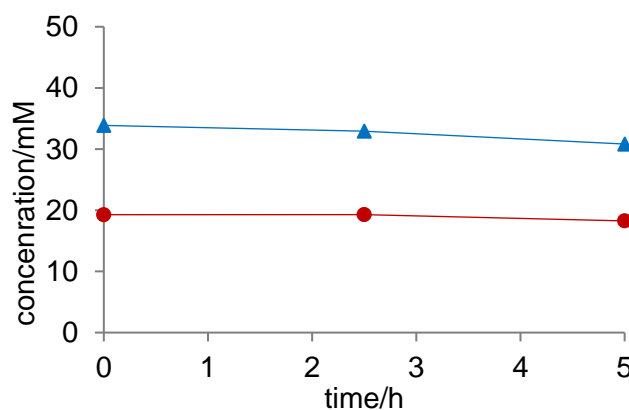

Figure S6. Volatility test of blue: dimethylphenylsilane (**1a**) and red: dimethylphenylsilanol (**1b**). Conditions: [**1a**] = 50 mM, [**1b**] = 50 mM, buffer: 50 mM KPi pH 7 containing **80% (v/v)** of acetonitrile, 25 °C, 600 rpm, H_2O_2 feeding-rate: 10 mM×h^{-1} (from a 1 M stock).
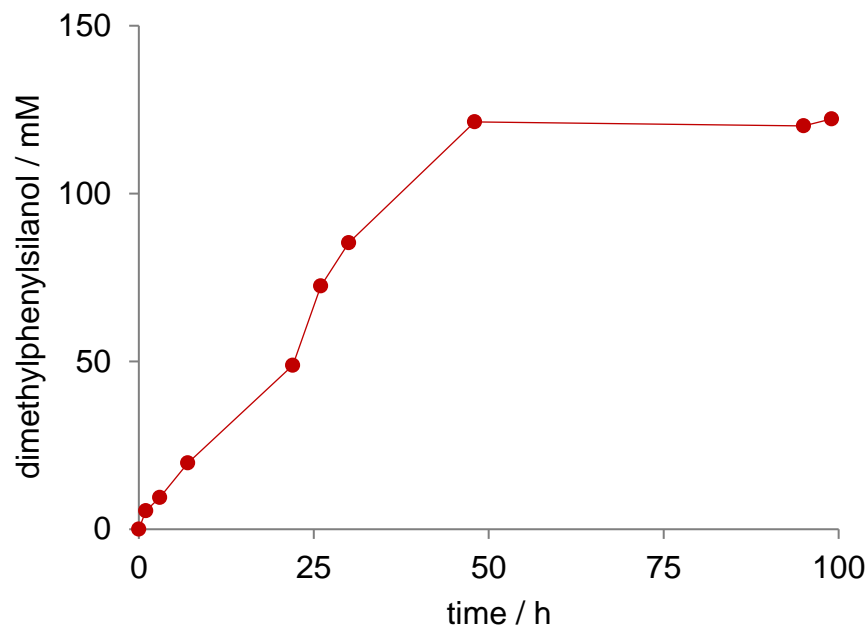
Figure S7. Time course of the *Aae*UPO-catalysed hydroxylation of **1a** in a 2LPS approach. Red: dimethylphenylsilanol (**1b**).
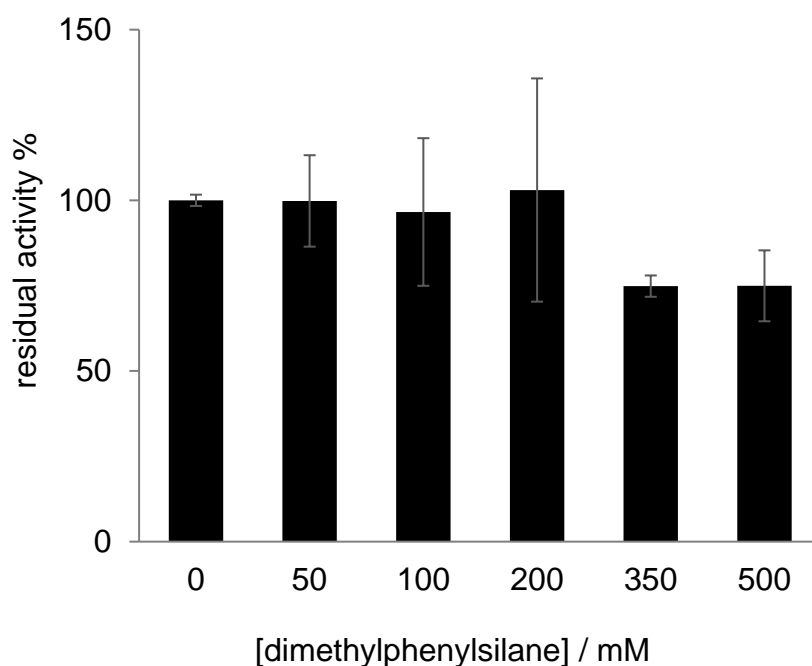

Figure S8. Influence of dimethylphenylsilane on the activity of *Aae*UPO. ABTS assay conditions: [ABTS]=0.5 mM, [H₂O₂]=2.0 mM, 50 mM sodium citrate buffer (pH 4.4). The reaction was started with the addition of 1 μM *Aae*UPO that was pre-incubated for 5 min with different amounts of dimethylphenylsilane. The error bars represent the standard deviation of triplicate experiments.

[dimethylphenylsilanol] / mM

Figure S9. Influence of dimethylphenylsilanol on the activity of *Aae*UPO. ABTS assay conditions: [ABTS]=0.5 mM, [H_2O_2]=2.0 mM, 50 mM sodium citrate buffer (pH 4.4). The reaction was started with the addition of 1 µM *Aae*UPO that was pre-incubated for 5 min with different amounts of dimethylphenylsilane. The error bars represent the standard deviation of triplicate experiments.
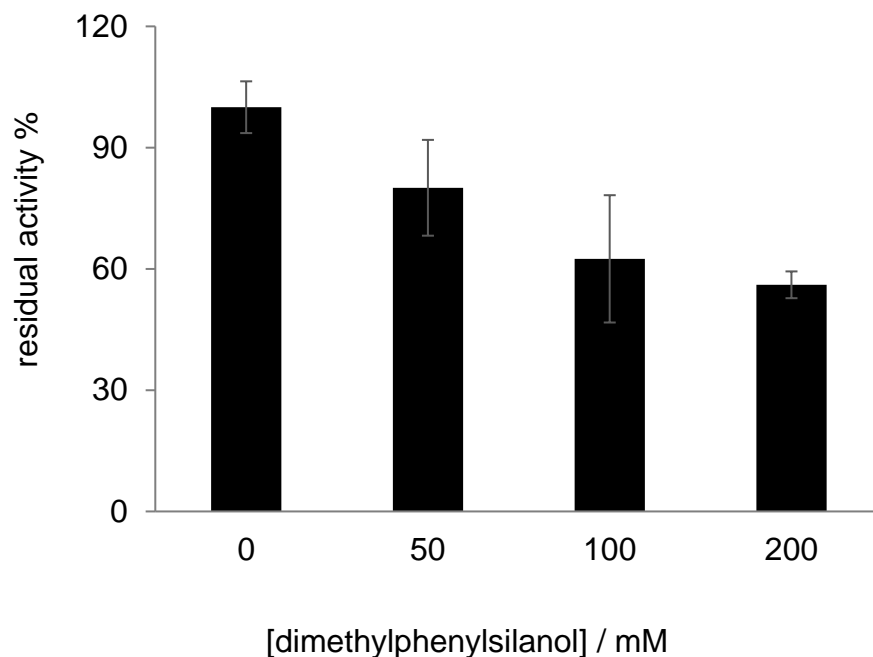
5

Towards preparative chemoenzymatic production of 3-cyanopropanoic acid from glutamate

The chemoenzymatic oxidative decarboxylation of glutamic acid to the corresponding nitrile using the vanadium chloroperoxidase from *Curvularia inaequalis* (*CN*CPO) as HOBr generation catalysts has been investigated. Product inhibition was identified as a major limitation. Nevertheless, 1,630,000 turnovers and a k_{cat} of 75 s^{-1} were achieved using 100 mM glutamate. The semi-preparative enzymatic oxidative decarboxylation of glutamate was also demonstrated.

5.1 Introduction

The production of biobased chemicals requires the removal of (oxygen) functionalities from biomass-derived compounds.[1–6] This is also the case of the oxidative decarboxylation of amino acids in the production of biobased nitriles. The oxidative decarboxylation of glutamic acid (Glu) – the most abundant amino acid in biomass[7] – generates the corresponding nitrile, 3-cyanopropanoic acid (CPA). CPA is a potential starting material for a range of products such as acrylonitrile, succinonitrile or pharmaceuticals.

The oxidative decarboxylation of amino acids can be mediated by hypobromite (HOBr). In order to minimise undesired oxidative side reactions, using HOBr in low concentrations is advisable. For this, next to some chemocatalytic,[8] or electrochemical methods[9] also an enzymatic approach has been developed (Scheme 1).[10,11]
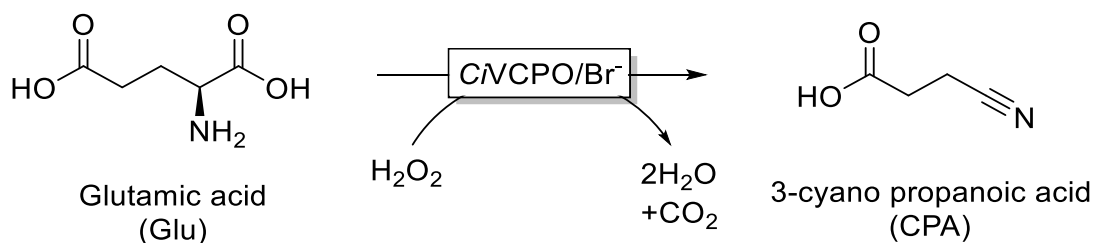
Scheme 1. Oxidative decarboxylation of glutamic acid yielding 3-cyanopropanoic acid using the vanadium-dependent chloroperoxidase from *Curvularia inaequalis* (*Ci*VCPO) and catalytic amounts of bromide.

High selectivity (>99%) and full conversion of glutamic acid into 3-cyanopropanoic acid were observed for the enzymatic procedure,[9–11] the substrate loadings, however, were as low as 5 mM, which is neither economically feasible nor environmentally acceptable.[12] Increasing the substrate concentration is an important task to demonstrate that highly selective catalysts like enzymes can be used at a preparative scale.[13]

The aim of this research was to scale up the conversion of glutamic acid into 3-cyanopropanoic acid by increasing the substrate loadings. The highly active and robust enzyme vanadium chloroperoxidase from *Curvularia inaequalis* (*Ci*VCPO),[14,15] was used in this endeavour.

5.2 Results and Discussion

5.2.1 First set reactions

As a starting point, we increased the initial L-glutamic acid concentration five-fold higher than in previous experiments,[10,11] H_2O_2 was added over time to the reaction mixture using a syringe pump. Pleasingly, we observed full conversion of the starting material into the desired CPA within approximately 5 h of reaction time (Figure 1).
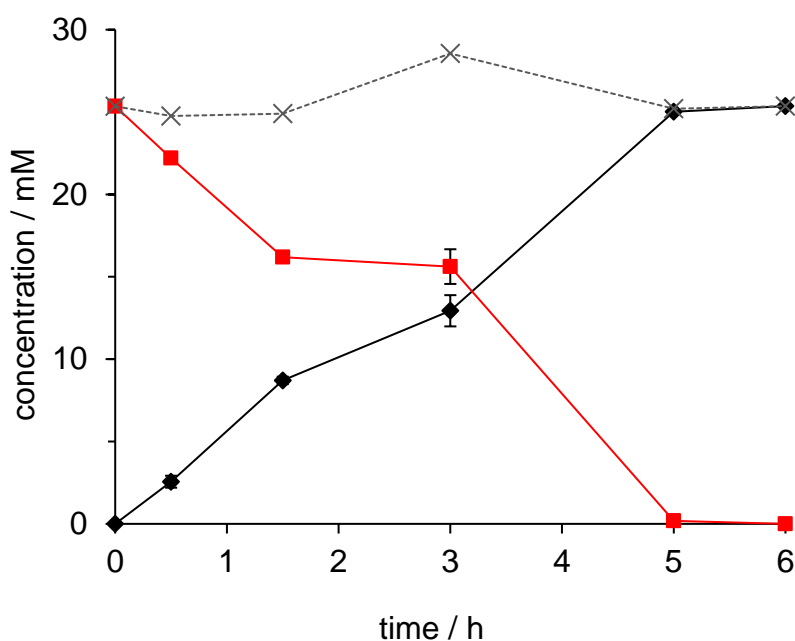

Figure 1. The conversion of glutamic acid (■) into 3-cyanopropanoic acid (◆), mole balance (X). Reaction conditions: [glutamic acid] = 25 mM, [NaBr] = 0.5 mM, [*Cl*VCPO] = 55 nM, H_2O_2-dosage: 12 mM×h^{-1} (from a 0.5 M stock solution, considering the final volume), 20 mM sodium citrate buffer (pH 5.6), room temperature (22 °C). The error bars represent the range of minimum duplicate experiments.

It should be noted that adding stoichiometric amounts of H_2O_2 from the beginning of the reaction had a rather detrimental effect on the product formation.[10,11] Under otherwise identical conditions, only half of the product was formed (Figure S1). In contrast to heme-dependent haloperoxidases, this phenomenon is not due to an inactivation of the biocatalyst but rather the result of an undesired reaction of H_2O_2 with HOBr yielding singlet oxygen ($^1O_2$, *vide infra*).[16] The biocatalyst performed 450,000 catalytic cycles corresponding to an average turnover frequency over 5 h of 25 s^{-1}. Even though these numbers are

convincing, they still somewhat fall back behind the catalytic potential of $C\textit{i}$VCPO.[13] We therefore systematically investigated several reaction parameters influencing the overall rate of the oxidative decarboxylation reaction.

5.2.2 H_2O_2 dosage rate

First, we varied the addition rate of H_2O_2 (Figure 2a) and observed a linear correlation between H_2O_2 dosage rate and overall product accumulation rate up to a H_2O_2 dose rate of 40 mM×h^{-1}. Higher dosing rates did not significantly increase the overall productivity. Consequently, the H_2O_2 yield decreased from 95% at 12 mM×h^{-1} to 34% at 12 mM×h^{-1} (Figure 2b).

b
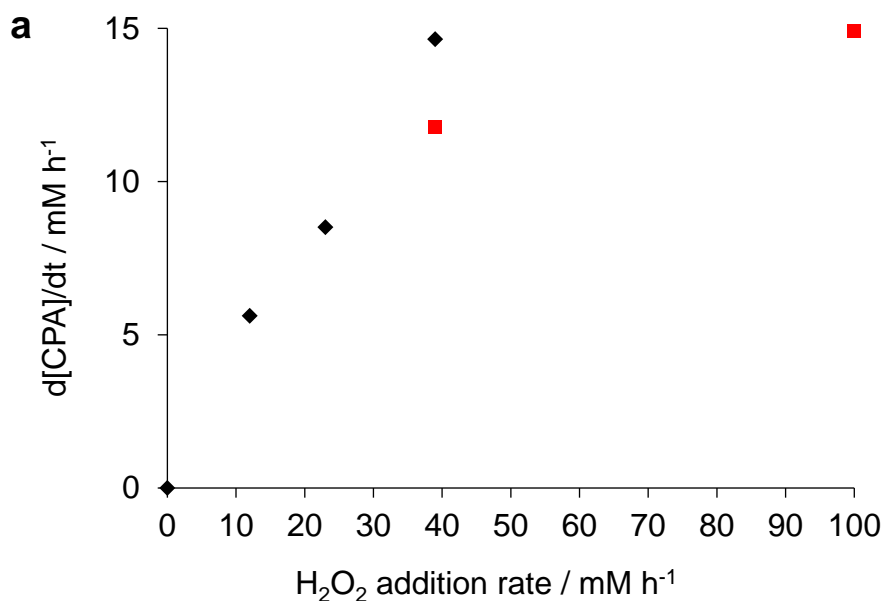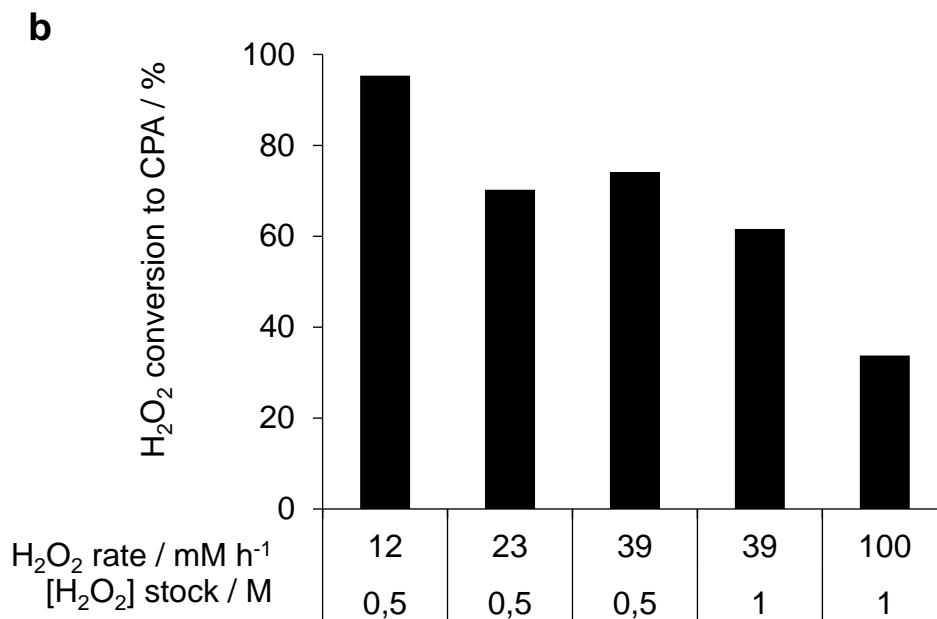
Figure 2. a) The correlation between the addition rate of H_2O_2 and the formation rate of the product (CPA). Reaction conditions: [glutamic acid] = 25 mM, [NaBr] = 0.5 mM, [ClVCPO] = 55 nM, H_2O_2-dosage: from a 0.5 M stock solution (◆) and from a 1 M stock solution (■), 20 mM sodium citrate buffer (pH 5.6), room temperature (22 °C). **b)** The yield in H_2O_2 as a function of the addition rate of H_2O_2.

The decrease H_2O_2 yield with increase in H_2O_2 addition rate we attribute to the above-mentioned undesired side reaction (Equation 1).[17]

$$H_2O_2 + OBr^- \xrightarrow{\text{spontaneous}} Br^- + H_2O + {}^1O_2$$

Equation 1. The formation of singlet oxygen by the spontaneous reaction between H_2O_2 and OBr^-.

In fact at a H_2O_2 addition rate of 100 mM, this reaction was so dominant that bubble formation was observed in the reaction vessel. Therefore, we limited the H_2O_2 addition rate to 39 mM h^{-1} for further experiments. Under these conditions, an average TF(ClVCPO) of more than 63 s^{-1} was calculated.

5.2.3 concentration of the co-catalyst Br⁻

Next, we varied the concentration of the Br⁻ co-catalyst (Figure 3). Interestingly, it turned out that the initially chosen 0.5 mM was already the optimal value as previously reported.[10] Lower concentrations resulted in reduced product formation rates while higher Br⁻ concentration seemingly did not influence the reaction rate.
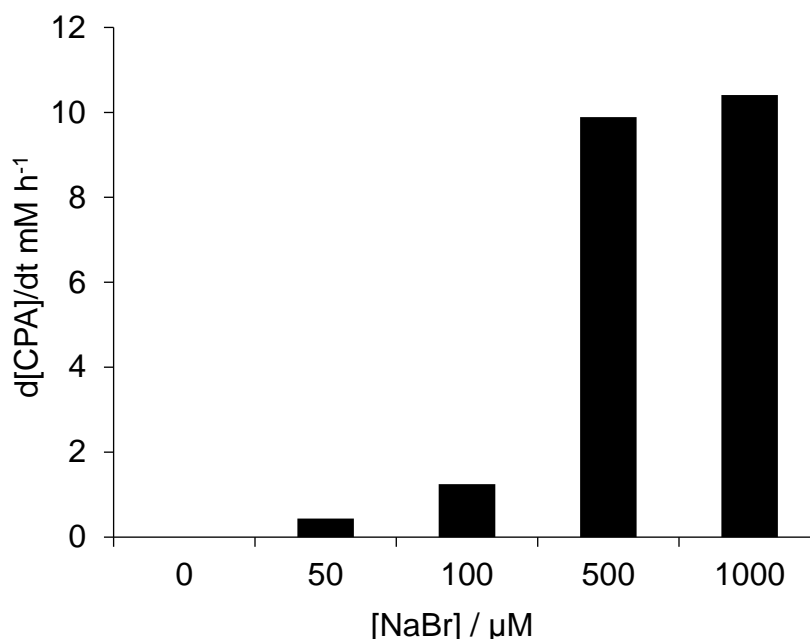
Figure 3. The influence of the concentration of NaBr on the overall CPA formation rate. Reaction conditions: [glutamic acid] = 25 mM, [*Ci*VCPO] = 55 nM, H_2O_2-dosage: 39 mM×h^{-1} from a 1 M stock solution, 20 mM sodium citrate buffer (pH 5.6), room temperature (22 °C).

5.2.4 Substrate loading

Next, the concentration of the glutamate in the reaction mixture was further raised to 100 mM. For reasons of solubility, we used sodium glutamate instead of glutamic acid (ensuring the pH of the final reaction mixture was 5.6 as in previous experiments). This switch had no significant influence on the rate of the reaction (Figure S2). Increasing the glutamate concentration to 100 mM gave excellent conversion rates and almost complete conversion (96%) of the starting material into the desired product (Figure 4).

Figure 4. Scale up of the oxidative decarboxylation of sodium glutamate ( ) to CPA ( ). [Sodium glutamate] = 100 mM, [NaBr] = 5 mM, [$CiVCPO$] = 55 nM, H_2O_2-dosage: 39 mM×h^{-1} from a 1 M stock solution, 20 mM sodium citrate buffer (pH 5.6), room temperature (22 °C). The error bars represent the range of duplicate experiments.
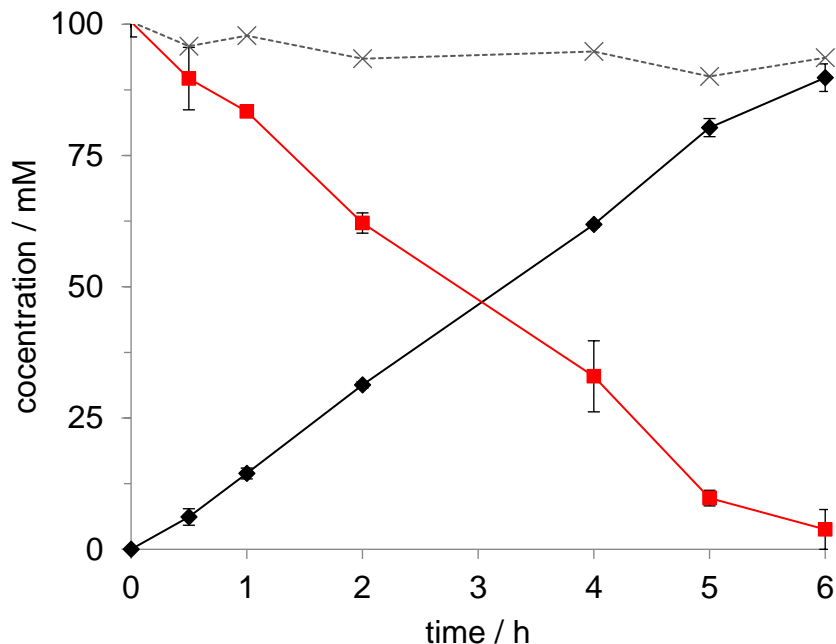
In these experiments, $CiVCPO$ performed excellent 1,630,000 turnovers at an average TF of 75 s^{-1}. Noteworthy, the H_2O_2 yield was also on average 80%. The latter observation may be attributed to an increased rate of the (desired) reaction between OBr$^-$ and gluta-mate over the (undesired) reaction with H_2O_2. Further increase of the glutamate concen-tration, however, did not lead to the anticipated improvements (Figure S3). On the con-trary, lower amounts of product (after prolonged reaction times) were obtained compared to the amounts shown in Figure 4. For example, using 500 mM glutamate resulted in only 31 mM of CPA after 24 h reaction.

5.2.5 Substrate/Product inhibition

We suspected substrate inhibition to account for this and therefore determined the $CiVCPO$ activity in the presence of different concentrations of glutamate (Figure 5). To our surprise, increasing glutamate concentrations showed limited influence on the activity

of *Ci*VCPO; even in the presence of 500 mM glutamate, its activity in the MCD assay was reduced by only 23%.

Next, the possibility of *Ci*VCPO inhibition by the product, 3-cyanopropanoic acid, was investigated (Figure 6). With increasing CPA concentration, the observed activity of *Ci*VCPO decreased. In the presence of 75 mM CPA, the enzyme activity was reduced by 50%, whereas in the presence of 200 mM, the enzyme lost almost entirely its activity in the MCD assay. It can be concluded that CPA, the product of oxidative decarboxylation, significantly inhibits *Ci*VCPO. Possibly, CPA coordinates to the prosthetic vanadate, thereby preventing the coordination of H_2O_2 to initiate the catalytic cycle but further studies will be necessary to fully elucidate the inhibitory mechanism.

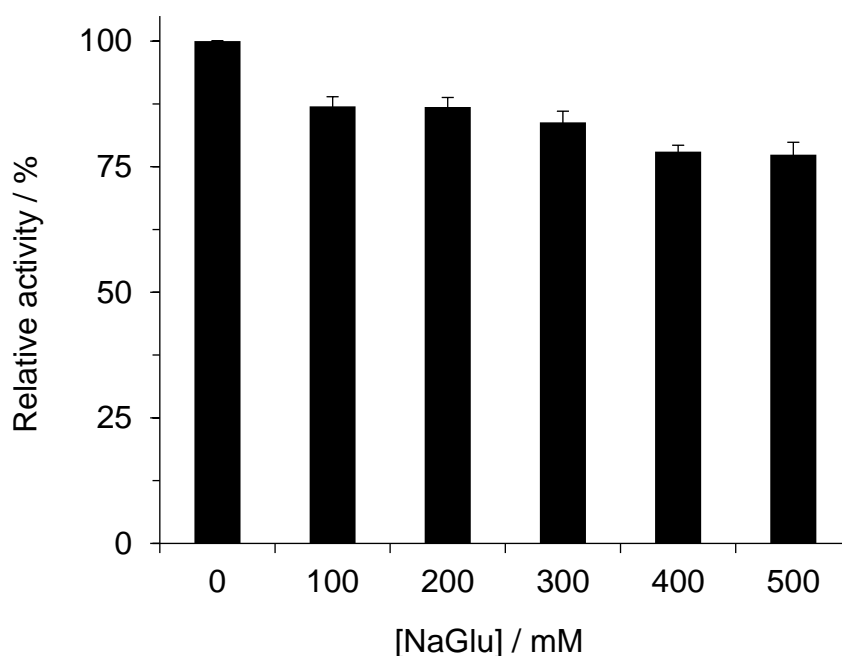**Figure 5**. Influence of sodium glutamate (NaGlu) on the activity of *Ci*VCPO. Assay conditions: [MCD]= 50 µM, [H_2O_2]= 1 mM, [NaBr]= 0.5 mM, [Na_3VO_4]= 100 µM, 50 mM sodium citrate buffer (pH 5), T= 25 °C, 290 nm. The reaction was started with the addition of 0.8 nM *Ci*VCPO that was pre-incubated for 5 min with different amounts of NaGlu. The error bars represent the standard deviation of triplicate experiments.

Figure 6. Inhibition of *Ci*VCPO by 3-cyanopropanoic acid (CPA). Assay conditions: [MCD]= 50 µM, [H$_2$O$_2$]= 1 mM, [NaBr]= 0.5 mM, [Na$_3$VO$_4$]= 100 µM, 50 mM sodium citrate buffer (pH 5), T= 25 °C, 290 nm. The reaction was started with the addition of 0.8 nM *Ci*VCPO that was pre-incubated for 5 min with different amounts of CPA. The error bars represent the standard deviation of triplicate experiments.
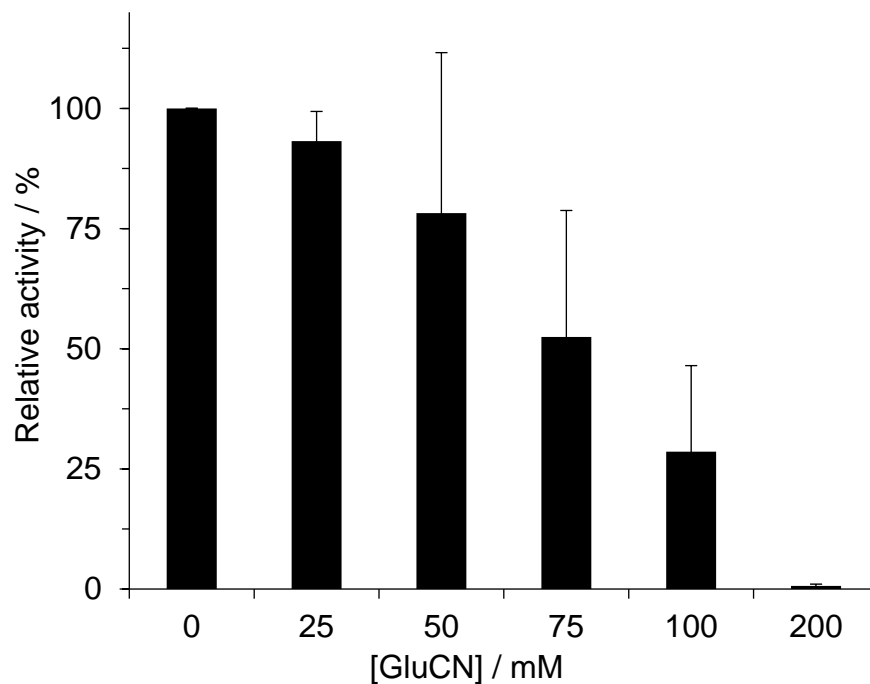
5.2.6 Semi-preparative reaction

Lastly, the oxidative decarboxylation of Glu by *Ci*VCPO was performed at a semi-preparative scale. From a 200 mL reaction scale (100 mM Glu), 0.827 g CPA (42% isolated yield, 96% pure) was obtained after 5 h reaction with 100 nM *Ci*VCPO. CPA was isolated by extraction in organic solvents, however, the extraction efficiency was low (see Experimental section). Based on the isolated yield, 420,000 turnovers were performed which is less than in the small scale (Figure 4), however, CPA remained in the aqueous phase even after the second extraction. The isolated yield is in agreement with previously reported chemical reaction with NaOCl/NaBr (43%),[18] but higher selectivity towards the nitrile was obtained by using *Ci*VCPO. Derivatisation to the corresponding ester or amide would certainly increase the efficiency of the extraction as demonstrated previously.[19] Also, continuous liquid-liquid extraction appears to be a promising method to increase the isolated yield. It is worth mentioning that the semi-preparative reaction was performed

without additional buffer (therefore less waste), and instead of the substrate, sodium glutamate was used as a buffer (where the pH was adjusted to pH 5.6 with H_2SO_4).

5.3 Conclusions

In conclusion, we demonstrate that the chemoenzymatic oxidative decarboxylation of glutamate is indeed a possible alternative to the established chemical and the new catalytic methods. The product inhibition and the isolation of the product are currently the main bottlenecks of this reaction which could be solved by selective *in situ* solid-phase extraction or by using a packed bed reactor with immobilised VCPO. Product isolation could be circumvented by direct conversion of CPA to a more hydrophobic product. Furthermore, this preparative scale opens the route towards the oxidative decarboxylation of other amino acids with different side chain functionalities and their corresponding nitriles.

5.4 Experimental section

5.4.1 Chemicals

L-glutamic acid (99.5% pure), sodium L-glutamate monohydrate (99% pure), NaBr (99.0% pure), H_2O_2 (50%, wt-%), citric acid, Na_3VO_4 (99.0% pure), MCD (monochlorodimedone), $HClO_4$ (70% pure) and H_2SO_4 (95-97% pure) were purchased from Sigma-Aldrich, 3-cyanopropanoic acid (95% pure) was provided by Interchim Uptima.

5.4.2 Enzyme preparation

Vanadium chloroperoxidase from *Curvularia inaequalis* (*Ci*VCPO) was obtained from heterologous expression in recombinant *Escherichia coli* and purified by heat treatment (see below).

***Ci*VCPO production.** *Ci*VCPO was obtained from heterologous expression in recombinant *E. coli* following a modified procedure.[1–6] Two 50 mL pre-precultures of LB medium containing 100 μg/mL of ampicillin were inoculated with 5 μL *E. coli* TOP10 pBADgIIIB

VCPO glycerol stock.[1–6] and incubated overnight at 37 °C and 180 rpm. Further, two precultures of 200 mL and 500 mL were inoculated with pre-preculture. The overexpression was carried out in a 15 L stirred tank fermenter. 13 L of TB medium containing 100 µg/mL of ampicillin was inoculated with 200 mL of pre-culture (OD_{600} = 4.08) to an OD of approx. 0.05 and incubated at 37 °C and 180 rpm. At OD_{600} = 1.0 (approx. 3 h), 15 mL 20% L-arabinose was added to reach a final inducer concentration of 0.02%. After induction, the culture was incubated for an additional 24 h at 25 °C and 180 rpm. The wet bacterial pellets obtained after centrifugation were washed with 50 mM Tris/H_2SO_4 buffer pH 8.2 and stored at -20 °C until processed as described below.

***Ci*VCPO purification.** About 30 g of wet cells were thawed on a hot water bath and re-suspended in 50 mM Tris/H_2SO_4 buffer pH 8.2 (0.5 g cells per mL). A spatula tip of DNase was added to the re-suspended cells, which were disrupted by sonication. The obtained suspension was centrifuged (10,000 rpm, 20 min), and the supernatant was incubated for 2×20 min at 70 °C (20 min were counted after the solution reached 70 °C). Each heat treatment was followed by centrifugation (10,000 rpm, 20 min) to remove the denatured proteins. The supernatant was concentrated and desalted by exchanging the buffer 4 times with Tris/H_2SO_4 buffer (50 mM, pH 8.2 + 100 µM Na_3VO_4) using Amicon membrane filters (30 kDa cut-off). The concentrated enzyme solution was stored at -20 °C in small aliquots (0.5 mL) until further use. The purity of the preparation was determined by SDS-PAGE comparing the band intensities by Image Lab™ software (version 6.0.1). The stock enzyme solution (approx. 10 mL) had a specific activity (based on monochlorodimedone assay) of 177 U/mg protein, a protein concentration of 2.85 mg/mL of which 78% *Ci*VCPO and a *Ci*VCPO concentration of 33 µM.

5.4.3 Enzymatic reaction conditions

In a 4 mL glass vial, a solution (2 mL starting volume) containing 0.5 mM NaBr, 55 nM *Ci*VCPO, different concentrations of glutamic acid or sodium glutamate monohydrate in 20 mM sodium citrate buffer (pH 5.6) was prepared. The reaction was started by the addition of H_2O_2, which was added with a continuous flow rate (see captions of figures) at room temperature (about 22 °C). The reaction was quenched by adding $Na_2S_2O_3$. For

each time point, a separate reaction vial was prepared. The conversion of Glu and the formation of CPA were analysed by two different HPLC methods (see below).

5.4.4 Enzyme activity assay

To assess *Ci*VCPO activity, a standardised assay reported previously was used.[20] In short: in a disposable UV plastic cuvette a solution (1 mL) containing 50 µM monochloro-dimedone (MCD), 1 mM H_2O_2, 0.5 mM NaBr, 100 µM Na_3VO_4 in 50 mM sodium citrate (pH 5.6) was prepared. The absorbance of MCD solution was followed at 290 nm, 25 °C. The reaction was started with the addition of *Ci*VCPO. The enzyme activity was calculated using a molar extinction coefficient for MCD of 20 mM^{-1} cm^{-1}. For the inhibition tests, the enzyme was incubated before the assay with different concentrations of inhibitor, for 5 min, at room temperature.

5.4.5 Semi-preparative reaction conditions

In a 500 mL round-bottom flask, an aqueous solution (200 mL deionised water) containing 100 mM monosodium glutamate monohydrate (3.78 g, 20 mmol) and 0.5 mM NaBr, was adjusted at pH 5.6 with a 2 M H_2SO_4 solution. Next, 100 nM *Ci*VCPO was added, and the reaction was started by the addition of H_2O_2 50 mM/h (10 mL of 1 M stock/h) by a syringe pump at room temperature (about 22 °C). After 5 h, the product was isolated by extraction in ethyl acetate and diethyl ether.

5.4.6 Product extraction from the semi-preparative reaction

The reaction mixture was acidified with H_2SO_4 at pH 3, saturated with NaCl and extracted with ethyl acetate (2×100 mL). The collected organic layers were dried over $MgSO_4$, and the solvent was evaporated. The ¹H NMR showed 3-cyanopropanoic acid as the main product (612 mg, 31% isolated yield, 96% purity). The ¹H NMR (water suppression) of the aqueous phase revealed the presence of unextracted nitrile. To increase the yield, an-other extraction was performed. For this, the aqueous phase was further acidified to pH 1

with H_2SO_4, extracted with diethyl ether (3×70 mL), dried over $MgSO_4$, and the solvent was evaporated and analysed by NMR. An additional 215 mg of 3-cyanopropanoic acid was isolated (97% pure based on NMR). Overall, 827 mg off-white oily solid (96-97% 3-cyanopropanoic acid, 42% isolated yield) was obtained.

5.4.7 Analysis

HPLC. Glutamic acid samples were analysed after appropriate dilution (0.05-5 mM range) in MQ water by a HPLC (Shimadzu) comprising LC-20AD pump, SIL-20AC HT autosampler, SPD-10A VP UV/Vis detector, and a CTO-20AC temperature-control unit. The column used was a Crownpak CR(+)/CR(-) column (150×4.0 mm, Chiral Technologies) with $HClO_4$ (pH 1.5, 10 °C, 0.5 mL/min, 210 nm). Retention time glutamic acid 13.1 min.

3-cyanopropanoic acid samples were analysed after appropriate dilution (0.1-100 mM range) in MQ water by a HPLC (Shimadzu) comprising of an LC-20AT pump, SIL-20A HT autosampler, RID 10A detector and a CTO-20A temperature-control unit. Detection was achieved by a refractive index detector set at 40 °C. The column used was an organic acid column CARBOSep CoreGel 87H3 (7.8×300 mm, Transgenomic) with H_2SO_4 (10 mM, 60 °C, 0.75 mL/min). Retention time 3-cyanopropanoic acid 14.1 min.

The yield in H_2O_2 (%) was calculated with the following formula: yield = $[CPA]_{t=x}$ / ($[H_2O_2]_{t=x}$ / 2)×100, where $[CPA]_{t=x}$ is the concentration of CPA at time x and $[H_2O_2]_{t=x}$ is the concentration of H_2O_2 added up to time x.

NMR. NMR spectra were recorded using an Agilent 400 MHz (^1H, 9.4 Tesla) spectrometer operating at 399.67 MHz for ^1H at 298 K. Water suppression was performed by using a PRESAT pulse sequence. 3-cyanopropanoic acid: ^1H NMR (400 MHz, D_2O): δ = 2.81-2.78 (t, 2H), δ = 2.76-2.74 (t, 2H); ^{13}C NMR (400 MHz, D_2O): δ = 174.9, 120.7, 29.3, 12.4.

References

1. G. J. S. Dawes, E. L. Scott, J. Le Nôtre, J. P. M. Sanders, J. H. Bitter, *Green Chem.* **2015**, *17*, 3231.

2. J. C. Philp, R. J. Ritchie, J. E. M. Allan, *Trends Biotechnol.* **2013**, *31*, 219.

3. J. J. Bozell, G. R. Petersen, *Green Chem.* **2010**, *12*, 539.

4. R. A. Sheldon, J. M. Woodley, *Chem. Rev.* **2018**, *118*, 801.

5. R. A. Sheldon, *ACS Sustain. Chem. Eng.* **2018**, *6*, 32.

6. H. L. Chum, R. P. Overend, *Fuel Process. Technol.* **2001**, *71*, 187.

7. T. M. Lammens, M. C. R. Franssen, E. L. Scott, J. P. M. Sanders, *Biomass Bioenergy* **2012**, *44*, 168.

8. L. Claes, J. Verduyckt, I. Stassen, B. Lagrain, D. E. D. Vos, *Chem. Commun.* **2015**, *51*, 6528.

9. R. Matthessen, L. Claes, J. Fransaer, K. Binnemans, D. E. De Vos, *Eur. J. Org. Chem.* **2014**, *2014*, 6649.

10. A. But, A. van Noord, F. Poletto, J. P. M. Sanders, M. C. R. Franssen, E. L. Scott, *Mol. Catal.* **2017**, *443*, 92.

11. A. But, J. Le Nôtre, E. L. Scott, R. Wever, J. P. M. Sanders, *ChemSusChem* **2012**, *5*, 1199.

12. Y. Ni, D. Holtmann, F. Hollmann, *ChemCatChem* **2014**, *6*, 930.

13. G. T. Höfler, A. But, F. Hollmann, *Org. Biomol. Chem.* **2019**, *17*, 9267.

14. J. W. P. M. van Schijndel, E. G. M. Vollenbroek, R. Wever, *Biochim. Biophys. Acta BBA - Protein Struct. Mol. Enzymol.* **1993**, *1161*, 249.

15. J. W. P. M. Van Schijndel, P. Barnett, J. Roelse, E. G. M. Vollenbroek, R. Wever, *Eur. J. Biochem.* **1994**, *225*, 151.

16. A. M. Held, D. J. Halko, J. K. Hurst, *J. Am. Chem. Soc.* **1978**, *100*, 5732.

17. R. Renirie, C. Pierlot, J. M. Aubry, A. F. Hartog, H. E. Schoemaker, P. L. Alsters, R. Wever, *Adv. Synth. Catal.* **2003**, *345*, 849.

18. J. L. Nôtre, E. L. Scott, M. C. R. Franssen, J. P. M. Sanders, *Green Chem.* **2011**, *13*, 807.

19. T. M. Lammens, J. Le Nôtre, M. C. R. Franssen, E. L. Scott, J. P. M. Sanders, *ChemSusChem* **2011**, *4*, 785.

20. R. Wever, P. Barnett, *Chem. Asian J.* **2017**, *12*, 1997.
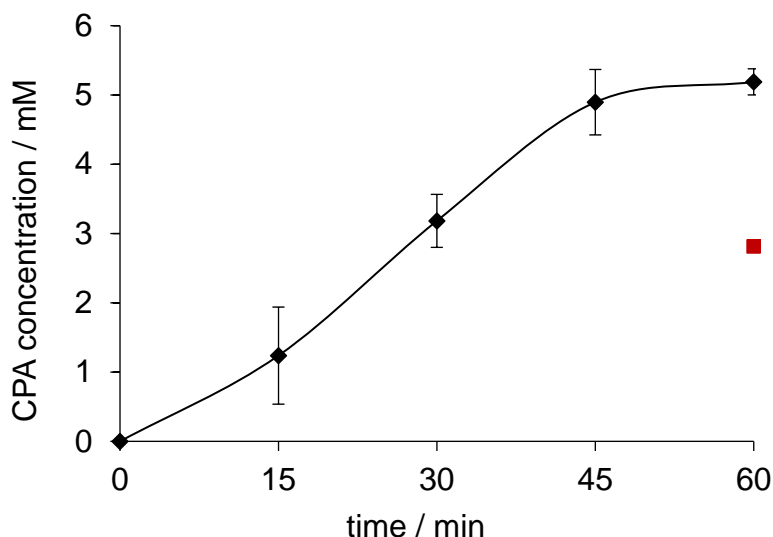
Supplementary Information

Figure S1. The conversion of 5 mM glutamic acid into CPA by continuous addition of H_2O_2 (◆) and by addition of H_2O_2 all (12 mM) at the beginning of the reaction (■). Reaction conditions: [glutamic acid] = 5 mM, [NaBr] = 0.5 mM, [*Ci*VCPO] = 55 nM, H_2O_2-dosage: 12 mM×h^{-1} (from a 0.5 M stock solution), 20 mM sodium citrate buffer (pH 5.6), room temperature (22 °C). The error bars represent the range of duplicate experiments.
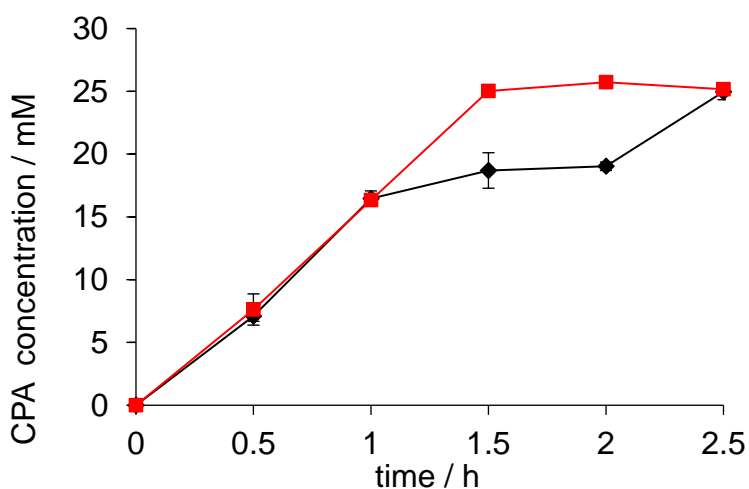
Figure S2. The conversion of 25 mM glutamic acid (◆) and sodium glutamate (■) into 3-cyanopropanoic acid. Reaction conditions: [glutamic acid/sodium glutamate] = 5 mM, [NaBr] = 0.5 mM, [*Ci*VCPO] = 55 nM, H_2O_2-dosage: 39 mM×h^{-1} (from a 1 M stock solution), 20 mM sodium citrate buffer (pH 5.6), room temperature (22 °C). The error bars represent the standard deviation of triplicate experiments.
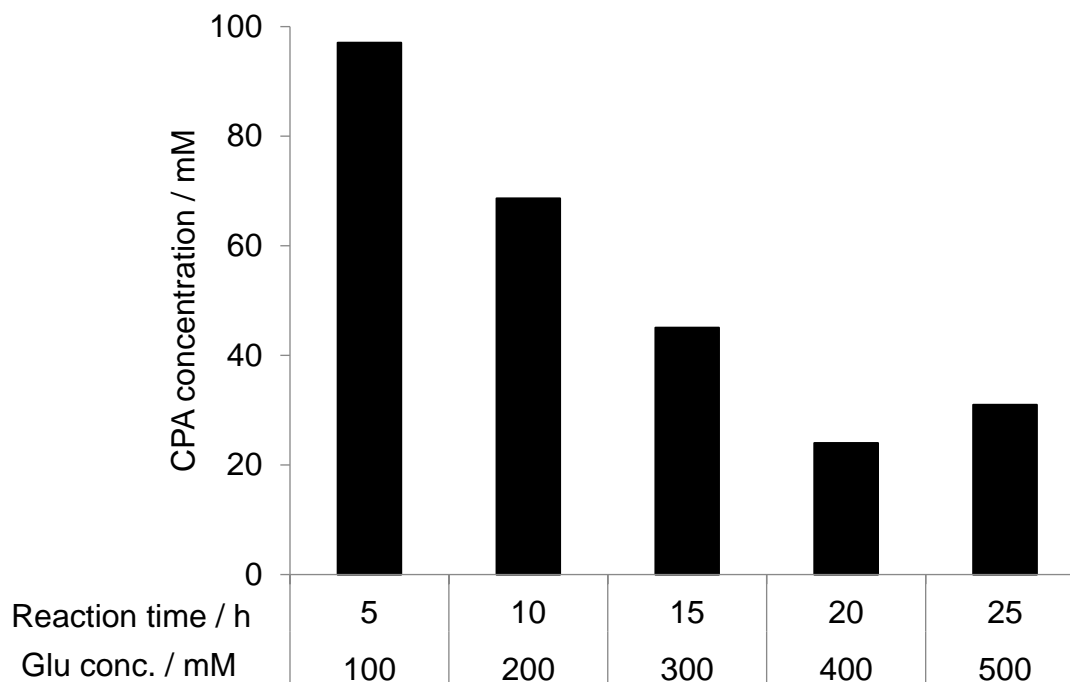
Figure S3. The conversion of sodium glutamate (different concentrations) into 3-cyanopropanoic acid. Reaction conditions: [NaBr] = 0.5 mM, [ClVCPO] = 55 nM, H_2O_2-dosage: 39 mM×h^{-1} (from a 1 M stock solution), 20 mM sodium citrate buffer (pH 5.6), room temperature (22 °C).
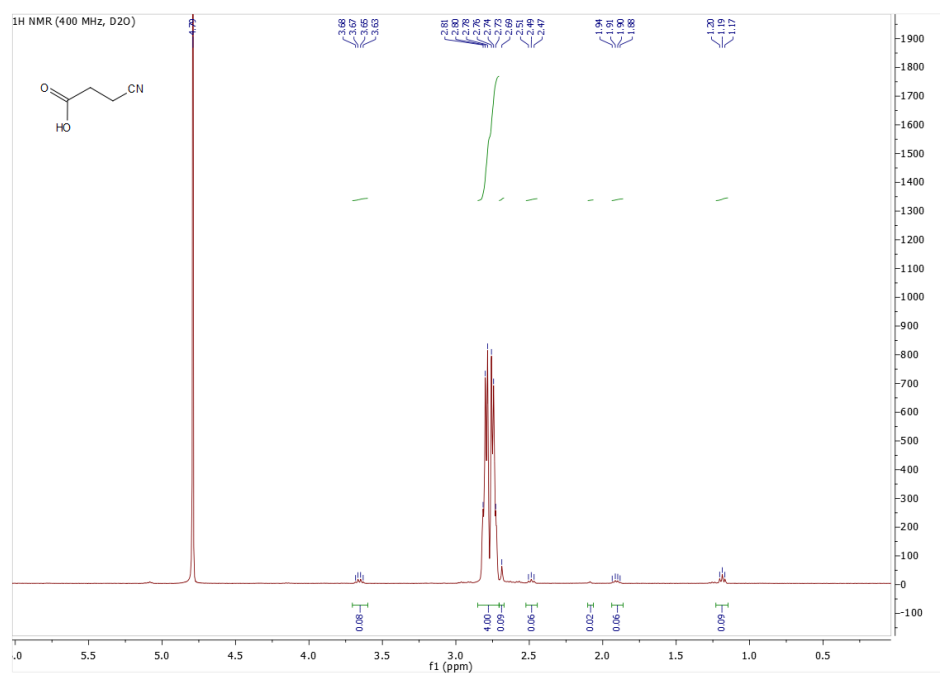
Figure S4. ^{1}H NMR of isolated 3-cyanopropanoic acid.

13C NMR (400 MHz, D2O)

174.93 120.74 29.29 12.41

f1 (ppm)
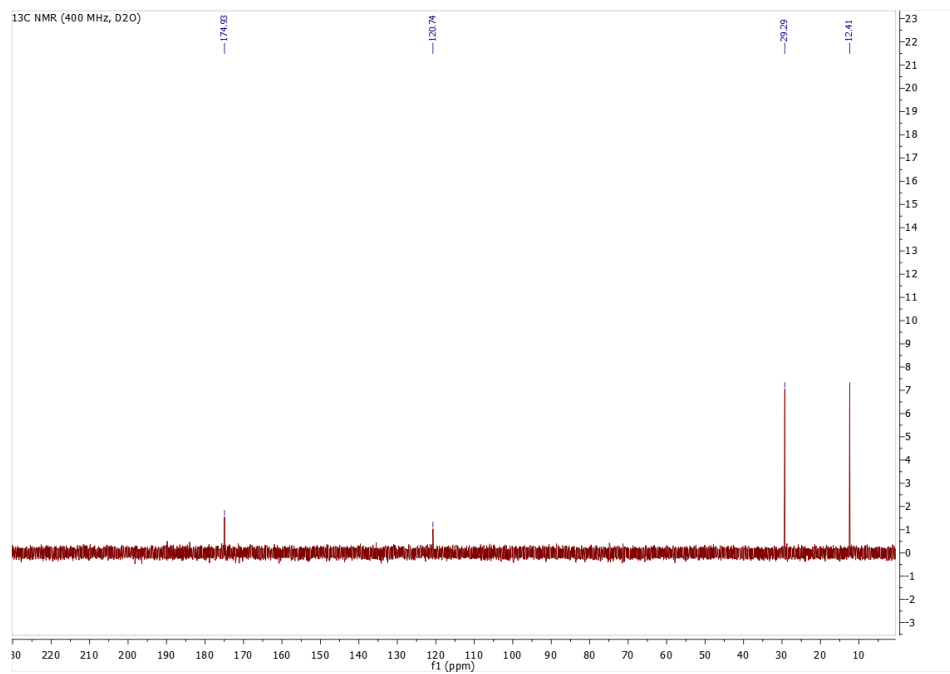
Figure S5. ^{13}C NMR of isolated 3-cyanopropanoic acid.

6

Peroxygenase-catalysed enantioselective hydroxylation of ethylbenzene derivatives driven by formate oxidase

The innovative formic acid oxidase from *Aspergillus oryzae* (*Ao*FOx) is an attractive catalyst for the generation of H_2O_2 with the oxidation of formic acid to CO_2. In this study, the *Ao*FOx was used to drive the r*Aae*UPO-catalysed hydroxylation of ethylbenzene derivatives. The combined enzyme system demonstrated a promising catalytic performance, a turnover number of 115,000 for both *Ao*FOx and r*Aae*UPO was obtained. However, the investigation of factors such as formate and enzyme spiking, pH, oxidase concentration, co-solvent, O_2 supply and production inhibition did not solve the premature ending of the reaction. In our opinion, the nature of the electronic donor for *Ao*FOx could be the breakthrough.

Xiaomin Xu, Caroline Paul, Frank Hollmann

6.1 Introduction

Chirality is very important for the targeted efficiency of many drugs.[1] Biocatalysts are increasingly applied to the manufacture of chiral intermediates as enzyme-catalysed reactions are selective and usually carried out under mild conditions,[2–4] which avoid the annoying problems of racemization, isomerization and compound rearrangement under extreme reaction conditions.[5]

Unspecific peroxygenases from *Agrocybe aegerita* (r*Aae*UPO) can catalyse the enantioselective hydroxylation of ethylbenzene into (*R*)-1-phenylethanol. As a heme-dependent enzyme, one of the main limitations of UPOs is a lack of resistance to H_2O_2. In order to make such H_2O_2-sensitive enzymes practical, biochemists are continuously trying to find a proper H_2O_2 generation system.[6] Formic acid oxidase from *Aspergillus oryzae* can oxidise formic acid to H_2O_2 and CO_2 without any byproducts,[7] representing a cleaning and promising H_2O_2 generation method. The aim of this study was to convert ethylbenzene derivatives to the corresponding (*R*)-1-phenylethanol derivatives using the *Ao*FOx-UPO combinatorial system and to investigate its reaction limitations.

6.2 Results and Discussion

6.2.1 Substrate scope

We first evaluated the substrate scope of r*Aae*UPO fuelled by *Ao*FOx (Table 1). Pleasingly, nearly all of the ethylbenzene derivatives **1-15a** tested could be converted to the corresponding alcohols **1-15b** under the combination of *Ao*FOx and r*Aae*UPO, with the exception of the *tert*-butyl substituted substrate **14a**. Moreover, according to previous reports,[7–9] while r*Aae*UPO converts ethylbenzene to (*R*)-1-phenylethanol, it also over-oxidises (*R*)-1-phenylethanol into the corresponding ketone. Thus, a proportion of acetophenone derivatives **1-15c** were also produced in this series of substrate range reactions (Table 1).

Table 1. Substrate scope of the enantioselective hydroxylation of ethylbenzene derivatives with *Ao*FOx and r*Aae*UPO.[a]

Substrate **a**		Alcohol[b] [mM] **b**	*ee* [%]	Ketone [mM] **c**	TON[c]
	1a	18.3	99	1.4	21,200
	2a	8.6	99	4.6	17,800
	3a	10.2	99	4.2	18,560
	4a	7.2	99	5.1	17,440
	5a	4.3	99	2.5	9,190
	6a	7.1	99	4.1	15,240
	7a	6.0	99	3.1	12,060
	8a	1.7	99	8.4	18,500
	9a	14.0	99	2.3	18,580
	10a	15.1	99	1.6	18,290
	11a	0.6	99	1.4	3,310
	12a	12.4	99	2.6	17,510
	13a	6.4	96	1.7	98,00
	14a	0	-	0	0
	15a	1.2	n.d[d]	0.9	3,000

[a] Reaction conditions: [substrate] = 50 mM, [r*Aae*UPO] = 1 µM, [*Ao*FOx] = 1 µM, [formate] = 250 mM, [ACN] = 10% v/v, 100 mM KPi buffer (pH 6.0), 25 °C , 600 rpm, 24 h. [b] The concentrations of **6-8a**,**10-12a** alcohol products were calculated using the calibration curves of the corresponding ketone. [c] TON = [product]/[enzyme]. [d] n.d = not determined. Data presented are an average of triplicates.

The *Ao*FOx-UPO combinatorial system showed promising catalytic performance. Encouraged by the above results, a series of experiments were conceived to further understand this system and increase turnover numbers.

6.2.2 Exploring factors influencing the overall reaction

We selected *p*-chloroethylbenzene as a model substrate for further investigation of the *Ao*FOx-UPO combinatorial system. As shown in Figure 1, 21 mM of *p*-chlorophenylethanol and 47 mM of *p*-chloroacetophenone with a turnover number of 115,000 for both *Ao*FOx and r*Aae*UPO has been obtained.
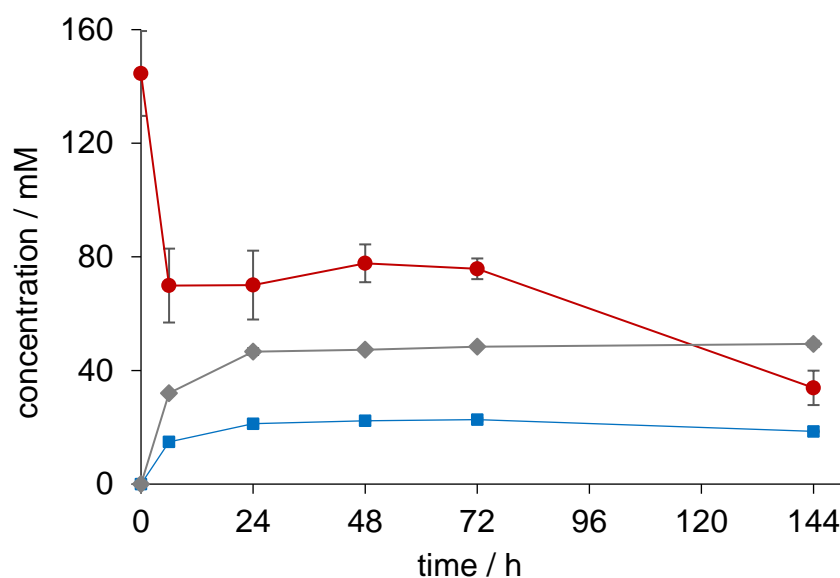
Figure 1. Time course of *p*-chloroethylbenzene hydroxylation. red: *p*-chloroethylbenzene, blue: p-chlorophenylethanol, grey: p-chloroacetophenone. Reaction conditions: [*p*-chloroethylbenzene] = 100 mM, [formate] = 250 mM, [r*Aae*UPO] = 1 µM, [*Ao*FOx] = 1 µM, 100 mM KPi buffer (pH 6.0), 25 °C, 600 rpm, 144 h. The error bars represent the standard deviation of duplicate experiments.

Initially, the reaction proceeded smoothly with a satisfying reaction rate. However, after 5 h, the concentration of each component remained constant, with a decrease in the *p*-chloroethylbenzene after three days most likely due to evaporation. Interestingly, r*Aae*-UPO is known to continuously catalyse the oxidation of ethylbenzene for more than 24 h

with H_2O_2 feeding.[10] To further understand why the catalytic reaction stopped after 5 h, we attempted to investigated possible reaction parameters and their influence on the overall reaction.

It should be noted that, due to the volatility of the substrates and products, the following results have more or less of mass balance issues.

6.2.2.1 Effect of the enzyme spiking

One possible reason may be poor stability of one of the enzymes. To confirm that the reaction contained sufficient amounts of active enzymes, we performed experiments by spiking the reaction mixtures with fresh enzyme after 5 h (Figure 2).

Figure 2. Effect of enzyme addition. red: *p*-chloroethylbenzene, blue: *p*-chlorophenylethanol, grey: *p*-chloroacetophenone. Reaction conditions: [*p*-chloroethylbenzene] = 100 mM, [formate] = 250 mM, [r*Aae*UPO] = 1 µM, [*Ao*FOx] = 1 µM, 100 mM KPi buffer (pH 6.0), 25 °C, 600 rpm, after 5 h, the reaction mixture was supplement with 1 µM r*Aae*UPO, 1 µM *Ao*FOx, or 1 µM r*Aae*UPO and 1 µM *Ao*FOx, all of the samples were incubated overnight. The error bars represent the standard deviation of duplicate experiments.

Interestingly enough, none of the spiking experiments increased the overall product formation. Reactions did not seem to restart after the fresh enzymes was added, therefore another factor must be influencing the premature ending of the reaction.

6.2.2.2 Effect of pH

We postulated the pH of the reaction may be the problem, with the formation of carbonate CO_3^{2-} during the reaction that may affect the pH. We therefore used up to 500 mM of buffer to ensure that the pH of the reaction remain stable at pH 6. However, from the results in Figure 3, with different buffer concentrations, product formation was the same over 24 h.
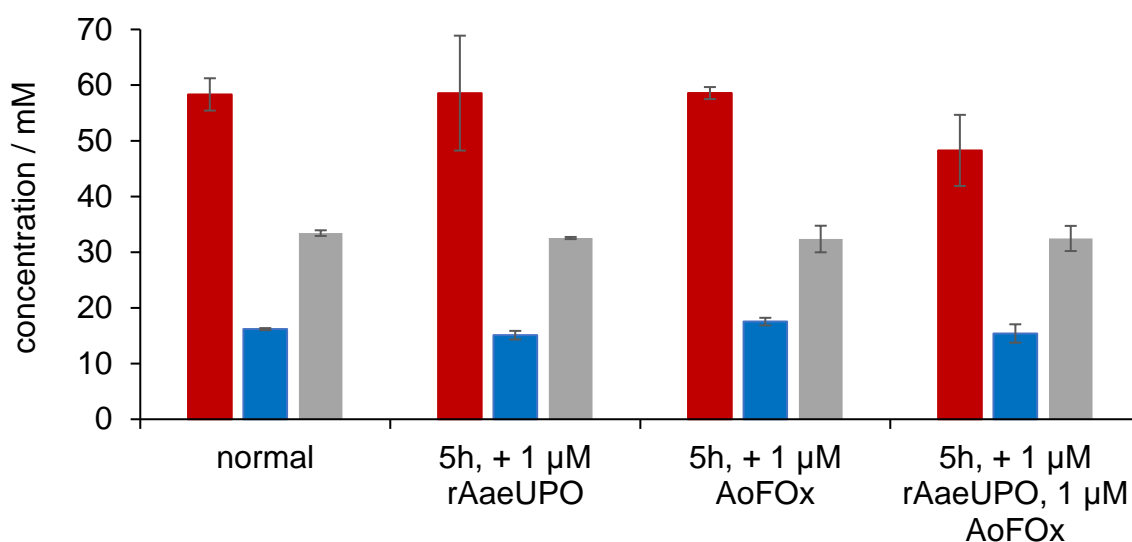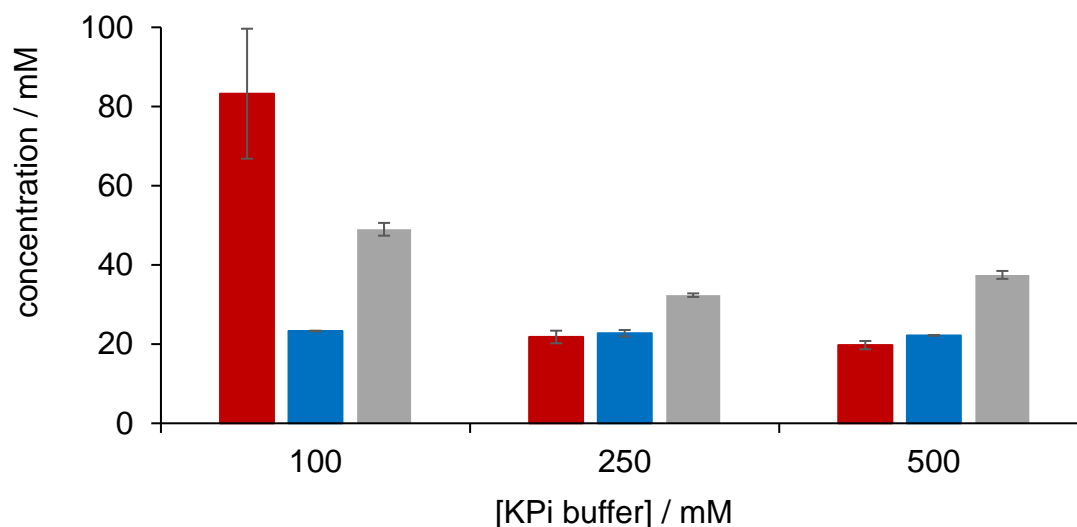

Figure 3. Effect of pH. red: *p*-chloroethylbenzene, blue: *p*-chlorophenylethanol, grey: *p*-chloroacetophenone. Reaction conditions: [*p*-chloroethylbenzene] = 100 mM, [formate] = 100-250 mM, [r*Aae*UPO] = 1 μM, [*Ao*FOx] = 1 μM, 100 mM KPi buffer (pH 6.0), 25 °C, 600 rpm, 24 h. The error bars represent the standard deviation of duplicate experiments.

6.2.2.3 Effect of the oxidase concentration

The next possible reason would be H_2O_2, because H_2O_2 is known to irreversibly inactivate r*Aae*UPO. The concentration of oxidase-*Ao*FOx determined the H_2O_2 generation rate. Therefore, we performed a series of experiments at various oxidase concentrations.
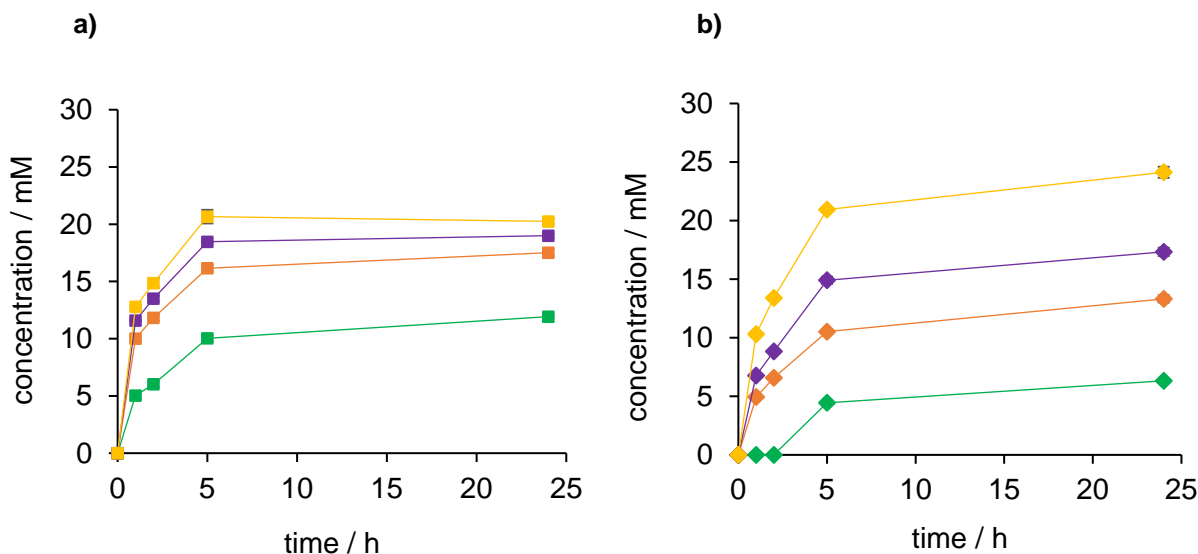
Figure 4. Effect of the H_2O_2 concentration. **a)** *p*-chlorophenylethanol (left, square), **b)** *p*-chloroacetophenone (right, diamond). green: 0.1 µM *Ao*FOx, orange: 0.6 µM *Ao*FOx, purple: 1 µM *Ao*FOx, yellow: 2 µM *Ao*FOx. Reaction conditions: [*p*-chloroethylbenzene] = 100 mM, [formate] = 250 mM, [r*Aae*UPO] = 1 µM, [*Ao*FOx] = 0.1-2 µM, [ACN] = 10% v/v, 100 mM KPi buffer (pH 6.0), 25 °C, 600 rpm, 24 h. The error bars represent the standard deviation of duplicate experiments.

As shown in Figure 4, there is certainly a positive effect of the concentration of *Ao*FOx on reaction initial rate. However, regardless of the concentration of *Ao*FOx, the reaction always stopped within 5 h. So the concentration of oxidase cannot explain why the reaction stops at 5 h.

6.2.2.4 Effect of the co-solvent

Next, we wondered if the substrate solubility may be the issue. The use of co-solvents in biocatalysis can enhance the solubility of hydrophobic substrates in aqueous phase, which may promote the reaction.[10] Therefore, a range of experiments in the presence of acetonitrile were performed.
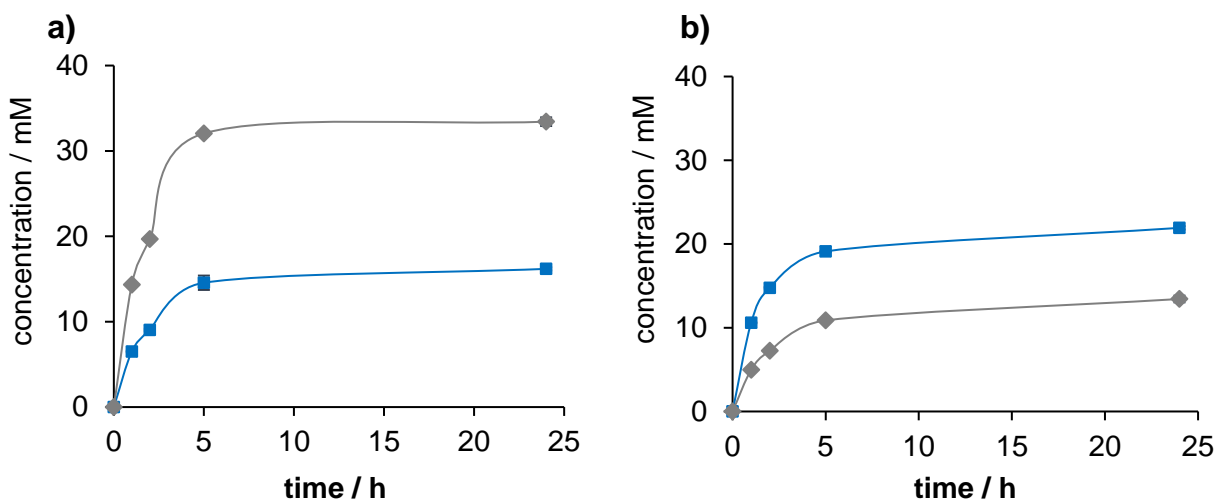
Figure 5. Effect of the co-solvent. **a)** no co-solvent, **b)** acetonitrile as co-solvent. blue: (*R*)-*p*-chlorophenylethanol, grey: *p*-chloroacetophenone. Reaction conditions: [*p*-chloroethylbenzene] = 100 mM, [formate] = 250 mM, [r*Aae*UPO] = 1 µM, [*Ao*FOx] = 1 µM, [ACN] = 10% v/v, 100 mM KPi buffer (pH 6.0), 25 °C, 600 rpm, 24 h. The error bars represent the standard deviation of duplicate experiments.

Interestingly, there was a pronounced change, wherein the acetonitrile co-solvent did not influence the amount of (*R*)-*p*-chlorophenylethanol but reduced the amount of the over-oxidised product *p*-chloroacetophenone (Figure 5), which may be due to a change in kinetic parameters.[10] However, we still could not find an explanation for the reaction stopping at 5 h.

6.2.2.5 Effect of O$_2$

Next, we suspected that it could be a problem of insufficient O$_2$ supply, as *Ao*FOx requires O$_2$. It is possible that with the reaction proceeding, the O$_2$ in reaction vial was consumed and its concentration decreased, which may have made the reaction unable to proceed.

Figure 6. Effect of the O_2 supply. red: *p*-chloroethylbenzene, blue: *p*-chlorophenylethanol, grey: *p*-chloro-acetophenone. Reaction conditions: [*p*-chloroethylbenzene] = 100 mM, [formate] = 250 mM, [r*Aae*UPO] = 1 μM, [*Ao*FOx] = 1 μM, [ACN] = 10% v/v, 100 mM KPi buffer (pH 6.0), 25 °C, 600 rpm, 24 h.

Therefore, in the following experiments, we adopted two ways to increase O_2 supply. The first was to decrease the reaction volume from 200 μL to 100 μL in the same vial, so that the O_2 supply per unit volume of the reaction was doubled. The second approach was to use a balloon filled with pure O_2 connected to the reactor through a tube to supply O_2 for the reaction. As can be seen in Figure 6, both methods to increase O_2 supply had no effect on the product formation over 24 h.

6.2.2.6 Effect of formate spiking

Then, it was assumed that after 5 h, the concentration of formate in the reaction was not sufficient enough and cause the reaction to stop. We therefore proceeded the experiment by spiking the reaction mixture with fresh formate after 5 h.
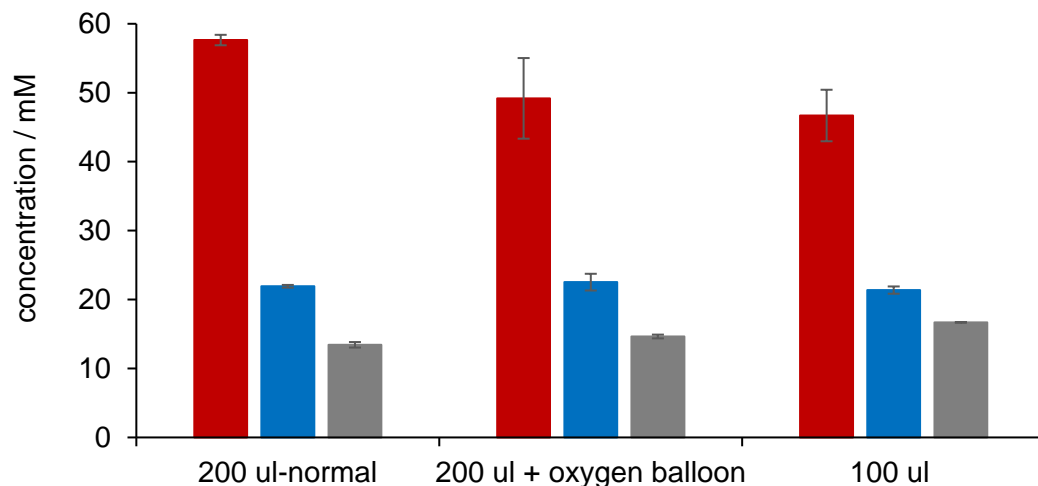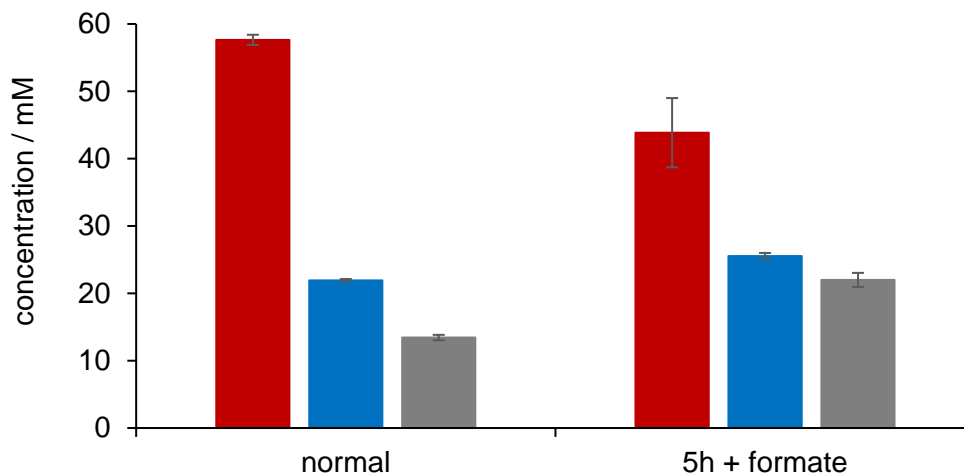
Figure 7. Effect of formate spiking. red: *p*-chloroethylbenzene, blue: *p*-chlorophenylethanol, grey: *p*-chloro-acetophenone. Reaction conditions: [*p*-chloroethylbenzene] = 100 mM, [formate] = 250 mM, [r*Aae*UPO] = 1 µM, [*Ao*FOx] = 1 µM, 100 mM KPi buffer (pH 6.0), 25 °C, 600 rpm, after 5 h, the reaction mixture was supplement with 250 mM formate, all of the samples were incubated overnight. The error bars represent the standard deviation of duplicate experiments.

From Figure 7, none of the spiking experiments increased the overall product formation. The addition of a fresh formate did not promote the reactions. Formate concentration also did not seem to be the main reason for the reactions stopping after 5 h.

6.2.2.7 Effect of ketone inhibition

Next, we investigated the issue of product inhibition of the enzyme. The final consideration was the possibility products would inhibit enzyme. For this purpose, 50 mM of *p*-chloro-acetophenone was added to the hydroxylation of ethylbenzene. It is noteworthy that, the addition of *p*-chloroacetophenone did not affect the behaviour of the enzymes (Figure 8).
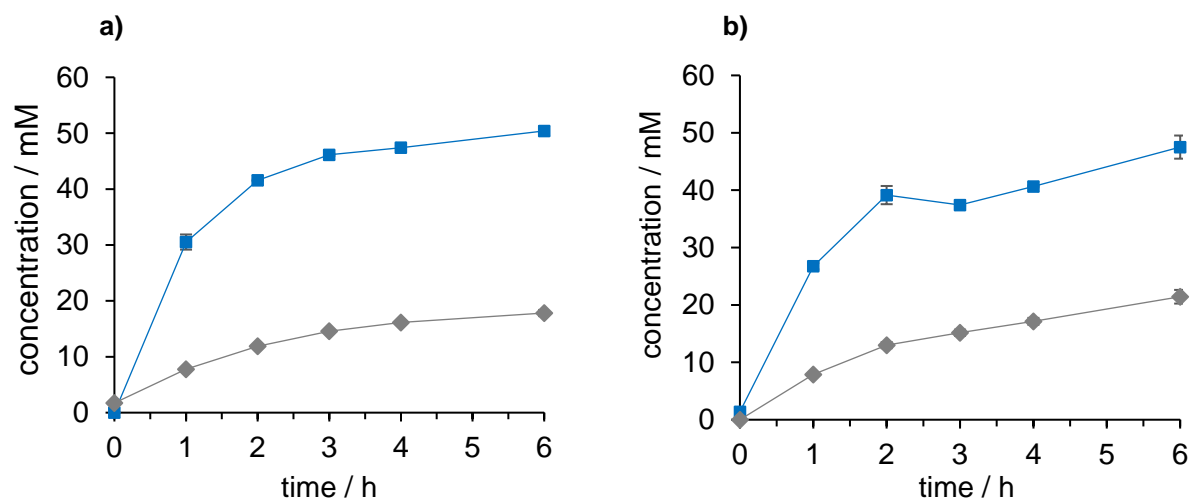
Figure 8. Effect of ketone inhibition. blue: (*R*)-phenylethanol, grey: acetophenone, **a)** normal, **b)** with 50 mM *p*-chloroacetophenone. Reaction conditions: [ethylbenzene] = 100 mM, [*p*-chloroacetophenone] = 50 mM, [formate] = 250 mM, [r*Aae*UPO] = 1 µM, [*Ao*FOx] = 1 µM, 100 mM KPi buffer (pH 6.0), 25 °C, 600 rpm, 6 h. The error bars represent the standard deviation of duplicate experiments.

Since *p*-chlorophenylethanol can be oxidised by r*Aae*UPO, adding *p*-chlorophenylethanol to ethylbenzene reaction may affect the results. We have not yet discovered a suitable method to test *p*-chlorophenylethanol inhibition.

6.2.2.8 Effect of carbonate inhibition

Does the carbonate formed during the reaction inhibit the enzyme activity? A range of carbonate concentrations were tested for their influence on *Ao*FOx and r*Aae*UPO activity.
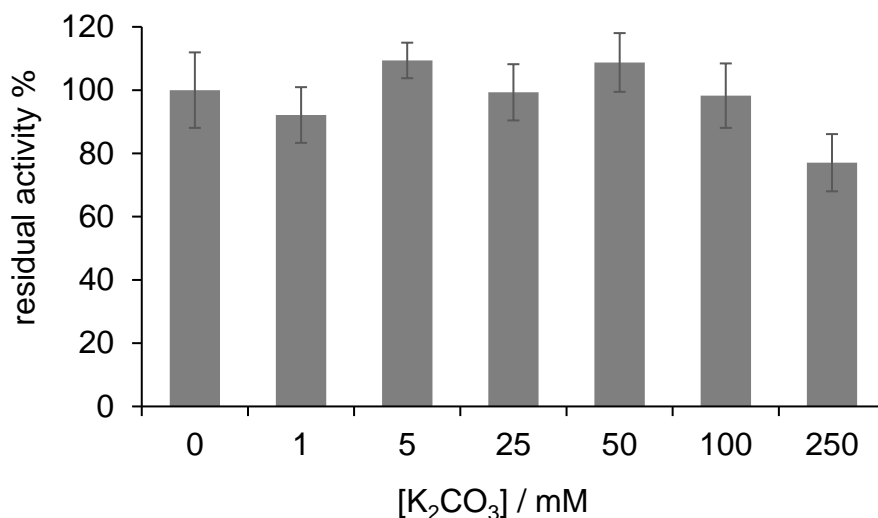
Figure 9. Influence of K_2CO_3 on the activity of r*Aae*UPO. ABTS assay conditions: [ABTS]= 0.5 mM, [H_2O_2]= 2 mM, [K_2CO_3] = 0-250 mM, 50 mM sodium citrate buffer (pH 4.4), T = 25 °C, 420 nm. 1 µM of enzyme was pre-incubated for 5 min in K_2CO_3 solutions. The error bars represent the standard deviation of triplicate experiments.
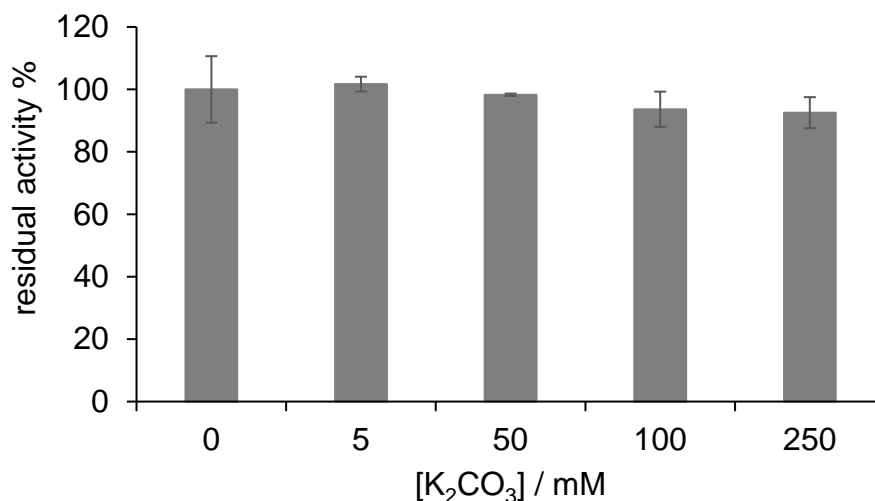
Figure 10. Influence of K_2CO_3 on the activity of *Ao*FOx. ABTS assay conditions: [ABTS] = 1 mM, [sodium formate] = 100 mM, [Horseradish peroxidase] = 10 U, [K_2CO_3] = 0-250 mM, 50 mM acetate buffer (pH 4.5), T = 25 °C, 420 nm. 1 µM of enzyme was pre-incubated for 5 min in K_2CO_3 solutions. The error bars represent the standard deviation of triplicate experiments.

As can be seen from Figures 9-10, the upside is that the effect of carbonate on enzyme activity was not significant. Therefore carbonate is probably not the reason for the reaction stopped within 5 h.

6.2.2.9 Effect of the electron donor

Formate oxidase (*Ao*FOx) can use methanol (MeOH) or formate as the electron donor,[8] thus we considered whether it was the electron donor that affected the reaction.
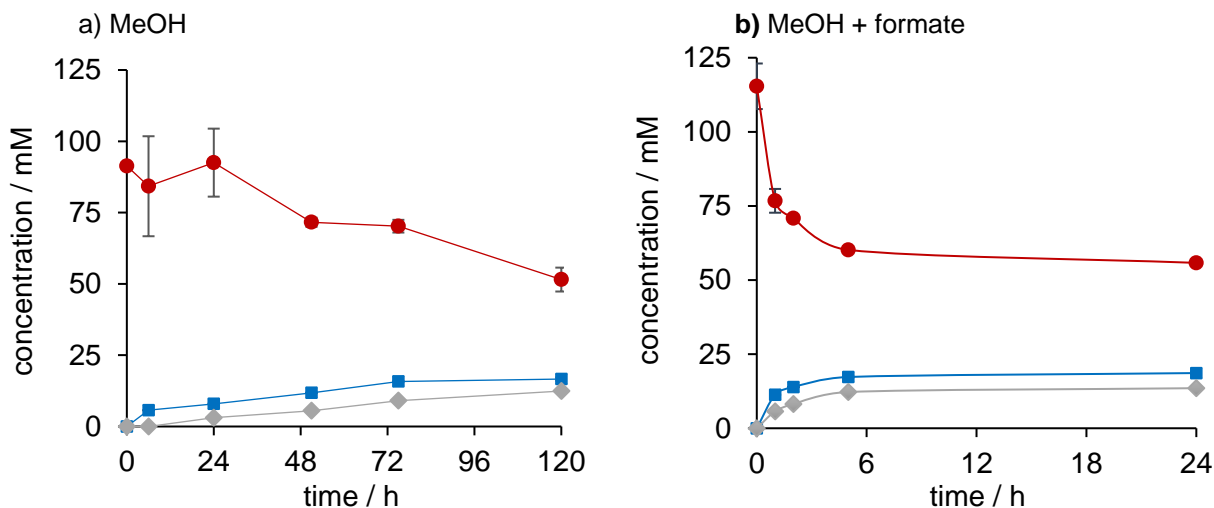
Figure 11. Effect of the electron donor. red: *p*-chloroethylbenzene, blue: *p*-chlorophenylethanol, grey: *p*-chloroacetophenone. Reaction conditions: [*p*-chloroethylbenzene] = 100 mM, [MeOH]= 10% v/v, [r*Aae*UPO] = 1 µM, [*Ao*FOx] = 1 µM, 100 mM KPi buffer (pH 6.0), 25 °C, 600 rpm, 120-150 h. The error bars represent the standard deviation of duplicate experiments.

Figure 11 can provide some information. When methanol was used as the electron donor, the reaction rate was relatively slow (TON 950 h^{-1}), but it could last for approximately 75 h. When both formate and MeOH were present, the reaction stopped at 5 h. It seems that there was a competitive relationship between formate and MeOH, with *Ao*FOx preferentially using formate, and this can be supported by the kinetic parameters of *Ao*FOx.[8]

Therefore, it is reasonable to suspect that by using formate as an electron donor, the catalytic rate of *Ao*FOx was relatively fast, but its stability was poor. By using MeOH as an electron donor, the catalytic rate of *Ao*FOx would be slow, but its stability would be better.

6.3 Conclusions

In conclusion, the *Ao*FOx-UPO combination system showed promising catalytic performance in the hydroxylation of ethylbenzene derivatives. However, the reaction usually stopped at 5 h. The investigation of factors such as formate and enzyme spiking, pH, oxidase concentration, co-solvent, O_2 supply and production inhibition did not solve our confusion very well. Finally the discussion of electron donor for *Ao*FOx gave us a guideline for the subsequent direction of effort.
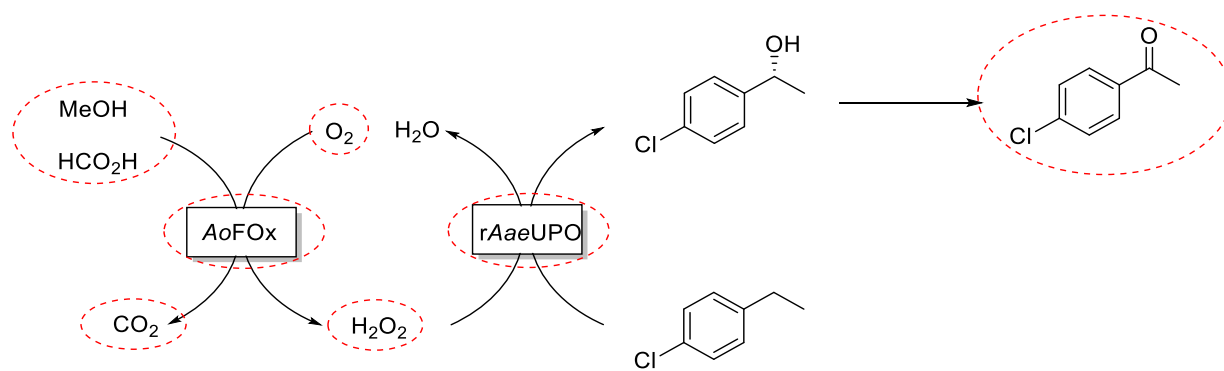
Scheme 1. Possible factors that have been investigated circled in dashed red.

6.4 Experimental section

6.4.1 General information

Unless otherwise mentioned, all chemicals were ordered from Sigma-Aldrich, TCI-Europe, or abcr GmbH and had been used without further purification. From GE Healthcare were purchased columns and column material for enzyme purification.

6.4.2 Enzyme preparation

The recombinant PaDaI variant of the evolved unspecific peroxygenase mutant from A. aegerita was expressed in P. pastoris and purified using the protocols mentioned in the previous publication.[11–13]

Formate oxidase from *Aspergillus oryzae* RIB40 (*Ao*FOx) was manufactured recombinantly in *E. coli* BL21(DE3), which was described in recent publications.[7,8]

6.4.3 Enantioselective hydroxylation of ethylbenzene derivatives

200 µl of a reaction mixture containing 100 mM KPi buffer pH 6.0, 1 µM r*Aae*UPO, 1 µM *Ao*FOx, 50 mM substrate, 250 mM formate, and 10% v/v CH_3CN were placed in a 1.5 ml glass vial. The reaction proceeded for 24 h at room temperature (25 °C) and 600 rpm. Reaction conditions were controlled using ThermoMixer C from Eppendorf.

6.4.4 Analysis procedures

6.4.4.1 Determination of r*Aae*UPO activity

The intrinsic activity was measured using an ABTS assay at 25 °C. The ABTS-assay was undertaken in a sodium citrate buffer (50 mM, pH 4.4) containing H_2O_2 (2.0 mM), ABTS (0.5 mM), and a diluted enzyme solution. Absorption change at 420 nm ($\varepsilon_{420} = 36.0$ mM^{-1} cm^{-1}) was used to track the oxidation of ABTS. The reactions were done in triplicates.

6.4.4.2 Determination of *Ao*FOx activity

An ABTS assay was used to determine the essential activity of *Ao*FOx. The ABTS assay was conducted using 50 mM of acetate buffer at pH 4.5 or phosphate buffer at pH 6.0 containing 1 mM of ABTS, 10 U mL^{-1} of HRP (horseradish peroxidase), 100 mM of formate, and different concentrations of *Ao*FOx. The reactions were monitored using an UV-Vis spectrometer at 420 nm (ε_{420} = 36.0 mM^{-1} cm^{-1}) at a temperature of 25 °C. 1 U of HRP is equivalent to the oxidation of 1 µmol ABTS per minute at pH 6.0, 25 °C.

6.4.4.3 GC measurements

On a Shimadzu GC-14A/FID or Shimadzu GC-2010 plus/FID equipped with various columns, GC measurements were conducted (see supplementary information). At different time intervals, the reactions were terminated by adding ethyl acetate containing 5 mM of n-octanol as an internal standard. Having followed extraction and centrifugation, the organic phase was dried with magnesium sulphate and analysed using gas chromatography. All given concentrations are derived from calibration curves established from authentic and synthetic standards.

References

1. W. Jiang, B. Fang, *Appl. Biochem. Biotechnol.* **2020**, *192*, 146.

2. C. K. Winkler, J. H. Schrittwieser, W. Kroutil, *ACS Cent. Sci.* **2021**, *7*, 55.

3. H. Renata, Z. J. Wang, F. H. Arnold, *Angew. Chem. Int. Ed.* **2015**, *54*, 3351.

4. S. Galanie, D. Entwistle, J. Lalonde, *Nat. Prod. Rep.* **2020**, *37*, 1122.

5. G. Rossino, M. S. Robescu, E. Licastro, C. Tedesco, I. Martello, L. Maffei, G. Vincenti, T. Bavaro, S. Collina, *Chirality.* **2022***, 1-16.*

6. H. L. Wapshott-Stehli, A. M. Grunden, *Enzyme Microb. Technol.* **2021**, *145*, 109744.

7. F. Tieves, S. J. P. Willot, M. M. C. H. van Schie, M. C. R. Rauch, S. H. H. Younes, W. Zhang, J. Dong, P. Gomez de Santos, J. M. Robbins, B. Bommarius, M. Alcalde, A. S. Bommarius, F. Hollmann, *Angew. Chem. Int. Ed.* **2019**, *58*, 7873.

8. S. J. P. Willot, M. D. Hoang, C. E. Paul, M. Alcalde, I. W. C. E. Arends, A. S. Bommarius, B. Bommarius, F. Hollmann, *ChemCatChem* **2020**, *12*, 2713.

9. Y. Ni, E. Fernández-Fueyo, A. G. Baraibar, R. Ullrich, M. Hofrichter, H. Yanase, M. Alcalde, W. J. H. van Berkel, F. Hollmann, *Angew. Chem. Int. Ed.* **2016**, *55*, 798.

10. T. Hilberath, A. van Troost, M. Alcalde, F. Hollmann, *Front. Catal.* **2022**, *2*.

11. P. Molina-Espeja, S. Ma, D. M. Mate, R. Ludwig, M. Alcalde, *Enzyme Microb. Technol.* **2015**, *73–74*, 29.

12. P. Molina-Espeja, E. Garcia-Ruiz, D. Gonzalez-Perez, R. Ullrich, M. Hofrichter, M. Alcalde, *Appl. Environ. Microbiol.* **2014**, *80*, 3496.

13. W. Stampfer, B. Kosjek, K. Faber, W. Kroutil, *J. Org. Chem.* **2003**, *68*, 402.

Supplementary information

Table S1. GC analytical data with achiral columns

Compound	GC column	Oven temperature program	Retention time
Ethylbenzene phenylethanol acetophenone	CP-Wax 52 CB (Agilent) (25 m×0.25 mm×1.2 µm); carrier gas: N₂ Split 150	135°C hold 4 min 20°C/min to 200°C hold 6.0 min 25°C/min to 250°C hold 1.0 min	3.56 min ethylbenzene 7.73 min n-octanol (IS) 9.72 min acetophenone 11.76 min phenylethanol
p-chloroethylbenzene *p*-chlorophenylethanol *p*-chloroacetophenone	CP-Sil 5 CB (Agilent) (25 m×0.25 mm×1.2 µm); carrier gas: N₂ Split 150	165°C hold 9 min 25°C/min to 345°C hold 1.0 min	3.74 min n-octanol (IS) 3.98 min *p*-chloroethylbenzene 7.02 min *p*-chloroacetophenone 7.49 min *p*-chlorophenylethanol
m-chloroethylbenzene *m*-chlorophenylethanol *m*-chloroacetophenone	CP-Wax 52 CB (Agilent) (50 m×0.53 mm×2.0 µm); carrier gas: N₂ Split 150	180°C hold 12 min 25°C/min to 250°C hold 1.0 min	1.58 min *m*-chloroethylbenzene 1.87 min n-octanol (IS) 4.97 min *m*-chloroacetophenone 10.27 min *m*-chlorophenylethanol
o-chloroethylbenzene *o*-chlorophenylethanol *o*-chloroacetophenone	CP-Sil 5 CB (Agilent) (25 m×0.25 mm×1.2 µm); carrier gas: N₂ Split 150	110°C hold 3 min 20°C/min to 145°C hold 5.0 min 20°C/min to 170°C hold 3.0 min 25°C/min to 345°C hold 1.0 min	7.72 min *o*-chloroethylbenzene 7.90 min n-octanol (IS) 11.86 min *o*-chloroacetophenone 12.67 min *o*-chlorophenylethanol
p-bromoethylbenzene *p*-bromophenylethanol *p*-bromoacetophenone	CP-Sil 5 CB (Agilent) (25 m×0.25 mm×1.2 µm); carrier gas: N₂ Split 150	170°C hold 10 min 25°C/min to 345°C hold 1.0 min	2.93 min *p*-bromoethylbenzene 6.49 min n-octanol (IS) 9.90 min *p*-bromoacetophenone

			14.37 min *p*-bromo-phenylethanol
m-bromoethylbenzene *m*-bromophenylethanol *m*-bromoacetophenone	CP-Sil 5 CB (Agilent) (25 m×0.25 mm×1.2 µm); carrier gas: N₂ Split 150	170°C hold 10 min 25°C/min to 345°C hold 1.0 min	3.39 min *m*-bromoeth-ylbenzene 4.62 min n-octanol (IS) 8.38 min *m*-bromoaceto-phenone 9.04 min *m*-bromo-phenylethanol
o-bromoethylbenzene *o*-bromophenylethanol *o*-bromoacetophenone	CP-Sil 5 CB (Agilent) (25 m×0.25 mm×1.2 µm); carrier gas: N₂ Split 150	170°C hold 10 min 25°C/min to 345°C hold 1.0 min	3.39 min *o*-bromoethylben-zene 4.48 min n-octanol (IS) 7.47 min *o*-bromoaceto-phenone 8.20 min *o*-bromo-phenylethanol
p-iodoethylbenzene *p*-iodophenylethanol *p*-iodoacetophenone	CP-Sil 5 CB (Agilent) (25 m×0.25 mm×1.2 µm); carrier gas: N₂ Split 150	190°C hold 15 min 25°C/min to 345°C hold 1.0 min	2.75 min n-octanol (IS) 4.82 min *p*-iodoethylben-zene 8.41 min *p*-iodoacetophe-none 8.75 min *p*-iodophenyleth-anol
p-fluoroethylbenzene *p*-fluorophenylethanol *p*-fluoroacetophenone	CP-Wax 52 CB (Agilent) (25 m×0.25 mm×1.2 µm); carrier gas: N₂ Split 150	160°C hold 11 min 20°C/min to 220°C hold 2.0 min 25°C/min to 250°C hold 1.0 min	3.36 min n-octanol (IS) 4.68 min *p*-fluoroethylben-zene 8.49 min *p*-fluoroacetophe-none 9.06 min *p*-fluoro-phenylethanol
p-ethylanisole *p*-methoxyphenylethanol *p*-methoxyacetophe-none	CP-Sil 5 CB (Agilent) (25 m×0.25 mm×1.2 µm); carrier gas: N₂ Split 150	160°C hold 6 min 20°C/min to 205°C hold 1.5 min 25°C/min to 345°C hold 1.0 min	4.05 min n-octanol (IS) 4.99 min *p*-ethylanisole 8.35 min *p*-methoxy-phenylethanol 9.12 min *p*-methoxyaceto-phenone
o-ethylanisole *o*-methoxyphenylethanol *o*-methoxyacetophe-none	CP-Sil 5 CB (Agilent) (25 m×0.25 mm×1.2 µm); carrier gas: N₂; Split 150	180°C hold 10 min 25°C/min to 345°C hold 1.0 min	3.06 min n-octanol (IS) 3.36 min *o*-ethylanisole 5.74 min *o*-methoxy-phenylethanol

Compound	GC column	Oven temperature program	Retention time
			5.99 min o-methoxyaceto-phenone
p-nitroethylbenzene p-nitrophenylethanol p-nitroacetophenone	CP-Sil 5 CB (Agilent) (25 m×0.25 mm×1.2 µm); carrier gas: N_2 Split 150	170°C hold 22 min 25°C/min to 345°C hold 1.0 min	3.48 min n-octanol (IS) 8.50 min p-nitroethylben-zene 13.32 min p-nitroacetophe-none 18.14 min p-nitro-phenylethanol
o-nitroethylbenzene o-nitrophenylethanol o-nitroacetophenone	CP-Sil 5 CB (Agilent) (25 m×0.25 mm×1.2 µm); carrier gas: N_2; Split 150	190°C hold 3 min 20°C/min to 215°C hold 4.5 min 30°C/min to 345°C hold 1.0 min	2.87 min n-octanol (IS) 4.33 min o-nitroethylben-zene 5.99 min o-nitroacetophe-none 6.16 min o-nitrophenyleth-anol
o-ethylnaphthalene o-naphthylethanol o-acetonaphthone	CP-Sil 5 CB (Agilent) (25 m×0.25 mm×1.2 µm); carrier gas: N_2 Split 150	160°C hold 5 min 20°C/min to 220°C hold 10.0 min 25°C/min to 345°C hold 1.0 min	3.87 min n-octanol (IS) 9.00 min o-ethylnaphtha-lene 12.54 min o-naphthyleth-anol 12.86 min o-acetonaph-thone

Table S2. GC analytical data with chiral columns

Compound	GC column	Oven temperature program	Retention time
ethylbenzene phenylethanol acetophenone	CP-Chirasil-Dex-CB (Agilent) (25 m×0.32 mm×0.25 µm); carrier gas: He Split 150	100°C hold 16 min 20°C/min to 140°C hold 3.0 min 25°C/min to 225°C hold 1.0 min	3.49 min ethylbenzene 10.07 min acetophenone 14.16 min n-octanol (IS) 18.65 min (R)-1-phenyleth-anol 19.10 min (S)-1-phenylethanol
p-chloroethylbenzene p-chlorophenylethanol p-chloroacetophenone	CP-Chirasil-Dex-CB (Agilent) (25 m×0.32 mm×0.25 µm); carrier gas: He Split 150	150°C hold 10 min 25°C/min to 225°C hold 1.0 min	2.70 min p-chloroethylben-zene 2.95 min n-octanol (IS) 4.52 min p-chloroacetophe-none

			7.54 min (*R*)-*p*-chloro-phenylethanol 8.08 min (*S*)-*p*-chloro-phenylethanol
m-chloroethylbenzene *m*-chlorophenylethanol *m*-chloroacetophenone	CP-Chirasil-Dex-CB (Agilent) (25 m×0.32 mm×0.25 µm); carrier gas: He Split 150	150°C hold 10 min 25°C/min to 225°C hold 1.0 min	2.77 min *m*-chloroethylben-zene 2.96 min n-octanol (IS) 4.12 min *m*-chloroacetophe-none 7.31 min (*R*)-*m*-chloro-phenylethanol 7.68 min (*S*)-*m*-chloro-phenylethanol
o-chloroethylbenzene *o*-chlorophenylethanol *o*-chloroacetophenone	CP-Chirasil-Dex-CB (Agilent) (25 m×0.32 mm×0.25 µm); carrier gas: He Split 150	150°C hold 10 min 25°C/min to 225°C hold 1.0 min	2,73 min *o*-chloroethylben-zene 2.96 min n-octanol (IS) 3.76 min *o*-chloroacetophe-none 6.89 min (*R*)-*o*-chloro-phenylethanol 7.73 min (*S*)-*o*-chloro-phenylethanol
p-bromoethylbenzene *p*-bromophenylethanol *p*-bromoacetophenone	CP-Chirasil-Dex-CB (Agilent) (25 m×0.32 mm×0.25 µm); carrier gas: He Split 150	135°C hold 8 min 25°C/min to 225°C hold 1.0 min	2.37 min *p*-bromoethylben-zene 3.66 min *p*-bromoacetophe-none 3.92 min n-octanol (IS) 5.99 min (*R*)-*p*-bromo-phenylethanol 6.41 min (*S*)-*p*-bromo-phenylethanol
m-bromoethylbenzene *m*-bromophenylethanol *m*-bromoacetophenone	CP-Chirasil-Dex-CB (Agilent) (25 m×0.32 mm×0.25 µm); carrier gas: He; Split 150	110°C hold 3 min 20°C/min to 140°C hold 3.0 min 20°C/min to 170°C hold 5.0 min 25°C/min to 225°C hold 1.0 min	5.95 min *m*-bromoethylben-zene 6.09 min n-octanol (IS) 9.51 min *m*-bromoacetophe-none 12.84 min (*R*)- or (*S*)-*m*-bro-mophenylethanol
o-bromoethylbenzene *o*-bromophenylethanol *o*-bromoacetophenone	CP-Chirasil-Dex-CB (Agilent) (25 m×0.32 mm×0.25 µm); carrier gas: He; Split 150	110°C hold 3 min 20°C/min to 135°C hold 3.0 min	6.0 min *o*-bromoethylbenzene 6.29 min n-octanol (IS) 9.33 min *o*-bromoacetophe-none

		20°C/min to 165°C hold 5.0 min 25°C/min to 225°C hold 1.0 min	13.41 min (*R*)- or (*S*)-*o*-bromophenylethanol
p-iodoethylbenzene *p*-iodophenylethanol *p*-iodoacetophenone	CP-Chirasil-Dex-CB (Agilent) (25 m×0.32 mm×0.25 µm); carrier gas: He Split 150	175°C hold 8 min 25°C/min to 225°C hold 1.0 min	2.31 min n-octanol (IS) 2.89 min *p*-iodoethylbenzene 5.00 min *p*-iodoacetophenone 6.848 min (*R*)-*p*-iodophenylethanol 7.08 min (*S*)-*p*-iodophenylethanol
p-fluoroethylbenzene *p*-fluorophenylethanol *p*-fluoroacetophenone	CP-Chirasil-Dex-CB (Agilent) (25 m×0.32 mm×0.25 µm); carrier gas: He Split 150	160°C hold 10 min 25°C/min to 225°C hold 1.0 min	2.72 min n-octanol (IS) 2.97 min *p*-fluoroethylbenzene 5.02 min *p*-fluoroacetophenone 8.03 min (*R*)-*p*-fluorophenylethanol 8.48 min (*S*)-*p*-fluorophenylethanol
p-ethylanisole *p*-methoxyphenylethanol *p*-methoxyacetophenone	CP-Chirasil-Dex-CB (Agilent) (25 m×0.32 mm×0.25 µm); carrier gas: He Split 150	110°C hold 3 min 20°C/min to 130°C hold 3.0 min 20°C/min to 170°C hold 3.0 min 25°C/min to 225°C hold 1.0 min	5.48 min *p*-ethylanisole 6.25 min n-octanol (IS) 10.39 min *p*-methoxyacetophenone 11.23 min (*R*)-*p*-methoxyphenylethanol 11.38 min (*S*)-*p*-methoxyphenylethanol
o-ethylanisole *o*-methoxyphenylethanol *o*-methoxyacetophenone	CP-Chirasil-Dex-CB (Agilent) (25 m×0.32 mm×0.25 µm); carrier gas: He; Split 150	110°C hold 3 min 20°C/min to 130°C hold 3.0 min 20°C/min to 180°C hold 5.0 min 25°C/min to 225°C hold 1.0 min	5.22 min *o*-ethylanisole 6.57 min n-octanol (IS) 10.83 min *o*-methoxyacetophenone 12.95 min (*R*)-*o*-methoxyphenylethanol
p-nitroethylbenzene *p*-nitrophenylethanol *p*-nitroacetophenone	CP-Chirasil-Dex-CB (Agilent) (25 m×0.32 mm×0.25 µm); carrier gas: He; Split 150	180°C hold 10 min 25°C/min to 225°C hold 1.0 min	2.31 min n-octanol (IS) 3.31 min *p*-nitroethylbenzene 4.97 min *p*-nitroacetophenone 9.88 min (*R*)-*p*-nitrophenylethanol 10.54 min (*S*)-*p*-nitrophenylethanol

o-nitroethylbenzene *o*-nitrophenylethanol *o*-nitroacetophenone	CP-Chirasil-Dex-CB (Agilent) (25 m×0.32 mm×0.25 µm); carrier gas: He; Split 150	180°C hold 13 min 25°C/min to 225°C hold 1.0 min	2.31 min n-octanol (IS) 2.74 min *o*-nitroethylbenzene 3.84 min *o*-nitroacetophenone 5.94 min (*R*)-*o*-nitrophenyleth-anol 6.23 min (*S*)-*o*-nitrophenyleth-anol

7

Conclusion and Outlook

With environmental problems becoming increasingly serious, biocatalysis, an environmentally friendly method for chemical synthesis, is gaining attention.[1] Biocatalysis has developed rapidly in recent years; growing numbers of enzymes are being discovered and applied, like the glucose isomerase, penicillin G acylase,[2] lipases,[3] and protease[4] etc. The capacity of enzymes to catalyse transformations with high reaction rates and selectivity under mild conditions while producing high-quality/purity products, making the concept of "green chemistry" into reality.[5] Oxidoreductases are considered very promising catalysts in organic synthesis as they can catalyse selective oxyfunctionalisation avoiding protecting group chemistry and complex synthetic routes. However, there are just very few examples of oxidoreductases applications on industry scale.[6,7] The introduction of H_2O_2-driven peroxyzymes, such as unspecific peroxygenase (UPO) and vanadium-dependent haloperoxidase (VCPO),[8] provides many opportunities for the application of oxidoreductases.

In this thesis, we investigated a variety of potential applications for vanadium-dependent haloperoxidase from *Curvularia inaequalis* (*Ci*VCPO) and unspecific peroxygenases from *Agrocybe aegerita* (r*Aae*UPO), as well as the associated enzymatic H_2O_2 regeneration systems. With the purpose of making some contributions to the application of enzymatic oxyfunctionalisation. The approach proposed has been divided into the following four sections:

1. Expanding the product scope of r*Aae*UPO–Chapter 3.
2. Innovative applications of r*Aae*UPO–Chapter 4.
3. Preparative-scale application of *Ci*VCPO–Chapter 5.
4. *Ao*FOx-driven H_2O_2 generation system–Chapter 6.

1. Expanding the product scope of *Aae*UPO

UPO can catalyse many types of selective oxyfunctionalisation reactions, for instance, the oxidation of C-H, C-C, or C=C bonds.[9] In particular, the enantioselective hydroxylation of ethylbenzene catalysed by UPO has received much attention. However, this reaction only produces (*R*)-phenylethanol with an overoxidation product-acetophenone. A valuable

point to note is that, with enough H_2O_2, ethylbenzene can be entirely converted to aceto-phenone–a very good raw material to produce chiral molecules. Therefore we designed this UPO-ADHs cascade of reactions. By adding a couple of different selective ADHs, we obtained not only (*R*)-phenylethanol but also (*S*)-phenylethanol. 10 pairs of enantiomeri-cally pure phenylethanol derivatives (>91% *ee*) were produced by using this cascade sys-tem. In comparison to the same period of photo-chemo-enzymatic systems[10], our UPO-ADHs system has advantages in terms of product concentration and purity (Table 1).

Table 1. The advantages of the project compared to the same period of photocatalytic systems.[10]

Advantages	Photons-UPO system	UPO-ADHs system
Product concentration	≤7 mM	~50 mM
(*S*)-1-phenylethanol	93% *ee*	99% *ee*
(*R*)-1-phenylethanol	99% *ee*	99% *ee*

The results obtained are promising, but the reaction system is not mature, and there is still the possibility of improvement. The one-pot one-step, for example, does not work here, probably because:

1. ACN as a co-solvent in *Aae*UPO reaction may inhibit ADHs.
2. 2-propanol as co-substrate and co-solvent in the reaction of ADHs is possibly in-hibited the activity of *Aae*UPO.
3. The reaction rates of *Aae*UPO and ADH are not in synchrony, with the accumula-tion of acetophenone intermediates that may cause the inactivation of ADHs.
4. The H_2O_2 added into the reaction system for *Aae*UPO may have influenced the activity of ADHs as well.

All of the above are issues that I think need to be solved in the future.

2. Innovative application: UPO catalysed Si-H oxyfunctionalisation

In contrast to the abundant enzymatic C-H selective oxyfunctionalisation reactions, the enzymatic Si-H bond oxyfunctionalisation reactions are uncommon. In fact, the possibility of using enzymes for organosilicon chemistry and producing new silicon-based materials is very valuable.[11] Arnold's first use of heme enzyme-P450 monooxygenase to oxidise silane to silanol inspired us.[12] The second approach is to use the unspecific peroxygenase *Aae*UPO, also a heme enzyme, for the first time in the selective oxyfunctionalisation of silanes. Nine silanes were investigated and 120 mM of dimethylphenylsilanol was obtained. 120 mM is a relatively high-level product concentration in the field of biocatalysis.

Table 2. The advantages of UPO compared to P450 in catalysing Si-H oxyfunctionalisation.[12]

Improvement	P450	*Aae*UPO
Product concentration	<2 mM	121 mM
Turnovers	19,100	120,000
k_{cat} (s^{-1})	0.2	84

It is very pleasing that we achieved such impressive results with *Aae*UPO for this first use, demonstrating that this enzymatic Si-H bond oxyfunctionalisation approach has great potential in application. As shown in Table 2, UPO seems more efficient in catalytic efficiency and product concentration than P450. However, we have to point out that this enzymatic Si-H oxyfunctionalisation route is not mature enough and also has many limitations:

1. This method does not always work, some silanes do not react, and some silanes obtained C-H-bond hydroxylation products. Molecular modelling calculation, and directed evolution to design a more suitable enzyme for those substrates may be the solutions.
2. During the reaction, we also found that the stability of UPO in the 2LPS system is difficult to keep long (<48 h), even with a low H_2O_2 addition rate (5 mM/h), so protein engineering and enzyme immobilisation to produce the UPO that can maintain activity in the reaction system are also the directions to be pursued.

3. There are many similarities between silicon and carbon. Enzymes that can catalyse transformations of C-H, C-C, and C-S bonds may also catalyse the transformations of Si-H, Si-Si, and Si-S bonds. So expanding the substrates scope of UPO catalysed Si-H oxyfunctionalisation reaction and developing more enzymatic organosilicon chemistry methods are also worth a try.

3. Preparative-scale application: *Ci*VCPO-catalysed oxidative decarboxylation

Following the study of the expanded and innovative application of enzymes, we moved on to reaction conditions optimisation and scale-up preparation. The third approach demonstrates the scale-up preparation of *Ci*VCPO-catalysed oxidative decarboxylation of glutamic acid.

Earlier work by But *et al.* using *Ci*VCPO established a clean oxidative decarboxylation that resulted in an nitrile.[13–15] Following this work, we investigated the reaction limitations and semi-scale preparation (827 mg of 3-cyanopropanoic acid (CPA) was isolated with 96-97% purity. As seen in Table 3, this approach has made some improvements compared to previous results, which indicates *Ci*VCPO is a potentially powerful tool in the production of 3-cyanopropanoic acid.

Table 3. Improvements in this project compared to previous reports.[13]

Improvement	Before	After
Substrate concentration	5 mM	100 mM
Reaction scale	2 mL	200 mL
Turnovers	91,000	1,630,000
k_{cat}	25 s^{-1}	75 s^{-1}

However, the limitation of this study is that the product 3-cyanopropanoic acid has a significant inhibition to *Ci*VCPO. Such inhibition is the problem that needs to be solved if we want to increase the product concentration. In my opinion, three approaches can be considered:

1. Designing an *in situ* product separation reactor.

2. Immobilising enzymes to make them reusable.

3. Using protein engineering to develop a stronger VCPO that can withstand highly substrate concentrations.

4. Formic oxidase-driven H_2O_2 generation system.

Peroxygenase has a well-known shortcoming: poor stability against H_2O_2.[16] Many enzyme-driven H_2O_2 generation systems have been developed for this reason. Our approach attempts was to use the *Ao*FOx (formic acid oxidase)-driven H_2O_2 generation system to guide *Aae*UPO-catalysed ethylbenzene derivatives hydroxylation. We extended the substrate scope of the previously developed *Ao*FOx/*Aae*UPO system,[17,18] 15 ethylbenzene derivatives were tested (*ee* value of (*R*)-alcohol: >95%). *p*-chloroethylbenzene was selected as the model substrate, and the reaction limitations were investigated. 21 mM of (*R*)-*p*-chlorophenolethanol and 47 mM *p*-chloroacetophenone with a turnover number of 115000 for both *Ao*FOx and *Aae*UPO was obtained.

We investigated factors such as formate and enzyme spiking, pH, oxidase concentration, co-solvent, O_2 supply and product inhibition, etc, that might affect the reactions. We have been unable to find a specific reason for the reaction to stop at 5 h. These data were recorded as a reference for following researchers in the hope that the reason can be found and solved in the future.

Is this H_2O_2 generation system genuinely green? The E factor developed in enzyme production and reactions seems to be very high; water from fermentations and reactions is the main reason. Therefore, optimising the reaction conditions of *Ao*FOx/*Aae*UPO to achieve a higher product concentration and a lower amount of waste in order to decrease the E factor could make this *in situ* system more attractive.

5. Final conclusion

Although biocatalytic oxyfunctionalisation is a promising transformation route, the chemical industry has not yet widely adopted it.[19,20] One main reason is the lack of stable and efficient biocatalysts to be used in practical synthesis. In this thesis, we have evaluated our catalysts in terms of extended applications of substrates scope, innovative applications of reaction types and semi-scale preparation, taking biocatalytic oxyfunctionalisation a small step closer to becoming a mature tool in chemical synthesis. We hope that in the near future, these very promising catalysts will come into regular use in chemical industry.

References

1. R. A. Sheldon, J. M. Woodley, *Chem. Rev.* **2018**, *118*, 801.

2. A. Bruggink, E. C. Roos, E. de Vroom, *Org. Process Res. Dev.* **1998**, *2*, 128.

3. F. Hasan, A. A. Shah, A. Hameed, *Enzyme Microb. Technol.* **2006**, *39*, 235.

4. D. A. Estell, T. P. Graycar, J. A. Wells, *J. Biol. Chem.* **1985**, *260*, 6518.

5. Y. Ni, D. Holtmann, F. Hollmann, *ChemCatChem* **2014**, *6*, 930.

6. P. Gomez de Santos, F. V. Cervantes, F. Tieves, F. J. Plou, F. Hollmann, M. Alcalde, *Tetrahedron* **2019**, *75*, 1827.

7. D. Holtmann, F. Hollmann, *ChemBioChem* **2016**, *17*, 1391.

8. B. O. Burek, S. Bormann, F. Hollmann, J. Z. Bloh, D. Holtmann, *Green Chem.* **2019**, *21*, 3232.

9. M. Hobisch, D. Holtmann, P. Gomez de Santos, M. Alcalde, F. Hollmann, S. Kara, *New Trends Ind. Biocatal.* **2021**, *51*, 107615.

10. L. Schmermund, S. Reischauer, S. Bierbaumer, C. K. Winkler, A. Diaz-Rodriguez, L. J. Edwards, S. Kara, T. Mielke, J. Cartwright, G. Grogan, B. Pieber, W. Kroutil, *Angew. Chem. Int. Ed.* **2021**, *60*, 6965.

11. M. B. Frampton, P. M. Zelisko, *Silicon* **2009**, *1*, 147.

12. S. Bähr, S. Brinkmann-Chen, M. Garcia-Borràs, J. M. Roberts, D. E. Katsoulis, K. N. Houk, F. H. Arnold, *Angew. Chem. Int. Ed.* **2020**, *59*, 15507.

13. A. But, J. Le Nôtre, E. L. Scott, R. Wever, J. P. M. Sanders, *ChemSusChem* **2012**, *5*, 1199.

14. A. But, A. van Noord, F. Poletto, J. P. M. Sanders, M. C. R. Franssen, E. L. Scott, *Mol. Catal.* **2017**, *443*, 92.

15. A. But, E. van der Wijst, J. Le Notre, R. Wever, J. P. M. Sanders, J. H. Bitter, E. L. Scott, *Green Chem.* **2017**, *19*, 5178.

16. B. Valderrama, M. Ayala, R. Vazquez-Duhalt, *Chem. Biol.* **2002**, *9*, 555.

17. F. Tieves, S. J.-P. Willot, M. M. C. H. van Schie, M. C. R. Rauch, S. H. H. Younes, W. Zhang, J. Dong, P. Gomez de Santos, J. M. Robbins, B. Bommarius, M. Alcalde, A. S. Bommarius, F. Hollmann, *Angew. Chem. Int. Ed.* **2019**, *58*, 7873.

18. S. J. P. Willot, M. D. Hoang, C. E. Paul, M. Alcalde, I. W. C. E. Arends, A. S. Bommarius, B. Bommarius, F. Hollmann, *ChemCatChem* **2020**, *12*, 2713.

19. G. W. Huisman, S. J. Collier, *Curr. Opin. Chem. Biol.* **2013**, *17*, 284.

20. A. T. Martínez, F. J. Ruiz-Dueñas, S. Camarero, A. Serrano, D. Linde, H. Lund, J. Vind, M. Tovborg, O. M. Herold-Majumdar, M. Hofrichter, C. Liers, R. Ullrich, K. Scheibner, G. Sannia, A. Piscitelli, C. Pezzella, M. E. Sener, S. Kılıç, W. J. H. van Berkel, V. Guallar, M. F. Lucas, R. Zuhse, R. Ludwig, F. Hollmann, E. Fernández-Fueyo, E. Record, C. B. Faulds, M. Tortajada, I. Winckelmann, J.-A. Rasmussen, M. Gelo-Pujic, A. Gutiérrez, J. C. del Río, J. Rencoret, M. Alcalde, *Biotechnol. Adv.* **2017**, *35*, 815.

Curriculum vitae

Name: Xiaomin Xu

Date of Birth: 07.04.1993

Place of Birth: Hubei, China
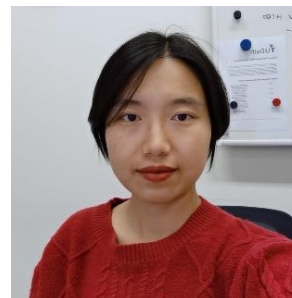
List of publications

1. 'Towards preparative chemoenzymatic production of 3-cyanopropanoic acid from glutamate'

   X. Xu, A. But, R. Wever, F. Hollmann. *ChemCatChem* **2020**, 12 (8), 2180–2183. DOI: 10.1002/cctc.201902194

2. 'A Peroxygenase-Alcohol Dehydrogenase Cascade Reaction to Transform Ethylbenzene Derivatives into Enantioenriched Phenylethanols'

   X. Xu, H. Brasselet, E. P. J. Jongkind, M. Alcalde, C. E. Paul, F. Hollmann, *ChemBioChem* **2022**, 23, e202200017. DOI: 10.1002/cbic.202200017

3. 'Peroxygenase-Catalysed Selective Oxidation of Silanes to Silanols'

   X. Xu, Y. Mao, M. Martinez, S. Roda, M. Floor, V. Guallar, C. E. Paul, M. Alcalde, F. Hollmann. *Manuscript in revision.*

4. 'Selective oxyfunctionalisation reactions catalysed by P450 monooxygenases and peroxygenases – a bright future for sustainable chemical synthesis'

   X. Xu, T. Hilberath, F. Hollmann. *Manuscript in revision.*

Acknowledgement

Thank you so much for finally turning to the end of this thesis after reading the previous sections. My four years as a PhD student have been a very memorable journey. I have benefited greatly from it. Four years ago, I came to the Netherlands alone, far from my family and friends. At first, I was shy, unconfident and confused. Now I have matured into a graduate who is self-assured and independent. Such growth and gains would not have been possible without the help of everyone in our warm BOC family.

First of all, I would like to give thanks to my promoter, Frank. He hasprovided me with a lot of practical ideas and advice. He has taught me how to consider the meaning behind the results of an experiment, how to tell a good scientific story and write a scientific paper. He has been always very patient in guiding me. Whenever he was available, his office door was open to me to answer any questions.

Secondly, I would like to thank my co-promoter Caroline. She has kept encouraging and supporting me throughout the four years, caring about my emotional and physical conditions. With her unlimited support, I started to become confident and outgoing. I am a person who is not so cautious in what I do, Caroline corrected many of the small mistakes I had made in the research. The details make the difference; thank you for taking the trouble to fix my errors in detail.

Thirdly I would like to appreciate are our secretaries: Mieke and Irma. Mieke, looked after us like mothers and helped us with almost everything relating to administration.. From the beginning, she assisted me in finding a house, getting a visa, and doing enrolment procedures; later, she provided timely notification of all meetings, events, and holidays; sent us surprising gifts at Thanksgiving and Christmas; and sent greetings at each Chinese New Year. All this made me feel warm. Irma helped me a lot during the last six months of my phd. She kept encouraging and supporting me with everything, which gave me a lot of courage for preparing the defence.

My fourth thanks go to Andrada, my daily supervisor during the first year of my phd. Even though I only worked with her for under a year, the effect she had on me was enormous. She taught me a lot of fundamental experiments and corrected my bad habits in research. Her support enabled me to complete my phd project independently over the next three

years. I am very fortunate to have had such a fantastic daily supervisor at the start of my phd.

In order of time, I would like to thank Morten, Sébastien, Georg, Marine, Fabio, Nati, and Alexandra for all their help when I first came to the Netherlands. In terms of life, they invited me to their homes for parties and helped me read the letters I received in Dutch. In terms of work, they gave me a lot of help and advice, helping me with my presentation and go/no go reports. Thanks to the help of these lovely people, I felt less lonely and homesick, rapidly adapted to life in the Netherlands.

Next, I would like to thank my big sister, Allison, for her constant encouragement and concern, which has warmed me throughout my four years. Thanks to Jose, we started our studies very closely together. I still remember the day we took the English exams together. In the blink of an eye, four years have passed. We have encouraged each other during these four years and I would like to thank you for all the help you have provided me in the lab. I hope that in the future, we might have the opportunity to meet again. I would also like to thank Jordi, a student from Spain, who accompanied me to the hospital when I hurt myself in the lab. Although Jordi has been away from the group for three years, I will never forget the help he gave me. I hope that in the future, we will have the opportunity to sit together again for a beer. Thanks to Hugo for his suggestions and assistance with my project; Loana, Eva and Chiara for their encouragement and warm hugs. Thanks to Jacob for helping me complete my project in my final months.

A big thanks to the enthusiastic and professional technicians in our group. Keeping busy every day fixing all sorts of GC problems for us is Remco; Very patient and supportive in teaching me how to use HPLC is Lloyd; Laura makes great carrots and banana cakes and help me with fermentations; Stephen, a fan of spice food, taught me many ways of using NMR; Linda brings much laughter to the office. Marc, the superman in the lab, can support me with anything.

Furthermore, I would like to thank the kind and helpful professors in the BOC group, Ulf, Kristina, Peter and Duncan, for their expertise and encouragement throughout the four years. Overall, thanks to the biocatalysis group for providing the most incredible work atmosphere. I also want to express my appreciation to Jinyuan, Marinka, Zhao Fu, Yuemei

for their support for me psychologically. Thank you for helping me to learn to love myself, love life, and love the world.

There are so many people that I would like to appreciate; if I could, I want to write down all of your names. I will keep you all in my heart forever and remember the beautiful memories I have made with you during my four years in TUDelft. Without you, I would not have been able to graduate.

As time flies, my journey at TUDelft has come to an end. The last person I would like to thank is myself. Thanks to Xiaomin, who decided to go to the Netherlands for the phd, it opened my eyes to a broader world. What this experience has given me is more than just the simple meaning of "getting a phd degree". This means that I defeated many challenges without escaping!

Finally, I dedicate this achievement to my beloved parents, family members, and friends for their constant understanding and support. It gave me the courage to overcome all the difficulties!